

# **Mafic-hosted zinc mineralisation, High Point, western Tasmania.**

**Rohan D. Hine B.Sc.**



Submitted in partial fulfilment of the requirements of the  
degree of Bachelor of Science with Honours

**Centre for Ore Deposit and Exploration Studies**

**University of Tasmania**

**1995**

*"For as birds are born to fly freely through the air, so are fishes born to swim through the waters, while to other creatures, Nature has given the earth that they might live in it, and particularly man that he might cultivate it and draw out of its caverns metals and other mineral products."*

(Georgius Agricola in *De Re Metallica*, 1556).

---

## Abstract

---

The High Point prospect is located on the northern slopes of Mount Charter in western Tasmania within the Que-Hellyer Volcanics of the Cambrian Mount Read Volcanic belt. The main lithologies include intrusive sub-ophitic dolerite, pyritic black shales, andesite dykes and sills, coherent basalt units, basalt breccias, dacite lavas and dacite breccias. The prehnite-pumpellyite grade of metamorphism recognised in the area is attributed to the Devonian Tabberabberan Orogeny. The structure of the area is dominated by N.E.-plunging synclines and by the Henty Fault zone to the east of the region, and the Mount Charter fault immediately to the southwest of the study area.

The previously enigmatic High Point dolerites are now considered to be broadly comagmatic with the upper basalts of the Que Hellyer Volcanics based on geologic relationships and geochemical analyses. Similarly, andesite units in the area are geochemical equivalents of the hornblende andesites of the southern Central Volcanic Complex. Dacites units in the High Point region correlate with the 'mixed sequence' dacites of the Que-Hellyer Volcanics (part of suite III of Crawford *et al.*, 1992).

Alteration of the High Point lithologies is considered to be a low intensity, low temperature equivalent of VHMS-related alteration at the Que River and Hellyer massive sulphide deposits. Typical alteration assemblages, considered to be Cambrian, include; silica-sericite in dacites, chlorite in basalts, sericite-fuchsite in the upper basalts and silica-albite in the andesites. Epidote alteration overprints the Cambrian alteration assemblages and is likely to be related to the Devonian Tabberabberan Orogeny.

The High Point prospect contains low grade, disseminated sphalerite mineralisation which occurs as fine-grained anhedral masses associated with minor galena and pyrite, and is predominantly hosted within the basalts and andesites. Lead isotope data suggests that the disseminated mineralisation is Cambrian and has a target signature similar to that of the Que River massive sulphide deposit, Zn ratios also indicate that the mineralisation is Cambrian VHMS style. Vein style sphalerite mineralisation is associated with minor pyrite, galena,

chalcopyrite and pyrrhotite and is attributed to remobilisation during the Devonian Tabberabberan Orogeny.

The heat source for the Cambrian mineralisation and alteration is interpreted to be related to the emplacement of the andesite dykes and sills. Hydrothermal fluids have preferentially precipitated sphalerite within the basalts and andesites, particularly below the contact of the Que River Shale. The Que River Shale has behaved as a chemical trap for the mineralised hydrothermal fluids. The mineralisation is currently subeconomic however, potential exists for economic mineralisation deeper within the stratigraphic sequence.

---

## Acknowledgments

---

The spine on this thesis bares but one name, however it would not have been possible without the help of so many people during all stages, from conception to final printing. If I forget to list your name below then I am sorry but you know who you are and that's all that counts.

Thanks goes to Aberfoyle Resources Limited for providing logistical support, in particular thanks are extended to Steve Richardson, David Wallace and Richard DeBomford (I owe you big time).

I would like to thank Dr Bruce Gemmell for his supervision of this project and Dr. David Cooke, Dr. Paul Kitto, Dr Tony Crawford and Dr Garry Davidson for reading various drafts of this thesis.

Thanks to all the honours students from the 1995 year for the many discussions, even though they may not have been all geological (Thank goodness!). In particular I would like to thank Bee and Pen for pushing me during those last days of hell and for the help with all the 'fiddly bits'. Thanks also to Johnny D for his masterful colouring in. Thanks guys.

My flat mates must also be thanked for reading the final drafts of this thesis and correcting the many combinations of '*et al.*' and 'Fig.'. Thankyou Dave, Tash, and Crow.

A very special thanks must go to Mum and Dad who provided so much for me during my undergraduate and honours years, and for initially introducing me to geology at a very tender age of 1.

A final thankyou must go to the makers of liquid paper and magic tape, and to Bushells, Coca-cola and Mykonos for keeping me going.

---

## Table of Contents

---

	<b>Page</b>
<b>Frontispiece</b>	i
<b>Abstract</b>	ii
<b>Acknowledgments</b>	iv
<b>Table of Contents</b>	v
<b>List of figures</b>	viii
<b>List of tables</b>	x
<b>List of plates</b>	xi
 <b>Chapter 1 Introduction</b>	
1.1 STUDY AREA	1
1.2 EXPLORATION HISTORY	2
1.3 PREVIOUS WORK	4
1.4 AIMS	4
1.5 METHODS	4
 <b>Chapter 2 Regional Geology</b>	
2.1 INTRODUCTION	6
2.2 MOUNT READ VOLCANICS STRATIGRAPHY	6
2.3 ANIMAL CREEK GREYWACKE	10
2.4 QUE-HELLYER VOLCANICS	11
2.5 DEFORMATION AND METAMORPHISM	13
2.6 MAJOR ORE DEPOSITS	13
2.6.1 Hellyer	13
2.6.2 Que River	15
2.6.3 Mount Charter	17
 <b>Chapter 3 Stratigraphy</b>	
3.1 INTRODUCTION	18
3.1.1 Classification of sedimentary lithologies	18
3.1.2 Classification of volcanics	19
3.2 ANIMAL CREEK GREYWACKE	20
3.3 DACITES	21
3.3.1 Dacite breccias	21
3.3.2 Interpretations	22
3.4. BASALTS	25
3.4.1 Basalt breccias	26
3.4.2 Interpretations	26
3.5 QUE RIVER SHALE	28
3.6 SANDSTONES AND SILTSTONES	29
3.7 ANDESITES	29
3.7.1 Andesite Breccias	30
3.7.2 Interpretation for andesites	31
3.8 DOLERITE	31
3.9 LOCAL STRUCTURE	33
3.10 STRATIGRAPHIC CROSS SECTIONS	33
3.11 SUMMARY	37

## **Chapter 4 Alteration**

4.1 INTRODUCTION	39
4.2 ALTERATION PETROGRAPHY	39
4.2.1 Silica alteration	39
4.2.2 Silica-sericite	40
4.2.3 Chlorite alteration	41
4.2.4 Fuchsite alteration	42
4.2.5 Silica-albite alteration	42
4.2.6 Potassic alteration	44
4.2.7 Epidote alteration	44
4.3 PARAGENESIS	44
4.4 ZONATION	46
4.5 DISCUSSION	48
4.5.1 VHMS related alteration	48
4.5.2 K-feldspar alteration	50
4.5.3 Epidote	51
4.6 SUMMARY	51

## **Chapter 5 Geochemistry**

5.1 INTRODUCTION	52
5.1.1 Analytical methods	53
5.2 RESULTS	53
5.2.1 Introduction	53
5.2.1.1 High Point results	53
5.2.1.2 Results from Que-Hellyer Volcanics	57
5.3 GEOCHEMICAL CLASSIFICATION OF VOLCANICS	59
5.4 IMMOBILE ELEMENT GEOCHEMISTRY	59
5.5 COMPARISON WITH QUE-HELLYER VOLCANICS	63
5.6 GEOCHEMICAL COMPARISON OF DOLERITES	64
5.7 ALTERATION INDICES	67
5.8 SUMMARY	68

## **Chapter 6 Mineralisation**

6.1 INTRODUCTION	69
6.2 VEIN ASSEMBLAGES	69
6.2.1 Comparison with stringer veins at Hellyer	71
6.3 MINERALOGY	72
6.3.1 Sphalerite	72
6.3.2 Galena	73
6.3.3 Chalcopyrite	73
6.3.4 Pyrite	74
6.3.5 Pyrrhotite	74
6.4 MINERAL PARAGENESIS	74
6.5 ZINC RATIO	77
6.6 METAL ZONATION	78
6.6.1 Depth zonation	80
6.6.2 Lateral zonation	83
6.7 LEAD ISOTOPES	83
6.8 DISCUSSION	85
6.9 SUMMARY	88

<b>Chapter 7.</b>	<b>Genetic Models</b>	
<b>Chapter 8.</b>	<b>Summary and Conclusions</b>	<b>89</b>
<b>References</b>		<b>93</b>
<b>Appendix 1:</b>	<b>Descriptive Logs</b>	
<b>Appendix 2:</b>	<b>Geochemical data</b>	
<b>Appendix 3:</b>	<b>Rock catalogue</b>	



## List of Figures

Figure	Page
1.1 Location map of the Mount Charter-High Point area in relation to Tasmania	1
1.2 Location of High Point in relation to the Que-Hellyer Volcanics	2
1.3 Location of the six main drill holes and the initial B.H.P. holes	3
2.1 Geology of the Mount Read Volcanics	7
2.2 Stratigraphic relationships between the major units of the M.R.V.	8
2.3 Stratigraphic relationships between the units of the Mount Charter Group	10
2.4 Schematic cross-section through the Que-Hellyer volcanics	12
2.5 Schematic cross section through the Hellyer orebody	14
2.6 Schematic cross section through the Que River deposit	16
3.1 Graphic log of MC 14	22
3.2 Graphic log of MAC 27	23
3.3 Graphic log of MC 13	23
3.4 Graphic log of MC 12	23
3.5 Graphic log of MAC 33	24
3.6 Graphic log of MAC 35	24
3.7 Location of cross section positions for High Point area	34
3.8 NE-SW schematic cross section for the High Point area	35
3.9 NNW-SSE schematic cross section for the High Point area.	36
4.1 Genesis of silica-sericite alteration rims around andesite clasts	41
4.2 Overprinting relationships of alteration at High Point	45
4.3 Paragenetic sequence of alteration assemblages	46
4.4 Downhole zonation of alteration	47
4.5 Zonation of major alteration at Hellyer	49
5.1 Graph of Cr versus Ti/Zr	60
5.2 Graph of Cr*P <sub>2</sub> O <sub>5</sub> versus Ti/Zr	60
5.3 Graph of P <sub>2</sub> O <sub>5</sub> versus Ti/Zr	60
5.4 Graph of Ti/Zr versus SiO <sub>2</sub>	62
5.5 Graph of Nb versus Y	62
5.6 Graph of Nb versus Zr	62
5.7 Graph of Al <sub>2</sub> O <sub>3</sub> versus Zr	63
5.8 Graph of P <sub>2</sub> O <sub>5</sub> versus Zr	63
5.9 Graph of TiO <sub>2</sub> versus SiO <sub>2</sub>	65
5.10 Graph of Ti/Zr versus SiO <sub>2</sub>	65
5.11 Graph of P <sub>2</sub> O <sub>5</sub> /TiO <sub>2</sub> versus SiO <sub>2</sub>	65
5.12 Graph of Cr*P <sub>2</sub> O <sub>5</sub> versus Ti/Zr	66
5.13 Graph of Cr versus Ti/Zr	66
5.14 Graph of P <sub>2</sub> O <sub>5</sub> versus Ti/Zr	66
5.15 Comparison of High Point alteration indices with Hellyer	67

6.1 Cartoon of cross-cutting vein relationships at High Point	71
6.2 Mineral paragenesis with superimposed vein stages	75
6.3 Zinc ratios for western Tasmania sulphide deposits	77
6.4 Zinc ratio for MAC 33	79
6.5 Zinc ratio for MAC 27	79
6.6 Zinc ratio for MAC 35	79
6.7 Zinc ratio for MC 14	80
6.8 Zinc ratio for all holes (combined data)	80
6.9 Down hole zonation of zinc grades for the NE-SW cross-section	81
6.10 Down hole zonation of zinc grades for the NW-SE cross-section	82
6.11 Lateral zonation of zinc grades in the High Point area	84
6.12 Lead isotopes signatures for High Point sphalerite	86
7.1 Genetic model for the formation of the High Point Stratigraphy	90
7.1 A). Basement (Animal Creek Greywacke)	90
7.1 B). Dacite lavas and hyaloclastites	90
7.1 C). Intrusion and extrusion of coherent basalts and basalt breccias	91
7.1 D). Deposition of the Que River Shale	91
7.1 E). Emplacement of andesite dykes and sills, Cambrian mineralisation	91
7.1 F). Intrusion of dolerite	92
7.1 G). Devonian metamorphism, and vein formation	92

---

## List of Tables

---

<b>Table</b>	<b>Page</b>
3.1 Modified Udden-Wentworth scale for classification of Sediments	19
3.2 Classification scheme for volcanic rocks (Compton, 1985)	20
5.1 Selected geochemical data from Mac 33	54
5.2 Selected geochemical data from Mac 35	55
5.3 Selected geochemical data	56
5.4 Que-Hellyer Volcanics geochemical data (basalts and andesites)	57
5.5 Que-Hellyer Volcanics geochemical data (dacites, dolerites)	58
5.6 Major element mobility in common rock types during hydrothermal activity	61
6.1 High Point lead isotope data	85

---

## List of Plates

---

Plate		Page
1	A/ Well preserved feldspar-phyric dacite lava with minor silica-sericite alteration, minor hematite dusting (Mac 35, 910m). B/ As above with Fe staining (Mac 33, 504 m).	27
2	Thin section of Plate 13 A. Well preserved plagioclase feldspars within a plagioclase-quartz groundmass (mag. x 25).	27
3	A/ Massive to weakly amygdaloidal basalt lava. Amygdales are infilled with mainly polygonal quartz. B/ Amygdaloidal, augite $\pm$ olivine-phyric basalt lava. Amygdales are cigar-shaped and 0.5 cm in length.	27
4	Thin section of amygdaloidal, augite $\pm$ olivine-phyric basalt lava (ppl, mag 25 x).	27
5	Cross polar view of plate 6, showing augite clusters and rare olivine phenocrysts (mag 25 x).	27
6	Rare resorbed quartz within a massive to weakly amygdaloidal basalt lava.	27
7	A/ Basalt lava showing the variability of the vesicularity. The vesicularity increases up hole (to right ). This section has carbonate-silica veins and silica veins cross-cutting the original lithology. B/ Basalt lava displaying the variable nature of vesicle size and intensity. Generally vesicle size, the intensity increases marginally for this sample (samples from Mac 35 between 600 and 610m).	27
8	A/ Monomict basalt lava derived from a poorly augite-phyric basalt. Polymict appearance is due to variable types and intensities of alteration.(Mac 33, 252m). B/ Dacitic hyaloclastite derived from a plagioclase-phyric dacite lava (Mac 33, 625.5m).	27
9	A/ Massive, black Que River Shale that is cut by pyrite-silica veins and silica-carbonate veins (Mac 27, 644.9). B/ Finely laminated volcanoclastic horizon in the Que River Shale. The white layer is composed of broken quartz and feldspar phenocrysts, small pyritic clasts are also visible. (MC 13, 260.1 m).	32
10	Thin section of the massive shale unit. Broken quartz phenocrysts (white) are set within a fine grained sediment matrix. Cross-cutting the section is a quartz-carbonate vein.	32

- |    |   |    |
|----|---|----|
| 11 | A/ Laminated volcanoclastic-andesite ash layer containing broken feldspar phenocrysts, pyrite clasts and a thin layer of Que River Shale (MC 13, 252.7 m) (Left is down hole). B/ Massive to laminated siltstone with minor pyrite clasts and quartz-carbonate veins (MC 13, 255.4 m).  | 32 |
| 12 | Thin section of laminated siltstone. Minor laminations can be partly seen to onlap a chloritically altered clast (mag 25x)  | 32 |
| 13 | A/ Chloritically altered, weakly feldspar-phyric andesite lava. Original mafic minerals have been replaced by a later stage chlorite alteration (Mac 33, 676m). B) Massive to weakly feldspar phyric andesite lava with regional prehnite-pumpellyite overprint.  | 32 |
| 14 | Chloritically altered andesite lava. Chlorite occurs as olive green patches on the original mafic phenocrysts. Other minerals include chromites (opaque) and plagioclase (brownish),(mag 25 x).   | 32 |
| 15 | A/ An aphyric-andesite lava that appears to have some hydrofracturing cross cutting the lithology (Mac 35, 780m). B/.Perlitically (?) cracked dacite to andesite lava (Mac 33, 524m).   | 32 |
| 16 | A/ Matrix supported monomict andesite breccia. The matrix has been overprinted by silica-sericite alteration (MC 14, 345 m). B/ Clast supported hydrofractured andesite breccia with infilling carbonate matrix. Andesite clasts are predominantly weakly feldspar-phyric. (Mac 35, 234.3m).  | 32 |
| 17 | A/ Silicified and sericitised andesite-mudstone peperite. The matrix of the peperite has been silicified. Clasts within the peperite have either silica-sericite rims or are totally altered by silica-sericite. B/ Silica-sericite and chlorite alteration of a basaltic peperite.   | 43 |
| 18 | A/ Light grey-white silica vein cross-cutting an andesite lava with smaller early stage veins.  | 43 |
| 19 | A/ Pseudo-fragmental appearance of silica-sericite alteration with an andesite lava. Minor chalcopyrite is visible within the alteration. B/ Pervasive silica-sericite-pyrite alteration texture.   | 43 |
| 20 | A/ Chlorite alteration of clasts within what was originally a peperite. The chlorite varies from dark green to light green. The matrix of the peperite has been altered by an early stage of silica alteration. B/ Light green disseminated fuchsite spots are within a lemon coloured sericite, which has been cross-cut by a carbonate-silica vein. | 43 |
| 21 | A/ Massive fuchsite alteration of basaltic lava with minor fine grained galena. B/ A relatively unaltered basalt lava.  | 43 |
| 22 | Silica-albite alteration with hematite dusting that is overprinting an earlier chlorite alteration (Mac 33, 364m-366m).   | 43 |
| 23 | A/ Potassic alteration of amygdaloides in an amygdaloidal basalt (Mac 35, 288.4m). B/ Carbonate hydrofracturing of andesite (Mac 35, 207).  | 43 |

24	A/ Complex alteration pattern of a basaltic peperite. The main features are the late stage cross-cutting epidote vein, the different colours of chlorite and the K-feldspar alteration of: the amygdales (Mac 35, 295.5 m). B/ (Bottom) Potassic alteration in the base of MC 13 (310m).	43
25	Cambrian mineralisation (Both A and B) The disseminated light brown mineral within the silica-sericite alteration (A) and disseminated throughout the basalt (B) is sphalerite and is associated with or without galena (Sp= Sphalerite and Gn= Galena).(Mac 33, 254 m) (MC 14, 171.0 m).	76
26	Disseminated Cambrian style mineralisation (Plate 25 B), showing fine grained anhedral sphalerite.	76
27	Polished slab of basalt showing sphalerite (light grey colour), minor pyrite (bright white; ppl, mag 50x).	76
28	Coarse grained sphalerite in Devonian quartz-carbonate veins. The sphalerite is subhedral and coarser grained than the Cambrian sphalerite (Plate 25).	76
29	Reflected light view of the coarser-grained sphalerite displaying chalcopyrite disease. Galena and minor pyrite are also associated with this form of sphalerite.	76
30	Chalcopyrite veins infilling tension gashes.	76
31	Reflected light view of the chalcopyrite tension gash infill. The chalcopyrite also has minor pyrrhotite and sphalerite (mag 25x).	76
32	A/ Carbonate-pyrrhotite vein cutting through shale (Mac 27, 729m; Po= pyrrhotite). B/ Interpillow pyrite at the margins of andesite and shale. Minor K-feldspar occurs at the edges of the andesite clast.	76

---

# Chapter 1

## Introduction

---

### 1.1 STUDY AREA

The High Point study area is located approximately 6 km south southwest of the old Que River mine site and 10 km southwest of the Hellyer mine, and is part of an exploration lease held by Aberfoyle Resources exploration division ( Fig. 1.1-1.2). The area, situated on the northern slopes of Mount Charter, is covered in dense myrtle rainforest and button grass plains forming part of an undulating plateau, that extends from the Hellyer mine area to Mount Charter (Komyshan, 1986). Access to the area can be gained via tracks constructed by logging contractors and mining companies which are now partially or totally overgrown. The dense nature of the vegetation and high rainfall allows only 10-15% of highly weathered outcrop to be visible.

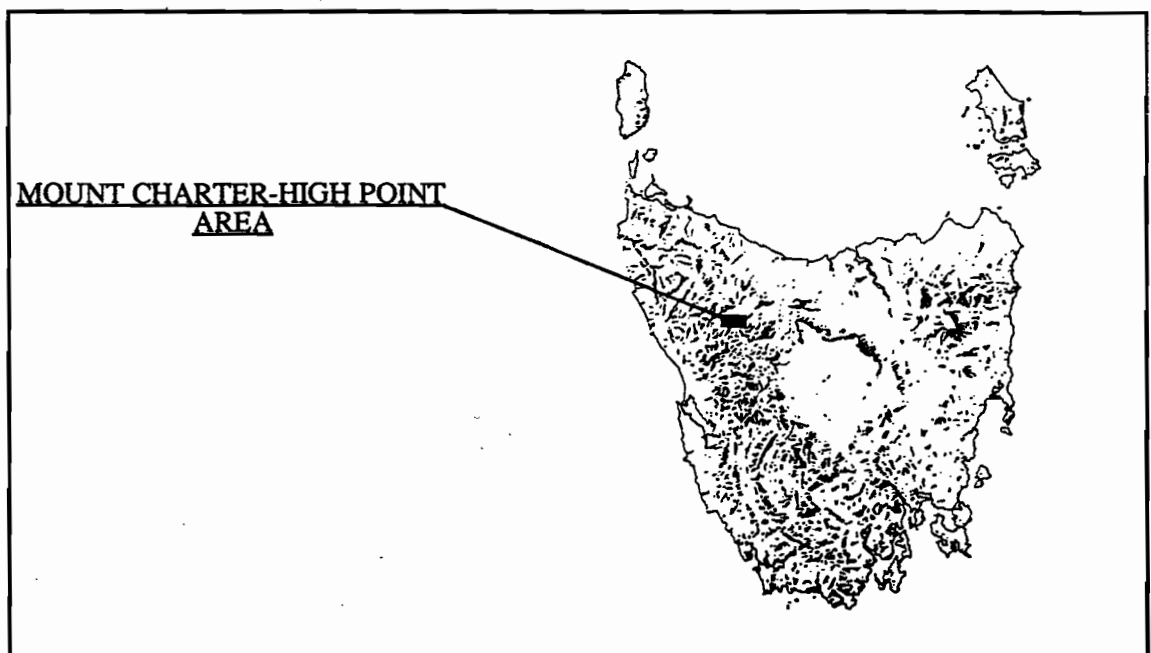


Figure 1.1: Location map of the Mount Charter-High Point area in relation to Tasmania.

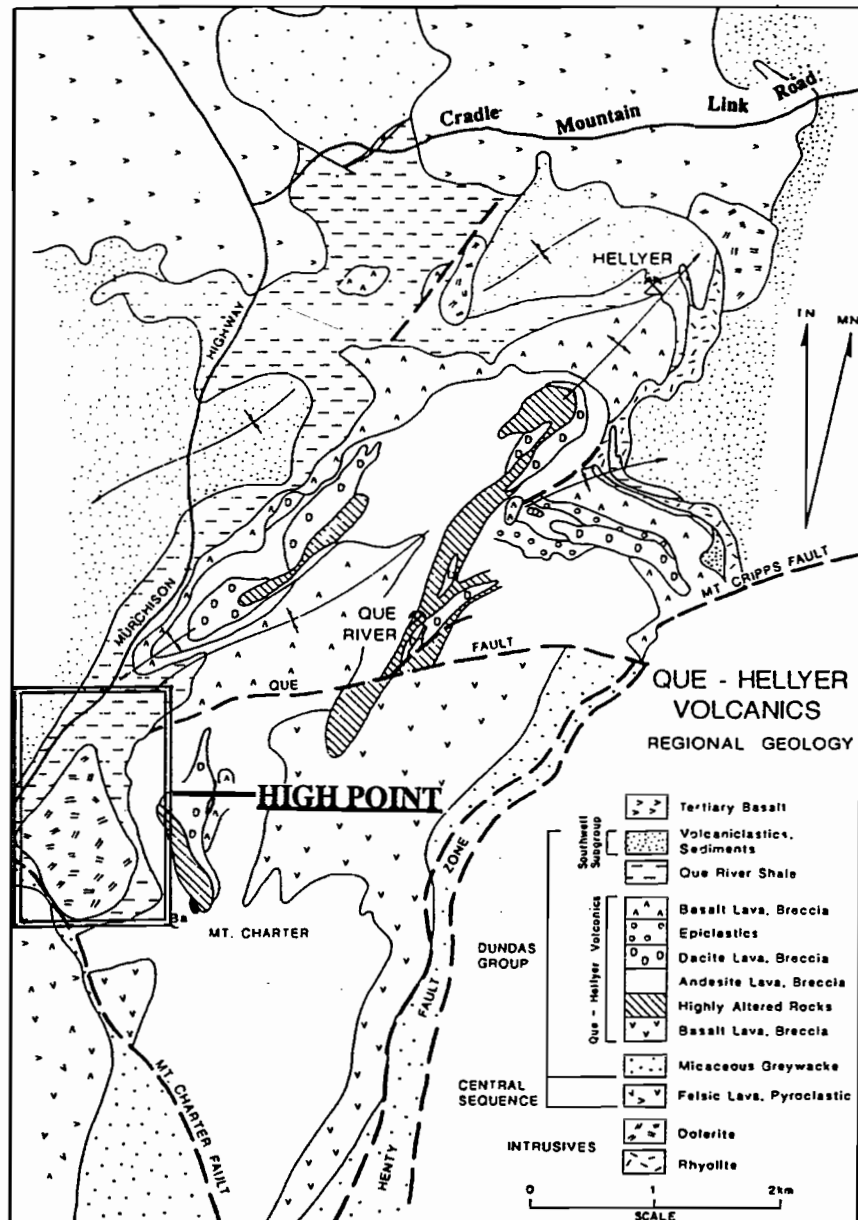


Figure 1.2: Location of High Point in relation to the Que-Hellyer Volcanics.

## 1.2 EXPLORATION HISTORY

High Point has been subject to intense exploration over several decades, with several companies still actively exploring in the immediate area including Aberfoyle exploration and Pasminco exploration. Exploration licence 5/63 was originally granted to Mt Costigan Mines Ltd. in 1963 and transferred to Comstaff Pl in 1964 (Anon, 1988). The tenement originally covered 4947 km<sup>2</sup>, but as a result of compulsory relinquishment, the tenement was reduced to only 32 km<sup>2</sup>. Sections of this ground were acquired by Aberfoyle Resources as part of an exploration program conducted in an attempt to find world class VHMS deposits similar to



Hellyer and Que River. Aberfoyle holds the ground on the eastern side of the Murchison highway, almost directly opposite the localities for the original High Point exploration conducted by Comstaff PL. Since the initial mapping and soil sampling programs, over 30 drill holes have been collared within a four kilometre radius. These were designed to test both the Mount Charter barite mineralisation and the High Point mineralisation. Of these holes, only ten are of relevance to the current study. This study will focus on information gathered from drill holes Mackintosh 27, Mackintosh 33, Mackintosh 35, (abbreviated Mac 27, 33 and 35), Mount Charter 12, Mount Charter 13, Mount Charter 14, (Abbreviated MC 12, MC 13 and MC 14) (Fig. 1.3). The initial intersection holes drilled by B.H.P. (HP 1-HP 4) will also be reviewed along with the six Aberfoyle holes.

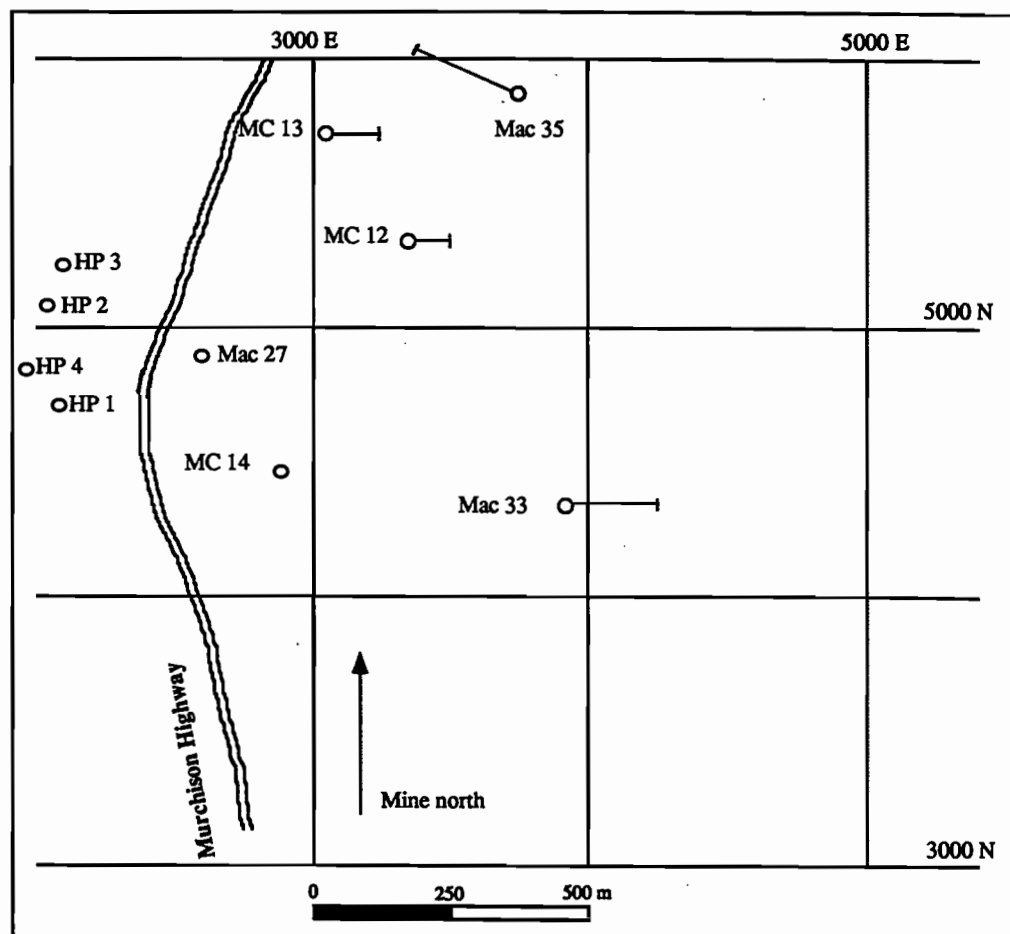


Figure 1.3: Location of the six main drill holes and the initial B.H.P. holes.

### **1.3 PREVIOUS WORK**

Previous work on the High Point region is limited. Comstaff and BHP submitted annual reports to Tasmanian Development and Resources - formerly known as the Tasmanian Department of Mines (eg Anon., 1988; Wilde and Kerr, 1989). The Tasmanian Department of Mines released a geological map of the area in 1966 as part of its regional mapping program. This map was updated in 1986 by Komysan with explanatory notes (Corbett and Komysan, 1989). Several reports have been produced by contract geologists and geophysicists, for example Crawford (1989) and Leaman (1990). The most recent work on the High Point mineralisation was by Barwick (1991). Barwick (1991) primarily focussed on the stratigraphy with reference to the disseminated sulphide mineralisation in drill core from HP 1, HP 2, HP 3 and HP 4.

### **1.4 AIMS**

There are five main aspects of the High Point prospect to be investigated, which in order of priority, are:

- 1/ To identify the main styles and types of mineralisation;
- 2/ To determine a possible heat source for the mineralisation;
- 3/ To characterise, both the host rocks for the mineralisation and other lithologies within the study area, using logging techniques, thin sections and geochemistry; and
- 4/ To develop genetic models for the mineralisation and the lithologies in an attempt to locate a possible ore body, leading to further exploration in the area.

### **1.5 METHODS**

Field work began in December 1994 and continued until early January 1995. During this six week period drill holes Mac 27, 33, 25, MC 12, 13 and 14 were logged at the Aberfoyle exploration core shed at the Hellyer mine site (where the holes are currently housed).

A further three days were spent at the Tasmanian Development and Resources core shed at Mornington, logging Holes HP 1-HP 4.

A sample suite of 20 rocks were selected for analysis at Analabs for both major and trace elements (Ti, Nb, Y, Rb, Sr, Cr, Pb, Zn, Cu and Ba). When choosing samples for analysis, care was taken to select the least altered samples in an attempt to avoid erroneous results. To aid with the interpretation of the geochemical data and hand sample description, thin sections were prepared from these samples and from other representative rock types. Polished thin sections and slabs were also prepared to examine the nature of the sulphide mineralisation i.e., mineralogy, relationships and paragenesis.

---

## Chapter 2

### Regional Geology

---

#### 2.1 INTRODUCTION

The Mount Read Volcanics (Campana and King, 1963) are an arcuate belt of predominantly calc-alkaline volcanics that are approximately 20 km wide and 200 km long. The Mount Read belt extends from Elliott Bay on the South west coast of Tasmania, through Queenstown, Rosebery and the Hellyer area to near Deloraine in the north (Campana and King, 1963; Corbett and Komyshan, 1989 ; Fig. 2.1). The volcanic sequence hosts five major VHMS base metal ore bodies (Mount Lyell, Rosebery, Hercules, Que River and Hellyer) as well as many other smaller prospects (Corbett, 1981; Corbett and Solomon, 1989).

#### 2.2 MOUNT READ VOLCANICS STRATIGRAPHY

The Mount Read Volcanics can be classified into seven major lithologic associations; several can be defined in stratigraphic positions and these are defined below:

1. The Sticht Range Beds form a basal clastic unit that overlies the Precambrian basement (Corbett, 1992).
2. Overlying the Sticht Range Beds to the east and north of Mount Murchison is a belt of quartz-phyric volcanics, intrusives and volcanoclastics with minor bedded sandstones, siltstones and shard rich mudstone (McNeill and Corbett, 1989). These rock types form the Eastern Quartz-phyric sequence. To the northwest of Mount Murchison the sequence is overlain by the Farrell Slates and interfingers with the Central Volcanic Complex (Corbett, 1992).

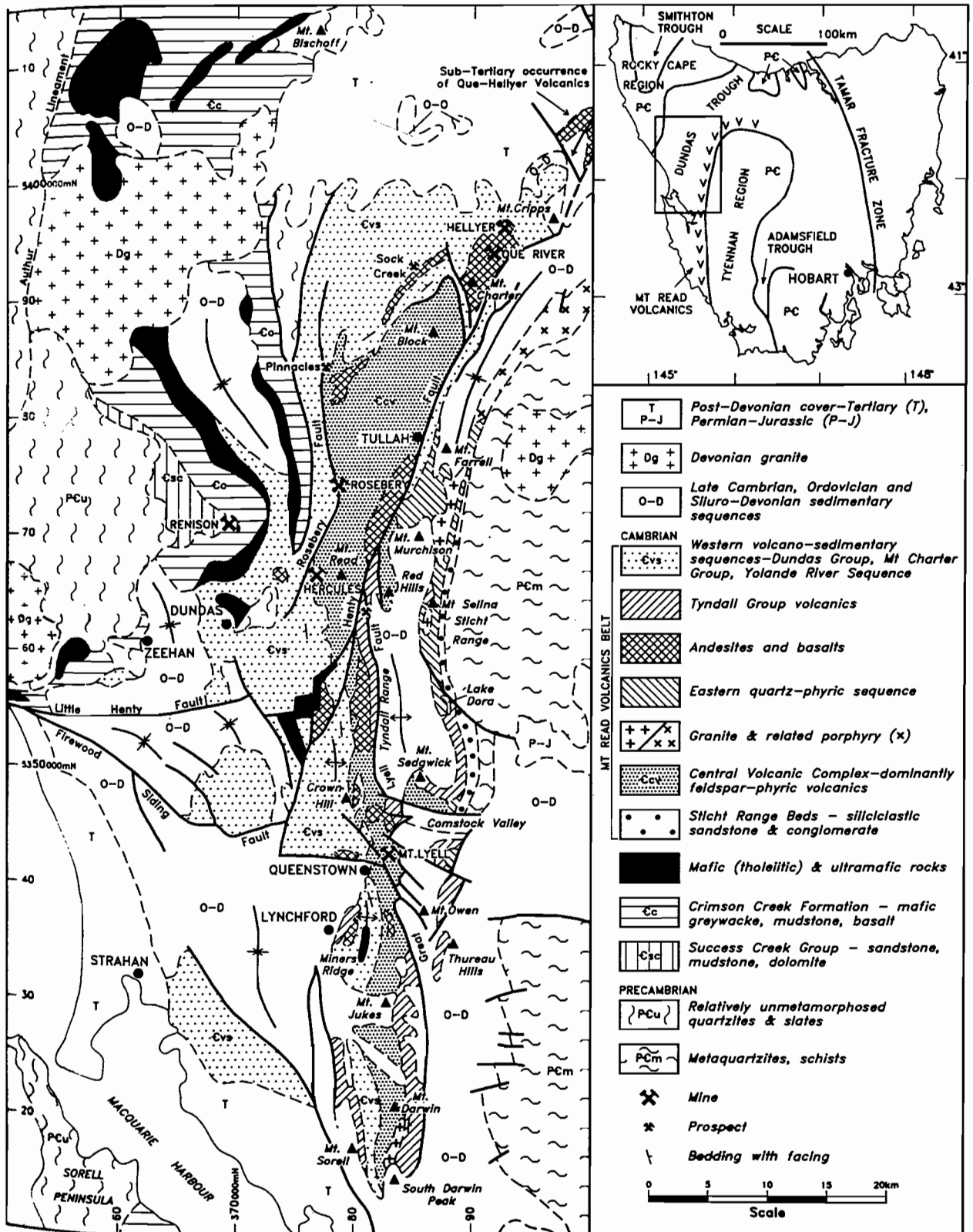


Figure 2.1: Geology of the Mount Read Volcanics (After Corbett, 1992)

3. Extending from Mount Darwin through Queenstown to Red Hills is a belt of predominantly feldspar-phyric lava-rich volcanics which has an interfingering relationship with most other units (Corbett, 1992). This belt is termed the Central Volcanic Complex. Other units within the Central Volcanic Complex include ignimbrites and rare bedded sedimentary units (Corbett, 1992) and significant andesites in the Queenstown and Tyndall range area (Crawford *et al.*, 1992 ; Fig. 2.1).

4. The Tyndall Group was recognised and defined as the unit that overlies the Central Volcanic Complex, the Eastern Quartz-phyric Sequence and the Yolande River Sequence (Fig. 2.2).

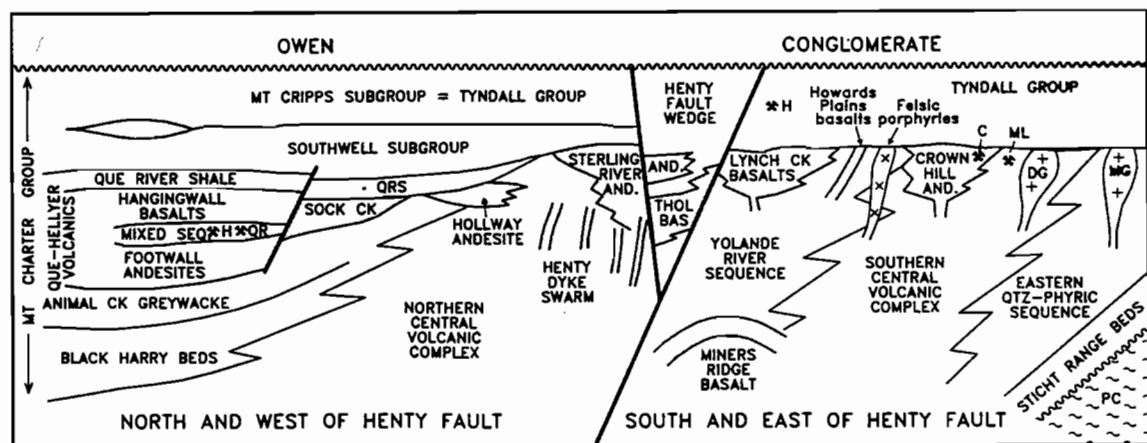


Figure 2.2: Stratigraphic relationships between the major units of the Mount Read Volcanics  
(After Crawford *et al.*, 1992).

The Tyndall Group are the youngest volcanics in the Mount Read belt (Pemberton *et al.*, 1991). This group is predominantly composed of volcanoclastics (including mass-flow breccias, sandstones and volcanolithic conglomerates) with minor quartz-feldspar-porphyrific rhyolitic-dacitic lavas and eroded blocks of the Darwin Granite (Corbett, 1992). The group extends northward from Queenstown along the Tyndall Range to Red Hills (Fig. 2.1), where rhyolite and minor andesite are interbedded in the lower part (Corbett, 1992).

5. Andesitic-basaltic lavas and associated intrusions of calc-alkaline compositions have been recognised to occur as separate lenses and masses within or between other

lithostratigraphic associations (Corbett, 1992). These rocks typically consist of interbedded flows and breccias, with minor pillow lavas and have a distinct geochemical signature (Crawford *et al.*, 1992).

6. Tholeiitic rocks occurring within the Mount Read Volcanics are also considered to be part of the major lithological units and include the Miners Ridge Basalt, Henty dyke swarm (basalt, dolerite, and gabbroic dykes) and the Henty fault wedge basalts (mainly porphyritic basalts and andesites that are tholeiitic in composition; Corbett, 1992).

7. The western volcano-sedimentary sequence comprises four major sub-units according to their position in relation to the Henty Fault system.

*Yolande River sequence:* The Yolande River sequence lies to the south of the Henty Fault system where it is folded about a major anticline. It has a tholeiitic basalt at its base in the core of the anticline and includes andesitic-basaltic sequences of the Lynch creek basalts (Corbett, 1992)

*Dundas Group:* The Dundas Group refers to the Cambrian rocks which flank the Mount Read Volcanics (Campana and King, 1963). The sequence lies to the north of the Henty Fault wedge, between the township of Dundas and the Hercules mine, to the Pinnacles area in the north (Crawford *et al.*, 1992; Fig. 2.1). Rock types include felsic tuffs, altered mafic-ultramafic bodies, conglomerates, sandstones, siltstones and shales (Crawford *et al.*, 1992; Corbett, 1992).

*Henty fault wedge sequence:* Refers to a complex sequence of sedimentary, volcanic and igneous rocks. The eastern section of the sequence is dominated by interbedded volcanolithic greywacke, siltstone and mudstone and minor felsic volcanoclastics, conglomerates and carbonates (Corbett, 1992). To the west the unit passes into a package of pyroxene-porphyritic calc-alkaline andesite lavas and breccias intruded by basalt and dolerite dykes, juxtaposed against serpentinised ultramafic rocks at the North Henty fault (Corbett, 1992; Fig. 2.2).

**Mt Charter Group:** Refers to the volcano-sedimentary sequence that contains the andesite and basalt hosts to the Que River and Hellyer massive sulphide deposits (Corbett, 1992). The group contains 7 main units (Fig. 2.3) which conformably overlie the Central Volcanic Complex and underlie the Owen Conglomerate (Corbett, 1992). The Que-Hellyer Volcanics is one such unit and is of interest as it hosts the Que River and Hellyer ore deposits. The Que Hellyer Volcanics are the main focus of this study.

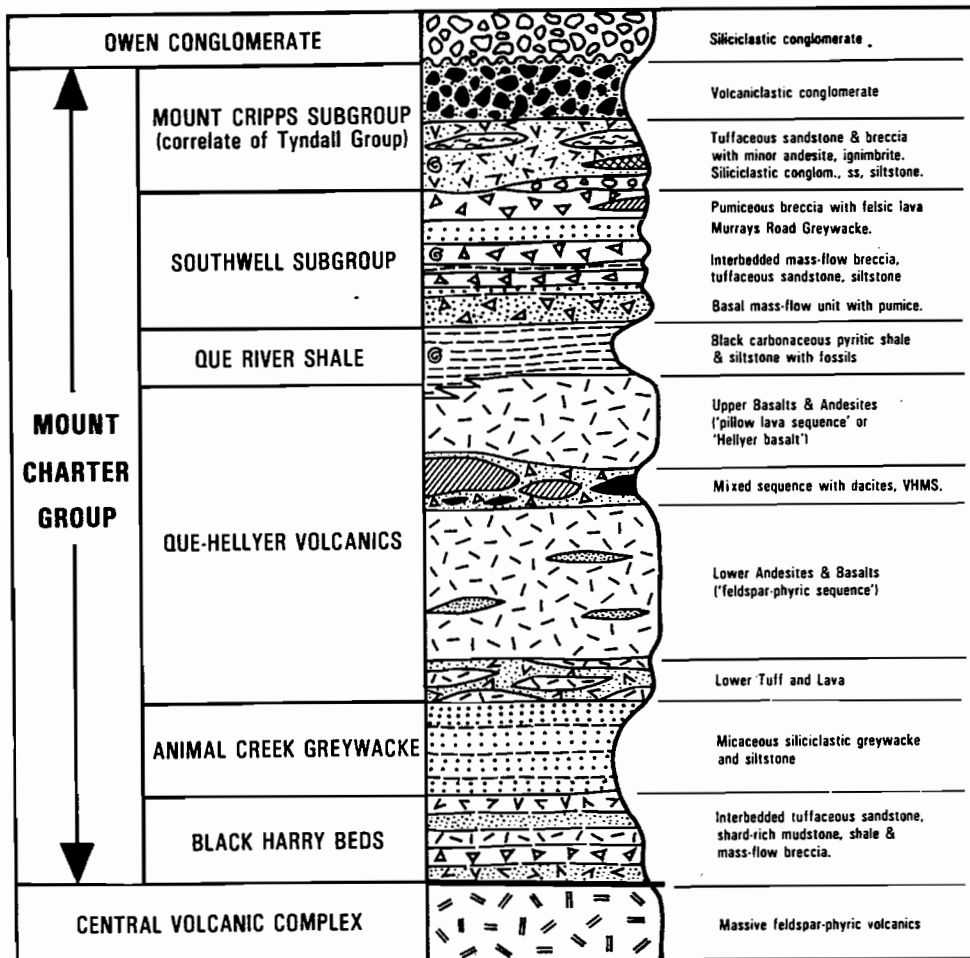


Figure 2.3: Relationships of the major units within the Mount Charter Group (After Corbett, 1992)

## 2.3 ANIMAL CREEK GREYWACKE

As redefined by Pemberton *et al.* (1991), the Animal Creek Greywacke comprises some 300 m of well-bedded grey micaceous siliciclastic sandstone interbedded with grey-black siltstone and shale. Other minor components of the sequence include tuffaceous sandstone,



shard rich mudstone and volcanoclastic breccias. A two fold subdivision into a lower tuffaceous part and an upper micaceous part is possible in regions between the Murchison highway and Sock Creek and East of Mount Block (Corbett and Komysan, 1989). The unit is found to underlie the Que-Hellyer Volcanics east of the Que River mine near the Henty fault zone (Corbett and Komysan, 1989).

## 2.4 QUE-HELLYER VOLCANICS

The Que-Hellyer Volcanics have been informally subdivided into four units. The basal unit of the volcanics is known as the lower basalt and conformably overlies and interfingers with the Animal Creek Greywacke (Fig. 2.4). The thickness of the lower basalt is highly variable and ranges up to a maximum of 100 m. At its thickest, this lower basalt sub unit consists of massive to pillowed porphyritic basaltic lavas, hyaloclastites, and minor thin, medium to coarse grained volcanic sandstones. The presence of the volcanic sandstone horizon has led to the interpretation that the lower basalt was formed through the rapid accumulation of volumetrically small eruptions (Waters and Wallace, 1992).

Conformably overlying the lower basalt unit is a 500 m thick horizon of predominantly andesitic to dacitic lavas, autoclastic breccias, and minor epiclastics, which comprise the lower andesites and basalts (Waters and Wallace, 1992). The lower andesites and basalts form the footwall sequence to mineralisation in the Que-Hellyer Volcanics (McArthur, 1986), and consist of a higher proportion of massive lavas that are up to 100 m thick at the top of the sequence to the south of the Que River deposit (Waters and Wallace, 1992).

The mixed or mine sequence hosts the Hellyer and Que River deposits and is a lithologically complex series of volcanics and volcanoclastics conformably overlying the lower andesites and basalts. On the immediate the ore deposits the unit reaches a maximum thickness of 100 to 150 m thick and is generally best developed in these regions. The mixed sequence can be further subdivided into the mixed sequence volcanoclastics and the mixed sequence dacites. The mixed sequence volcanoclastics are in excess of 20 m thick at Hellyer and thin laterally away from the mineralisation . In comparison the mixed sequence volcanoclastics at the Que

River deposit are in the order of 120 m thick and show a complex interfingering relationship with the dacitic lavas. The mixed sequence dacites consist of lava flows, domes and autoclastic breccias and occur toward the top of the mixed sequence (Waters and Wallace, 1992).

The uppermost unit in the Que-Hellyer Volcanics, the Hellyer basalt, consists of pillowed to massive basalt lavas, hyaloclastites, peperites, and minor interbedded fine grained sediments which are up to 220 m thick (Waters and Wallace, 1992). Toward the outer margins of the Que-Hellyer Volcanics the Hellyer basalt conformably overlies the lower andesites and basalts. In contrast the Hellyer basalt interfingers and conformably overlies the coarse volcanics and dacites in the vicinity of the ore bodies (Waters and Wallace, 1992).

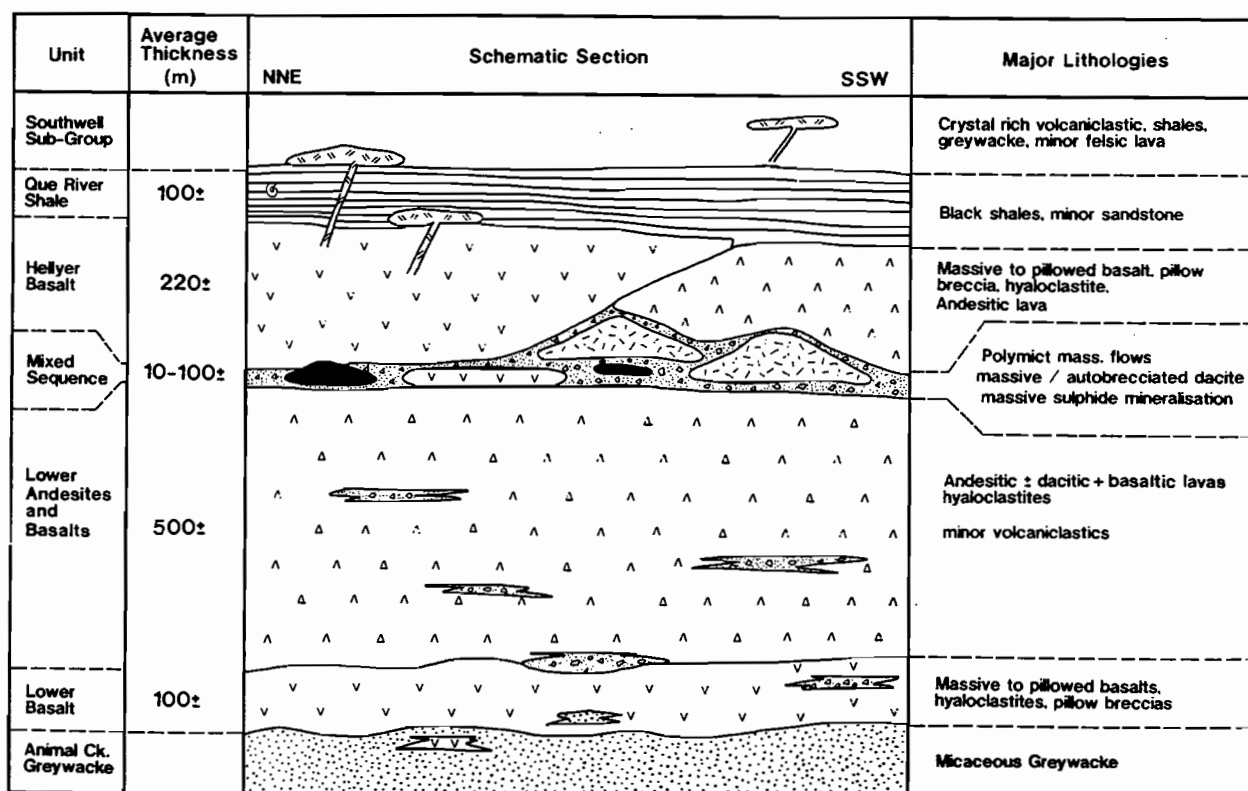


Figure 2.4: Schematic cross section through the Que-Hellyer Volcanics  
(After Waters and Wallace, 1992).

## 2.5 DEFORMATION AND METAMORPHISM

Deformation of the Mount Read Volcanics has occurred in two main phases-during the late Cambrian and during the Middle Devonian (Williams, 1989). The late Cambrian event is characterised by brittle failure and appear to follow similar trends to the Devonian deformation and a weak local cleavage development (Corbett and Lees, 1987). Devonian deformation initially produced an early north-north west-trending open fold stage. This initial phase was followed by a second phase of faulting and folding on west-north west to north west trends during the middle to late Devonian (Williams, 1978; Corbett and Lees, 1987).

Regional metamorphism of the Mount Read Volcanic belt occurred during the middle to late Devonian (Williams, 1989). A maximum grade of lower greenschist facies is evident around the Hercules and Rosebery mine sites in the middle to southern section of the Mount Read Volcanics. At the northern end of the Mount Reads, near Que River and Hellyer the local metamorphic grade has only reached prehnite-pumpellyite (Whitford *et al.*, 1982).

## 2.6 MAJOR ORE DEPOSITS

### 2.6.1 Hellyer

The Hellyer ore body is an elongate, faulted massive sulphide lens hosted within the Que-Hellyer Volcanics of the Mount Read Volcanics (Corbett, 1989). The host sequence to the body consist of the footwall Feldspar Phyric Sequence of massive lavas and volcanoclastics that are predominantly andesitic in composition (McArthur, 1986) (Fig. 2.5). Overlying the Feldspar Phyric Sequence is a thin package of interbedded poorly sorted volcanic breccias and a well sorted finely laminated ash unit termed the Hangingwall Volcaniclastic Sequence (Staff Aberfoyle Resources Limited, 1990). The finely sorted unit onlaps the ore body, however, it is absent where the sulphide obtains it maximum thickness. The massive sulphide lens is directly overlain by the basalts of the Pillow Lava Sequence. These consist of pillowed and amygdaloidal basalt with minor pyritic chert, cherty shale or hyaloclastic interpillow margins (McArthur, 1989).

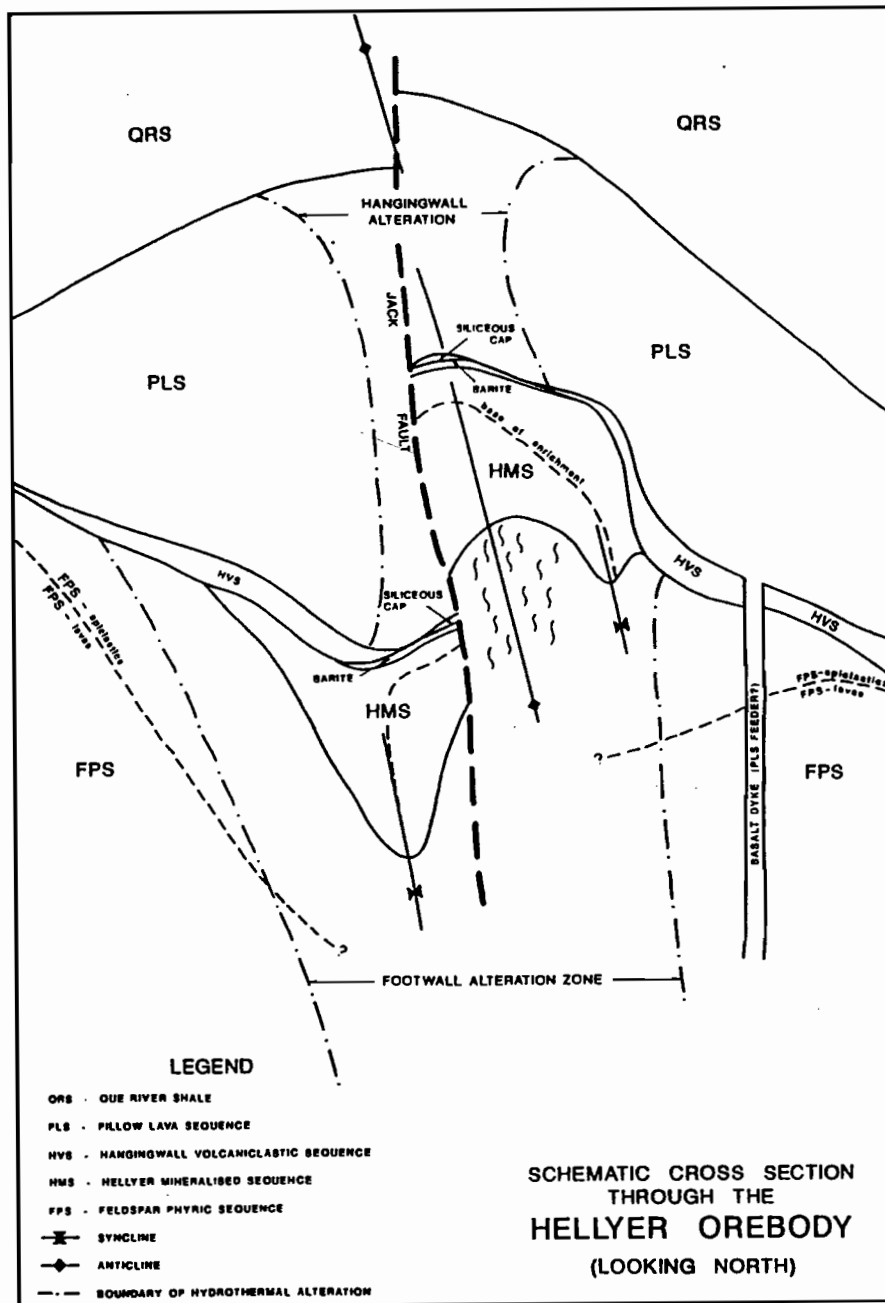


Figure 2.5: Stratigraphic cross section through the Hellyer massive sulphide deposit. (FPS= Feldspar Phyric Sequence, HVS= Hangingwall Volcaniclastic Sequence, PLS= Pillow Lava Sequence, HMS= Hellyer Mineralised Sequence and QRS= Que River Shale) (After Drown, 1990).

The Hellyer massive sulphide deposit is approximately 17 million metric tons of high grade polymetallic ore (13.0 % Zn, 6.8 % Pb, 0.3 % Cu, 160 g/t Ag and 2.3 g/t Au) (Gemmell and Large, 1992). The textures of the sulphide are diverse and are classified from McArthur (1989) as follows:

1/ Planar banded sulphides with alternating layers < 5mm thick of fine grained sphalerite/galena;

- 2/ Contorted and discontinuously banded sulphides as above, set in a generally massive fine grained pyrite/ sphalerite/ galena matrix;
- 3/ Massive featureless fine grained pyrite /sphalerite /galena locally with coarse grained sphalerite and or chalcopyrite gashes;
- 4/ Reworked fragmental ore with sub-rounded clasts to 10 mm diameter of varied textured sulphides set in a massive fine grained pyrite/ sphalerite/ galena matrix;
- 5/ Disseminated partially recrystallised pyrite/sphalerite/galena set in a sericite-rich matrix;
- 6/ Recrystallised and locally porous pyrite-rich ore with minor fine grained sphalerite/ galena;
- 7/ Irregular pyrite/ sphalerite/ galena/ tetrahedrite masses set in a dominant glassy quartz matrix;

Massive barite caps the orebody and is up to 15 m thick in places, whereas other places a silica cap occurs containing up to 40 % sulphide (Drown, 1990).

### 2.6.2 Que River

Que River, the second of the large VHMS deposits within the Que-Hellyer Volcanics, was discovered as the result of drilling a coincident electromagnetic and soil geochemistry anomaly. The oldest rocks in the Que River mine area are calc-alkaline andesite lavas and volcaniclastics (Fig. 2.6). Unaltered lithologies of this sequence occur as green, weakly altered breccias and volcaniclastics that consist of angular to sub-rounded clasts set in a fine-grained quartz chlorite matrix. Within the alteration zone, the lithologies consist of predominantly lapilli sized altered volcaniclastics that are andesitic in composition. Intercalated with the altered volcaniclastics are units of polymict volcaniclastics that are commonly associated with the ore lenses. Clasts of this unit are typically lapilli to ash sized, subrounded dacite and andesite with minor chert and other indeterminate lithologies (Wallace, 1989). A coarse polymict volcaniclastic unit immediately overlies the ore lenses. This consists of angular clasts of amygdaloidal basalt, dacite, and base metal sulphides set in a fuchsite carbonate matrix. The youngest unit in the local mine area is an elongate wedge of generally massive fawn to cream coloured dacite (Wallace, 1989).

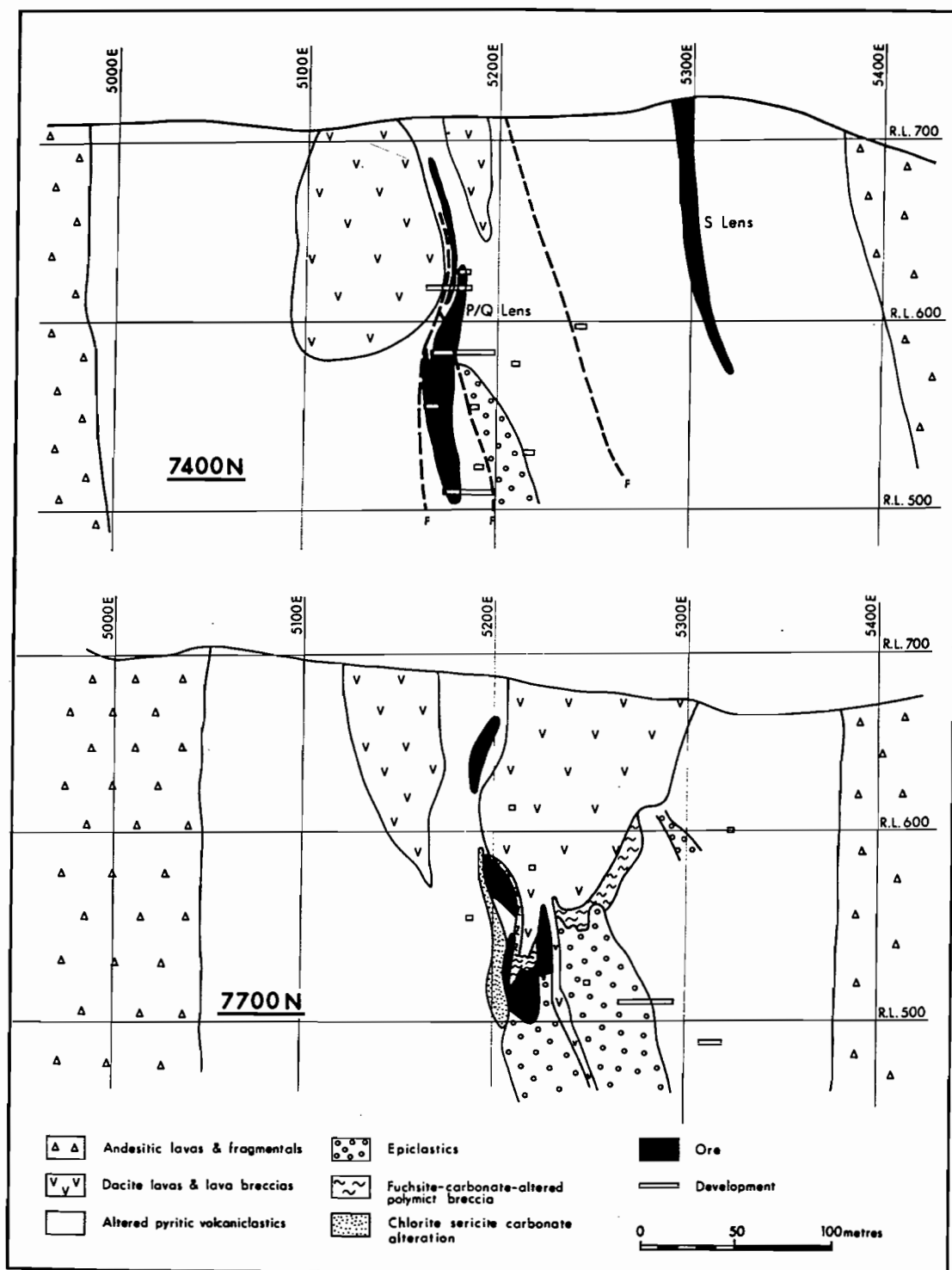


Figure 2.6: Cross sections of the Que River deposit at mine grid lines 7700 mN and 7400 mN.  
(After Wallace, 1989).

The Que River deposit was folded into a tight syncline, during the Devonian (Large and McGoldrick, 1986) and originally consisted of five lenses of mineralisation that were near vertical, sub parallel and stratabound orientations with north-north east strike (Wallace, 1989). Of the five lenses only three were economic to mine, PQ, S and P North. The largest of the economic lenses, PQ, consisted of approximately 30 % pyrite, 24 % sphalerite, 10 % galena and minor chalcopyrite and arsenopyrite (Waters and Wallace, 1992). S lens consisted of a northern, zinc rich zone (dominated by sphalerite, galena, and chalcopyrite) and a southern copper zone (mainly chalcopyrite and pyrite) (Waters and Wallace, 1992). The P North lens lays just to the west of the PQ lens and consisted of similar mineralogy to the main lens (Waters and Wallace, 1992). Sulphide textures of the PQ lens included:

- 1/ Disseminated ore - coarse recrystallised sulphides occur in a sericite  $\pm$  silica matrix that is common around the margins of the lens;
- 2/ Fragmental ore - consists of discrete clasts of base metal sulphides occurring with either a sericite matrix or a sphalerite, galena annealed sulphide matrix (Large *et al.*, 1987);
- 3/ Banded ore - layered and recrystallised sphalerite, galena and pyrite;

### **2.6.3 Mount Charter**

At the southern limits of the Que-Hellyer Volcanics sub-economic massive barite and sulphide mineralisation outcrops on the northern ridge of Mount Charter. The mineralisation is in a comparable stratigraphic position to the Que River and Hellyer deposits, having similar mineralisation to that of the precious metal zone at Que River. The ore minerals at Mount Charter include pyrite, sphalerite, tennantite, galena and minor chalcopyrite with very minor gold as electrum, proustite and tetrahedrite. Footwall rocks to the deposit include rhyodacite to dacite lavas, lava breccias and volcaniclastics, whereas the hangingwall is formed by the lower andesites and basalts of the Que-Hellyer volcanics (Rand, 1988).

---

## Chapter 3

### Stratigraphy

---

#### 3.1 INTRODUCTION

The stratigraphy of the High Point region has been described and interpreted from diamond drill holes Mac 27, 33, 35 and MC 12, 13, 14 (localities shown on Fig. 1.3). Graphic logs (Figs. 3.1-3.6) and descriptive logs (Appendix 1) are provided for each hole. Initial descriptions by Aberfoyle geologists of the igneous horizons identified them either as lavas or lava breccias. In this study the breccias are further subdivided into autobreccias, *insitu* hyaloclastites and resedimented hyaloclastites. Other units recognised during this study include dolerite, black shales, volcanoclastic sandstones and siltstones and epiclastic sands and siltstones. Lithologies observed in the High Point area are discussed in stratigraphic order from oldest to youngest due to the intimate associations between the units.

The main aims of this chapter are to:

- 1/ Provide detailed descriptions of the various lithologies based on hand samples and thin section petrography;
- 2/ Interpret the depositional setting for each unit; and
- 3/ Construct N.E.-S.W. and N.W.-S.E cross sections through the area.

##### 3.1.1 Classification of sedimentary lithologies

Classification of sedimentary rocks is based on a modified Udden-Wentworth scale (Table 3.1). The sedimentary lithologies in the High Point area range from coarse grained



sandstones to fine mudstones. Genetic names of the sediments were not used in the field but have been assigned in some cases after examination of thin sections.

		U.S. Standard sieve mesh	Millimeters	Phi ( $\phi$ ) units	Wentworth size class
GRAVEL			4096	-12	
			1024	-10	Boulder
			256	-8	
			64	-6	Cobble
			16	-4	
			4	-2	Pebble
	5	4	4	-2	
	6	3.36		-1.75	
	7	2.83		-1.5	Granule
	8	2.38		-1.25	
SAND	10	2.00	2	-1.0	
	12	1.68		-0.75	
	14	1.41		-0.5	Very coarse sand
	16	1.19		-0.25	
	18	1.00	1	0.0	
	20	0.84		0.25	
	25	0.71		0.5	Coarse sand
	30	0.59		0.75	
	35	0.50	1/2	1.0	
	40	0.42		1.25	
	45	0.35		1.5	Medium sand
	50	0.30		1.75	
	60	0.25	1/4	2.0	
	70	0.210		2.25	
	80	0.177		2.5	Fine sand
	100	0.149		2.75	
	120	0.125	1/8	3.0	
	140	0.105		3.25	
	170	0.088		3.5	Very fine sand
	200	0.074		3.75	
MUD	230	0.0625	1/16	4.0	
	270	0.053		4.25	
	325	0.044		4.5	Coarse silt
		0.037		4.75	
		0.031	1/32	5.0	
		0.0156	1/64	6.0	Medium silt
		0.0078	1/128	7.0	Fine silt
		0.0039	1/256	8.0	Very fine silt
		0.0020		9.0	
		0.00098		10.0	Clay
CLAY		0.00049		11.0	
		0.00024		12.0	
		0.00012		13.0	
		0.00006		14.0	

Table 3.1: Modified Udden-Wentworth scale showing the classification of sediments based upon grain size.

(After Boggs, 1987).

### 3.1.2 Classification of volcanics

Classification of the volcanic units logged during the field work has been based on thin section and hand sample petrography and using compositional classification methods. The

classification scheme of Compton (1985), which is based on phenocryst assemblage (Table 3.2), has been used in preference to Ewarts (1982) classification which is based upon chemical composition. Ewarts scheme was not used because the units in the High Point area are variably altered and compositional changes have undoubtedly occurred since deposition.

Rocks with quartz	Alkali feldspar : plagioclase ratio typically > 1:2; biotite or pyroxene generally < 5%	RHYOLITE
	Alkali feldspar : plagioclase ratio < 1:2 and alkali feldspar commonly absent; quartz may be scarce; hornblende, pyroxene, and biotite all likely	DACITE
Rocks without quartz, feldspathoids, melilite, or analcite	Alkali feldspar : plagioclase ratio > 4:1; biotite or pyroxene ± scarce olivine	TRACHYTE
	Alkali feldspar : plagioclase ratio < 4:1; hornblende, biotite, or pyroxene ± scarce olivine	LATITE
	Alkali feldspar absent; plagioclase abundant; pyroxene and (or) hornblende ± scarce olivine	ANDESITE
	Olivine and plagioclase abundant (high-alumina basalt), or pyroxene abundant and plagioclase and olivine abundant to scarce	BASALT
Rocks with feldspathoids, melilite, or analcite	Alkali feldspar abundant and > plagioclase; pyroxene, biotite, and amphiboles all possible	PHONOLITE
	Plagioclase abundant and > alkali feldspar; clinopyroxene abundant; no olivine	TEPHRITE
	Plagioclase abundant and > alkali feldspar; clinopyroxene abundant; with olivine	BASANITE
	Feldspathoids abundant; little or no feldspar; clinopyroxene abundant ± olivine	NEPHELINITE, etc.

Table 3.2 Classification scheme of primary volcanics (After Compton, 1985).

### 3.2 ANIMAL CREEK GREYWACKE

In DDH Mac 33, grey-black interbedded siltstones and crossbedded sandstones conformably underlie the volcanic units. Sedimentary features such as cross bedding indicate that the sediments are younging up hole. These sediments are interpreted to be similar to the Animal Creek Greywacke as they display similar characteristics to the units described in section 2.3.1. The Animal Creek Greywacke is in contact with a coherent andesite horizon in Mac 33 where baked margins are observed.

### 3.3 DACITES

Dacites were only intersected in drill holes Mac 27, Mac 33, and Mac 35 (Figs. 3.2, 3.5, 3.6). The dacites typically occur in the deeper sections of the drill holes as either coherent or brecciated facies. The coherent facies and the brecciated dacites are observed to have gradational contacts. Interbedded volcanoclastics are present within the dacite and have conformable contacts. Maximum thickness is up to 45 m for individual coherent facies eg. Mac 35 (Fig. 3.6), while thinner (10-30 m) coherent units are observed in Mac 27 and Mac 33 (Figs. 3.2, 3.5). The coherent facies of the dacites are mottled pink and grey through to black in colour and are massive to feldspar-phyric (Plates 1A, 1B), with individual euhedral phenocrysts up to 3 mm long. Other features typical of the coherent dacite are abundant perlite cracks that have been highlighted by secondary quartz and calcite veins. Some sections of the dacite lavas appear to be weakly flow banded indicating that the lavas were partially fluidal during emplacement.

Petrographic analyses of the dacites revealed diverse textures and mineralogies. The dacites are moderately to sparsely plagioclase-phyric and have undergone varying degrees of alteration. Plagioclase phenocrysts are up to 1 mm long, are subhedral to euhedral in shape and comprise between 5 and 10 modal % of the dacites (Plate 2A). Minor hornblende phenocrysts occur as subhedral to euhedral shaped rare phenocrysts up to 0.5 mm long.

#### 3.3.1 Dacite breccias

Dacite breccias are observed to be in close association with the coherent dacites in drill holes, Mac 27, Mac 33 and Mac 35 and attain thicknesses in the order of 100 m (Mac 35)(Fig. 3.6). The dacite breccias are restricted to clast-supported breccias that have jigsaw-fit texture (Plate 8B). The clasts are angular to sub-angular with a maximum length of 6 cm. Margins of the clasts are observed to have occasional chilled margins with possible tiny normal joints. The matrix is up to 5 mm thick and is composed of fine grained glassy plagioclase-phyric dacite. In thin section glassy shards have been observed within the matrix of the breccias.

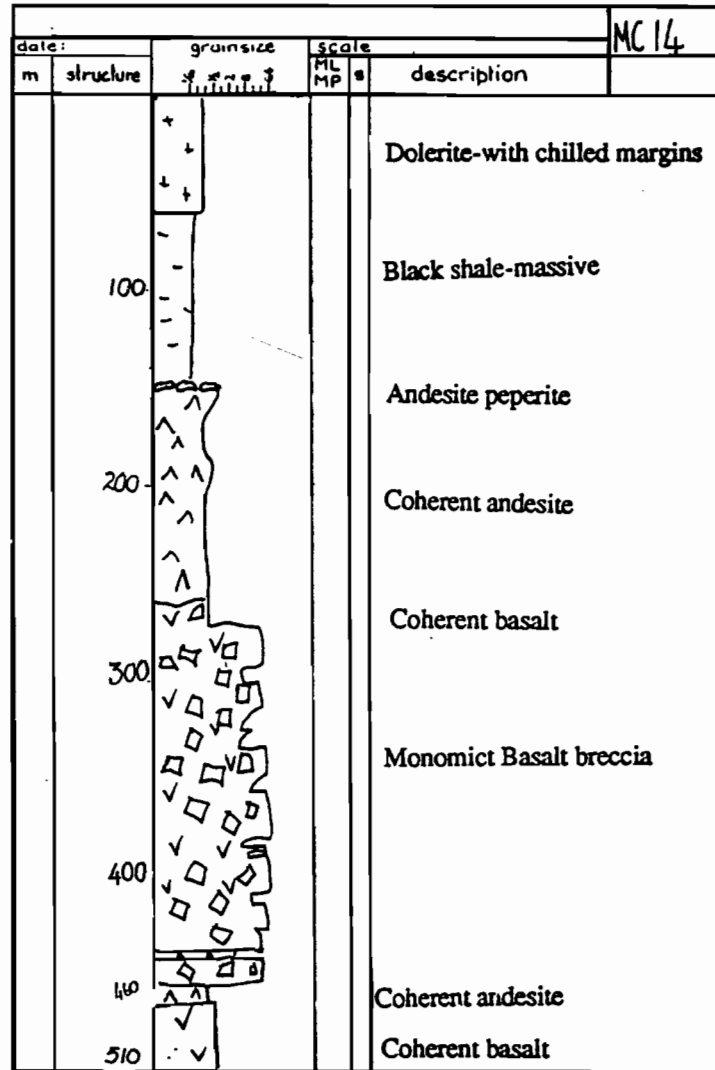


Figure 3.1: Summarised graphic log of MC 14.

### 3.3.2 Interpretations

The dacite units are interpreted to be sparsely plagioclase-phyric, glassy dacite to plagioclase  $\pm$  augite-phyric, dacite. Corbett and Komyshan (1989) describe similar coherent dacites from elsewhere in the Que-Hellyer Volcanics and define them as tabular lava flows. This explanation is also preferred for the coherent dacites at High Point. The jigsaw-fit clast supported dacites are defined as *insitu* dacite-hyaloclastites (McPhie *et al.*, 1993). Evidence for this interpretation includes the gradational contact between coherent dacites and the dacite breccias, jigsaw-fit textures, the tiny normal joints and minor perlitic cracking. The presence of volcaniclastic layers interbedded within the dacite units suggest that this unit is equivalent to the mixed sequence at Hellyer, as described by Waters and Wallace (1992) and Corbett (1992).

Figure 3.2: Summarised graphic log of Mac 27

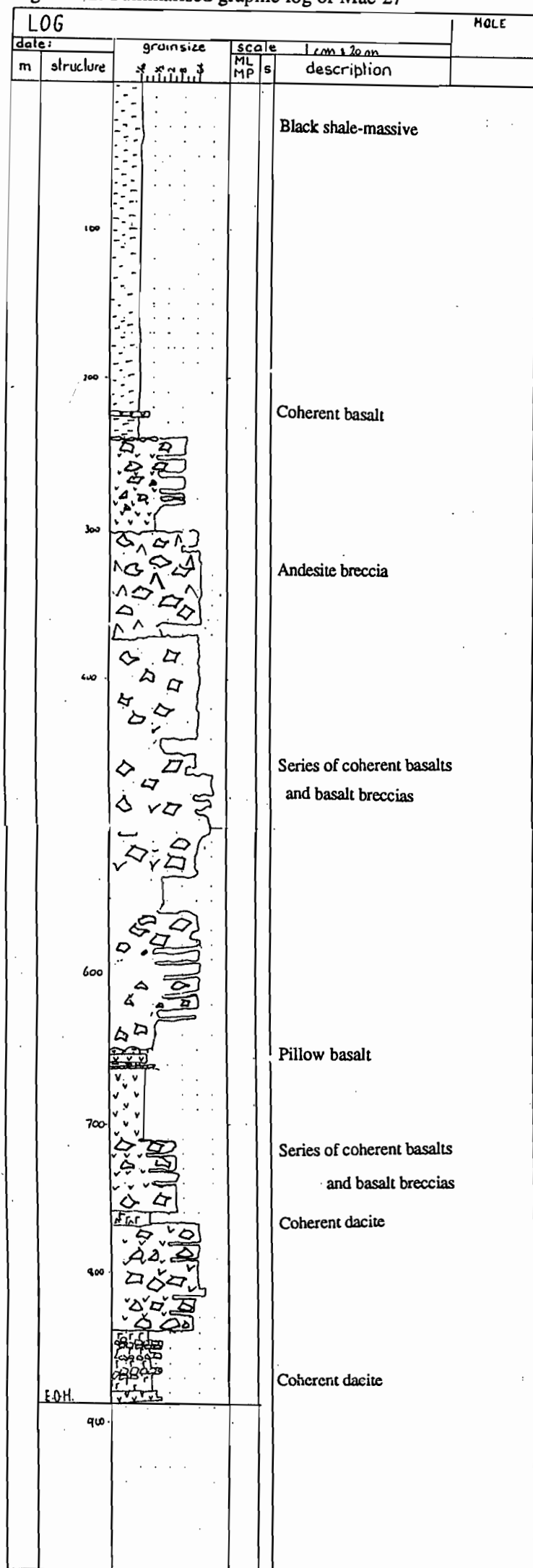


Figure 3.3: Summarised graphic log of MC 13

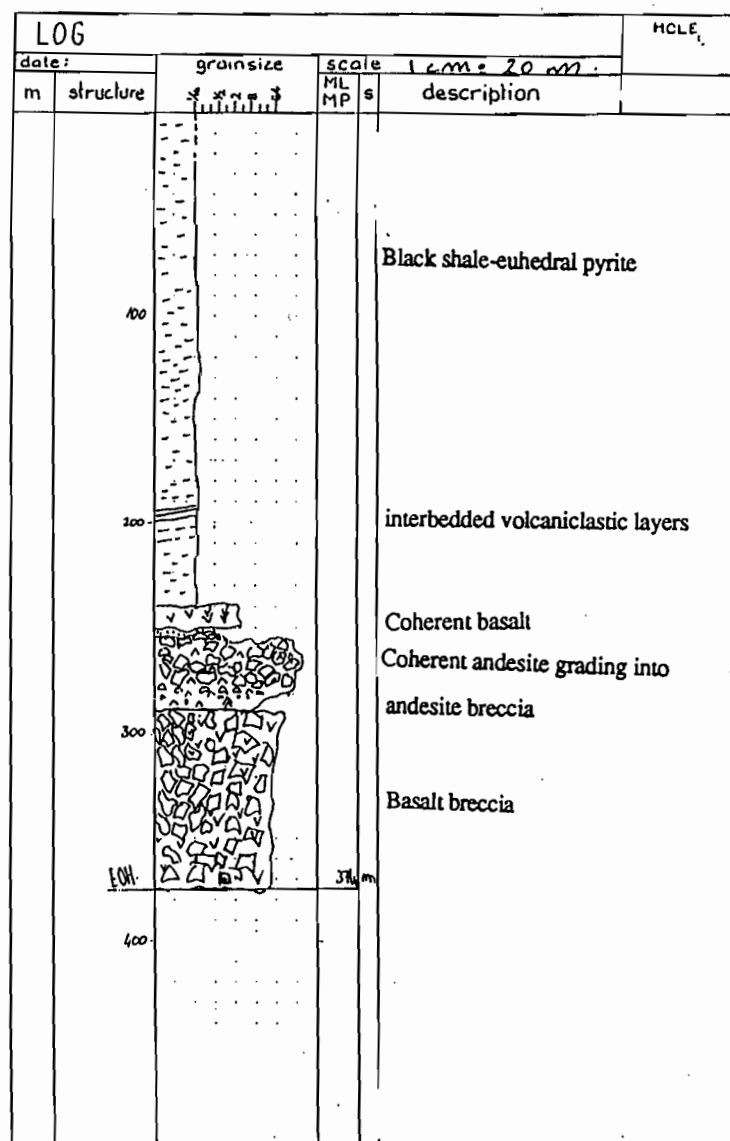
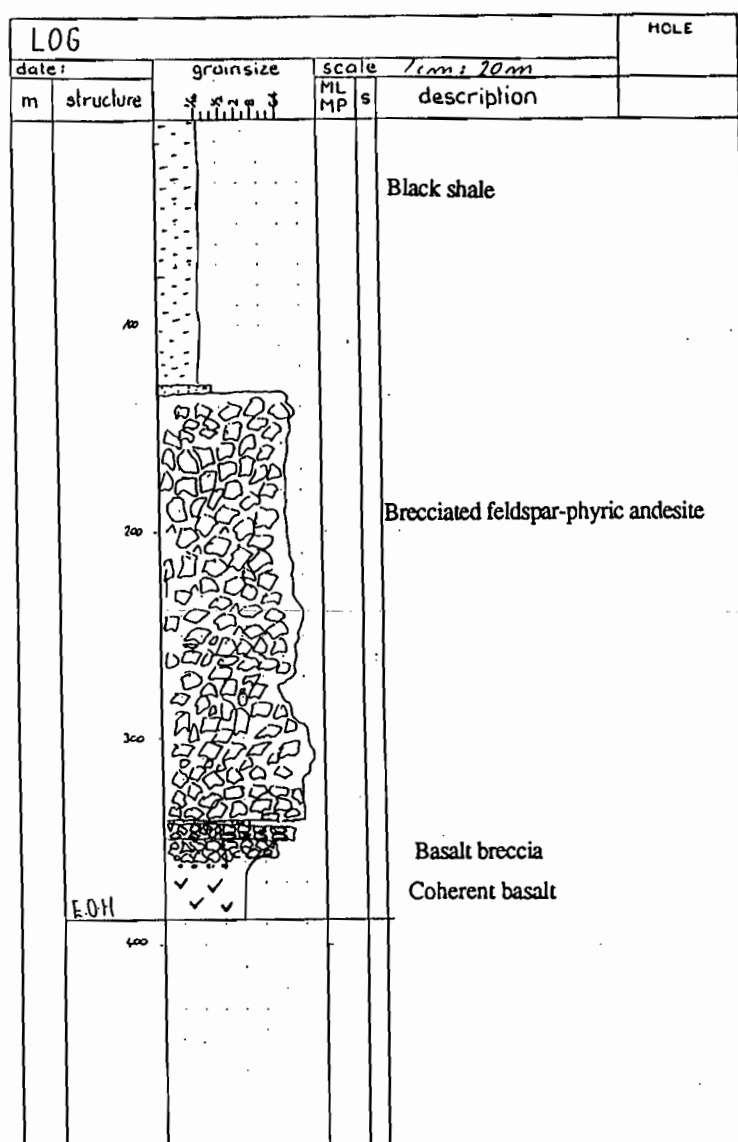


Figure 3.4 : Summarised graphic log MC 12



LOG		grainsize		scale		1 cm 20 m	
date:				ML	S	description	
m	structure			MP		page of	
20						Dolerite	
40							
60							
80						interbedded volcanoclastic layers	
100						Black shale	
120							
140							
160						Dolerite	
180							
200						Black shale-massive	
220							
240						Basalt breccia	
260	No Core						
280							
300						Coherent basalt and basalt breccia	
320						Coherent feldspar-phyric andesite	
340						Brecciated feldspar-phyric andesite	
360							
380							
400							
420							
440							
460						Dacite breccia (Hyaloclastite)	
480							
500						Mottled pink-dark green siliceous	
520						feldspar phyric coherent dacite	
540						with minor flow banding	
560							
580							
600						Coherent andesite-dacite	
620							
640							
660						Coherent basalt	
680							
700							
720						Coherent dacite	
740							
760						Andesite breccia	
780							
800						Coherent andesite	
820							
840							
860						Interbedded sandstones and siltstones	
880						(Animal Creek Greywacke)	
900							
920							

LOG			HOLE	
date:		grainsize	scale 1cm/1 20m Core	
m	structure	ML MP	s	description
				page of
100				Brecciated feldspar-phyric andesite
150				
200				Coherent feldspar-phyric andesite
				Basalt breccia
				Pillow basalt
300				Coherent basalt
400				
500				Monomict Basalt breccia
600				
700				Coherent basalt
				Basalt breccia
800				
900				Dacite breccia
1000				
				Dacite breccia (Hyaloclastite)
				Coherent dacite
1100				Interbedded sandstones and siltstones
				Coherent andesite-dacite
1200				

### 3.4 BASALTS

Basaltic units were encountered in all but one of the drill holes (MC 12), and have a maximum thickness of up to 400 m in drill hole Mac 27 (Fig. 3.2). The basalt package can be further subdivided into coherent horizons and brecciated horizons. Individual coherent horizons are up to 50 m thick compared to the lava breccias which are up to 110 m thick (Figs. 3.1-3.5). Contact relationships between the basalts and other lithologies are either peperitic (Que River Shale contact), or as chilled margins (dacite contact). Within the whole basaltic sequence gradational contacts are also observed between the coherent units and the breccias. Unaltered basalts in the High Point area are grey to green and are generally massive, with local amygdale rich zones (Plates 3A-3B). The amygdales are generally cigar shape to well rounded spheres and are a maximum of 8 mm in diameter. Amygdale concentration is variable with the average concentration being approximately 3-5 % (Plate 7B). In drill hole Mac 35 and DDH Mac 33, amygdales comprise up to 30-35% of the basalt in a 40 cm thick zone (Plate 7A). In this zone the average diameter of the amygdales decreases from 5 mm to 1 mm uphole.

Depositional features of the basalt lavas include pillow lobes, peperitic margins and possible chilled margins. The peperitic margins are observed at the contact between the basalt lavas and the Que River Shale (Fig. 3.1) and consist of subrounded to rounded amygdaloidal basalt clasts set in a silicified mud matrix. Individual clasts sizes within the basalt-mudstone peperites are less than 5 cm in length. Pillow lobes in core are interpreted to be up to 1.5 m thick and are typically enclosed by lava breccias. The pillow lobes occur sporadically throughout the basalt package and display variable amygdale concentrations (as described above).

The basaltic units have consistent mineralogies and are predominantly augite + olivine-phyric primitive basaltic lavas that are typical of many of the Hellyer basalts (Plates 4-5). Olivines have commonly been replaced by silica and minor amounts of calcite, whereas the augites have remained relatively unaltered. The augites crystals range from 0.6 mm to 1.8 mm in length, and are generally found as glomeroporphyritic crystal clusters. The groundmass is a

brown aggregate of albite and augite microlaths with amygdales infilled by quartz and chlorite. In drill holes Mac 33 and Mac 35, the basalt lavas contain between 6-10 modal % augite, and 3-10 modal % altered olivines. These lavas can therefore be described as olivine + augite-phyric to augite + olivine-phyric lavas. An interesting petrographic feature of the basalts are rare resorbed quartz clasts (Plate 8), that are thought to represent an inclusion from a quartz rich assemblage that has been incorporated within the basalt melt.

### **3.4.1 Basalt breccias**

Occurring with the basaltic package are a series of basalt lava breccias that occur in close association with the basalt lavas. As stated previously (section 3.4.1), individual basalt breccia units are more variable in thickness with some individual sections being over 100 m thick. The breccia units range from clast supported units to matrix supported units (Appendix 2). The clasts are angular to sub-angular with a maximum width of 20 cm and a minimum diameter of a few millimetres. Hand samples have the appearance of being polymict, but thin section analysis reveals that the breccia clasts are almost exclusively monomict and composed of massive to amygdaloidal, olivine + augite-phyric to augite  $\pm$  olivine-phyric basalt lava.

Several of the clasts supported breccias display a jigsaw texture (Figs. 3.4-3.5). Clast shapes of these breccias are angular to sub-angular and are generally less than 8 cm in length and 4 cm in width. The matrix between the clasts is composed of predominantly quartz and calcite as veins up to 4 mm thick. Compositionally, the clasts are identified as augite + olivine-phyric basalts that are similar to those described in the previous section. Other features of the clasts include possible quenched margins with tiny normal joints.

### **3.4.2 Interpretations**

The basaltic units are interpreted to be intrusive, where as others were most likely extrusive (or shallow intrusive) lavas and lava breccias. The extrusive or shallow intrusive units are characterised by peperitic margins and pillow lobes, indicating emplacement was in a subaqueous environment into minor sediment. The shallow intrusives or extrusive lavas appear to be comprised of several smaller flows rather than one large flow, based on the massive to



**Plate 1:** A/ (Top) Well preserved feldspar-phyric dacite lava that has had minor silica-sericite alteration (with minor hematite dusting) (Mac 35, 910m). B/ (Bottom) As above with Fe staining (Mac 33, 504 m).

**Plate 2:** Thin section of Plate 13 A. Well preserved plagioclase feldspars set within a quartz-plagioclase groundmass (mag. x 25).

**Plate 3:** A/ (Top). Massive to weakly amygdaloidal basalt lava . Amygdales are infilled with predominantly polygonal quartz. B/ (Bottom). Amygdaloidal, augite  $\pm$  olivine-phyric basalt lava. Amygdales are generally cigar shaped and 0.5 cm in length.

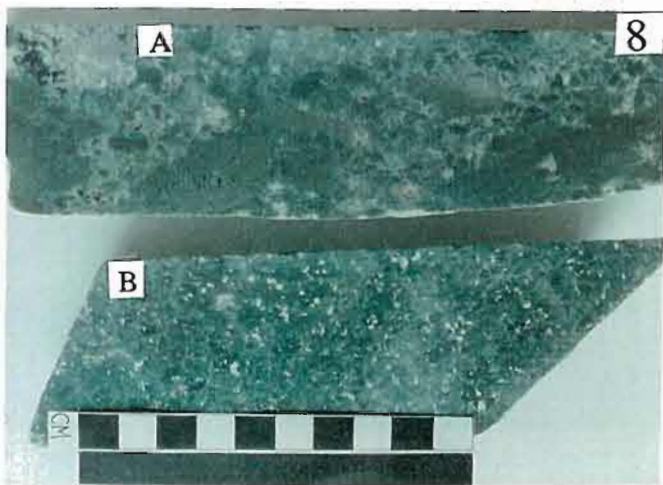
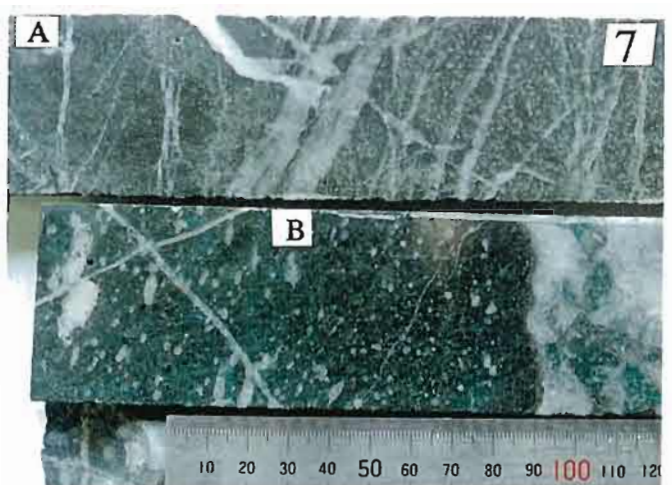
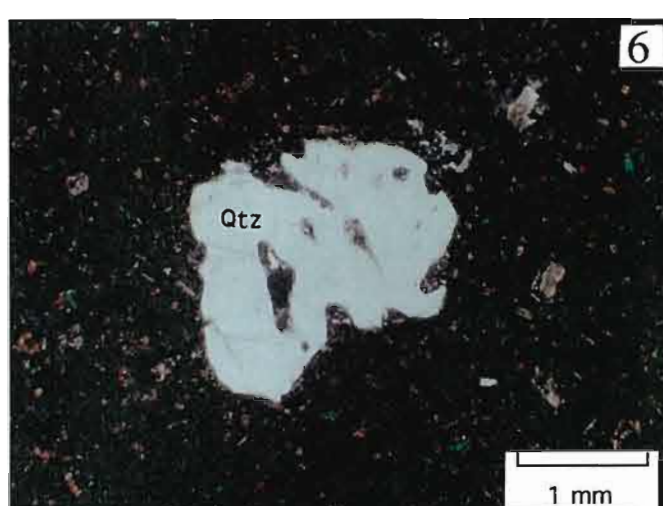
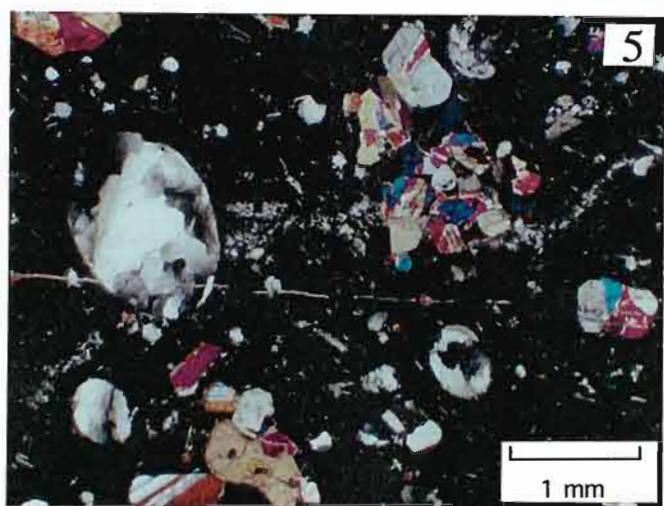
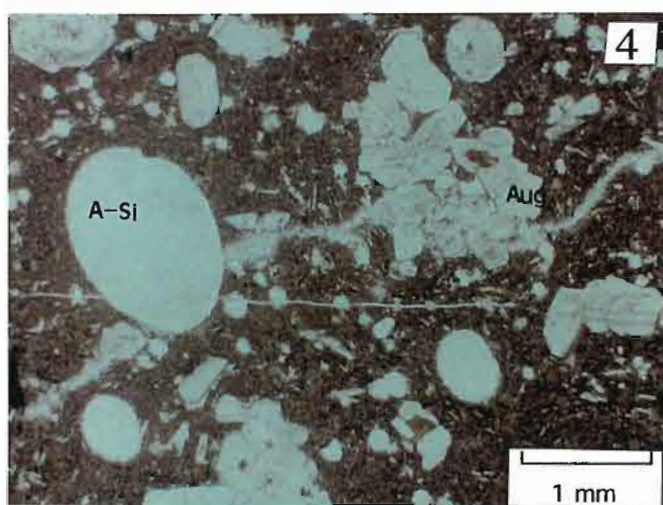
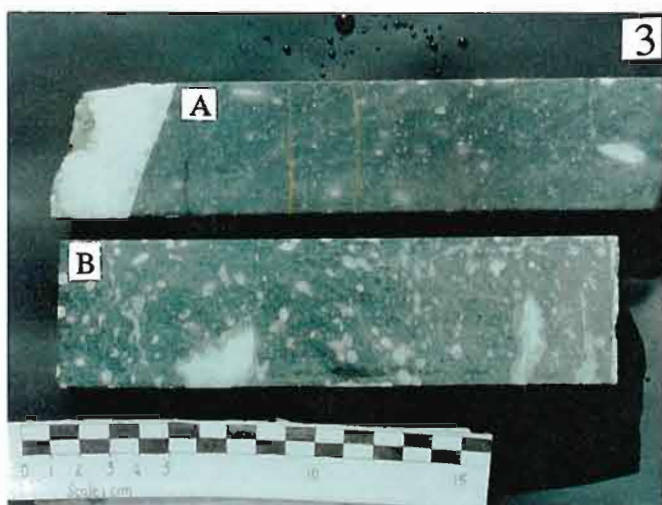
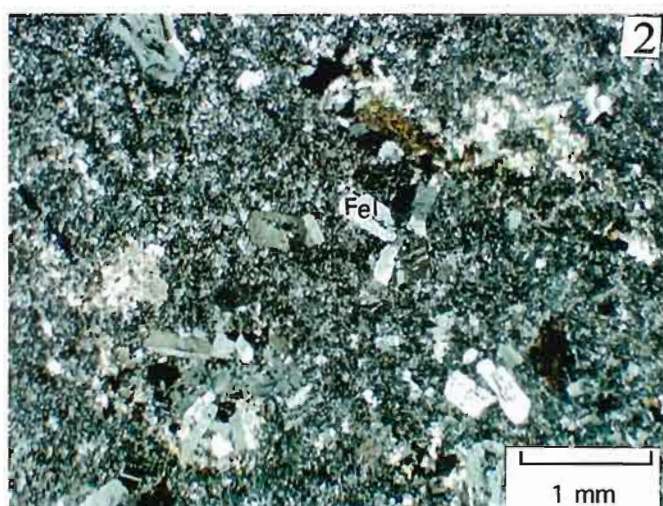
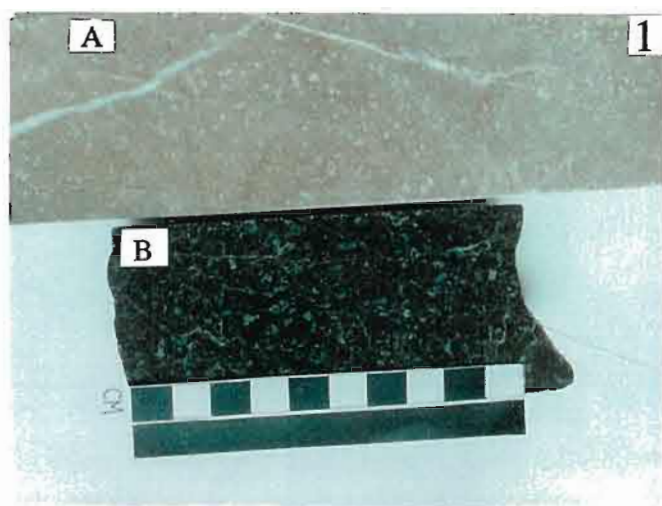
**Plate 4:** Thin section of amygdaloidal, augite  $\pm$  olivine-phyric basalt lava in normal light (mag 25 x).

**Plate 5.** Cross polar view of plate 6, showing augite clusters and rare olivine phenocrysts (mag 25 x).

**Plate 6:** Rare resorbed quartz within a massive to weakly amygdaloidal basalt lava.

**Plate 7:** A/ (Top) Basalt lava reflecting the variable intensity of the vesicularity. The vesicularity increases up hole (to right ). This section has carbonate-silica veins and silica veins cross-cutting the original lithology. B/ (Bottom) Basalt lava displaying the variable nature of vesicle size and intensity. Generally vesicle size decreases up hole and the intensity increases marginally for this sample (both are from Mac 35 between 600 and 610m)

**Plate 8:** A/ (Top) Monomict basalt lava derived from a poorly augite-phyric basalt. The polymict appearance is due to variable types and intensities of alteration. (Mac 33, 252m). B/ (Bottom). Dacitic hyaloclastite derived from a plagioclase-phyric dacite lava (Mac 33, 625.5m)





amygdale-poor lavas grading into zones of intense amygdaloides, the presence of lava breccias overlying and underlying the amygdaloidal lavas and the sharp contact between lavas and the lava breccias. The clast supported lava breccias that have a jigsaw fit are interpreted to be hydrofractured lavas, whereas the matrix breccias are classified as autobreccias. The intrusive basalts (sills) are generally massive, with chilled margins where the basalts are in contact with the dacites. The basaltic sills and the extrusive lavas (or shallow intrusives) are part of the same event, where the lower intrusive basalts represent the sub-surface expression of the pillow basalts and the basalt-mudstone peperite. The thickness for the basalts is greater than other localities within the Que-Hellyer Volcanics and is attributed to structural thickening by Devonian folding. The basalts occur at a similar stratigraphic position to the hangingwall basalts overlying Hellyer (Waters and Wallace, 1992).

### 3.5 QUE RIVER SHALE

The dominant sedimentary unit in the study area is the Que River Shale. This lithology has been described elsewhere as a distinctive unit of black carbonaceous, pyritic shales and siltstones that overlies the Que-Hellyer Volcanics (Corbett and Komysan, 1989) and is interpreted to have been deposited in a deep marine environment with quiet reducing conditions (Jago, 1973). The shale in hole MC 13 (Fig. 3.3) is typical of the Que River Shale in that it is a black, fine-grained, massive unit with minor laminations (Plates 9A-9B). The two distinct lithotypes (massive and laminated) correspond to lithotype 1 (massive to weakly laminated) and 2 (well-laminated) of Sinclair (1994). Petrographic analysis of the shale has revealed subparallel sericite-muscovite flakes, silt-sized angular quartz and carbonate grains with minor carbonate veinlets (Plate 10). Sulphide mineralisation is disseminated throughout the shale units. The predominant sulphides are pyrite, sphalerite and galena with accessory chalcopryrite. These minerals are associated with quartz and carbonate (calcite) veins and constitute less than 1 % of the shale.

Thin horizons (1-2m thick) of fine to coarse crystal rich volcanoclastic sediments are interbedded within the Que River Shale (Plate 9B). These units are polymict in composition and

contain shale clasts with minor quartz and feldspar fragments and possible volcanic glass (obsidian) in an altered ash-size feldspathic matrix. The fine volcanoclastics horizons and the coarse volcanoclastic horizons are separated by a 4 m massive layer of the Que River Shale. Both volcanoclastic layers display well sorted graded beds that indicate that the sequence is facing upwards

The Que River Shale represents a major hiatus in local volcanism, marking a change from proximal mafic to intermediate volcanism to distal felsic volcanism (Corbett, 1992). Current models for the Que River Shale suggest that the sediment was deposited in a quiet marine basin (Jago, 1973).

### **3.6 SANDSTONES AND SILTSTONES**

A second package of sediments exists below the Que River Shale at High Point in drill holes MC 12 and MC 13 (Figs. 3.3-3.4). This package consists of interbedded volcanoclastic siltstones and sandstones having 3-4 mm thick laminations (Plates 11A-11B). They are comprised predominantly of volcanic glass, altered lithic fragments, fractured volcanic quartz and minor feldspar fragments (Plate 12). The volcanoclastic sandstones and siltstones interfinger with the volcanic packages in MC 12 and MC 13 and have conformable contacts. The volcanic sandstones and siltstones that have probably been sourced from intermediate to felsic volcanics owing to the felsic components of the layers.

### **3.7 ANDESITES**

Andesite units in the High Point area consist of coherent and brecciated horizons and are observed in all drill holes (Figs. 3.1-3.6). Thickness of the brecciated horizon is in excess of 200 m (MC 13) compared to the coherent units that rarely exceed 30 m in thickness. Contact relationships with other units are variable. Peperitic margins occur at the contact between the andesites and the overlying Que River Shale, with individual andesite clasts up to 6 cm in length. These clasts are generally rounded and occur in a silicified mudstone/shale matrix. The total thickness of the andesite-mudstone peperites reaches approximately 10 m. The andesites can also be seen to have an interfingering relationship with the basalts (Figs. 3.6-3.7). The

contacts between the units are sharp to gradational over 20 cm. Within one metre of a basalt-andesite contact deep within Mac 33 a basalt clast is incorporated in the coherent andesite horizon. Contacts between the andesites and dacites are also observed to be sharp to gradational over 20 cm. The coherent andesites in hand sample are green to grey in colour that are massive to weakly feldspar-phyric (Plates 13A-13B).

Petrographic examination of the andesites has revealed that the feldspar-phyric lavas have euhedral to subhedral feldspar phenocrysts between 2 and 4 mm that comprise between 5 and 10% of some andesites. The more massive units range from weakly feldspar-phyric to aphanitic (Plate 15 A). Where phenocrysts are visible in hand specimen they are subhedral, 1mm in length and comprise a maximum of 2% of the rock. The only textural features observed in the coherent andesites are perlitic cracks.

The coherent andesite horizons are plagioclase  $\pm$  augite-phyric perlitically cracked, glassy andesite lavas. In thin section, the andesites contain between 8 and 12 modal % (Plate 14). Plagioclase phenocrysts are typically less than 1 mm in length (Plate 14), and have been albitized. Rare chloritised augite phenocrysts that comprise 3 % of the rock are also observed in thin section. The groundmass is an assemblage of predominantly fine-grained quartz and feldspar aggregates after devitrified glass. Perlite cracks occur throughout the groundmass; they have been highlighted by secondary chlorite alteration.

### **3.7.1 Andesite breccias**

Andesite breccias have been intersected in all drill holes (Figs. 3.1-3.6). The breccia units are in excess of 200m thick (MC 13, Mac 33) and have gradational contacts with the coherent andesites. Contacts observed with other lithologies are generally sharp with chilled margins. There are two main forms of andesite breccias: clast-supported (Plate 16B) and matrix-supported (Plate 16A). The matrix supported breccias have sub-angular to sub-rounded clast shapes and range in size from several cm to 50 cm in length. The matrix supporting the clasts is composed of predominantly andesite that is altered by silica-albite. The clast-supported breccias have smaller (less than 10cm) clasts that are predominantly angular in shape. The

matrix supporting these breccias is composed of silica-albite and quartz carbonate alteration assemblages. Both styles of breccias are poorly sorted monomict units.

### 3.7.2 Interpretation for andesites

The occurrence of the andesite package is observed as a coherent facies and a brecciated facies and are intersected in all drill holes. The interfingering relationships and the contacts between the andesites, and the basalts, dacites, and Que River Shale suggest that the andesites were emplaced later than these three lithologies. The andesite-mud fluidal peperites are indicative of deposition occurring while the Que River Shale was still wet and unconsolidated suggesting that the emplacement of the andesite was partially penecontemporaneous with the shale deposition. The matrix-supported andesite breccias are considered to be autobreccias that have formed during the emplacement of the andesite body, whereas the clast-supported breccias are due to hydrofracturing of the coherent facies. The andesites are typical of the upper basalts and andesites of Corbett (1992).

## 3.8 DOLERITE

A green to brown massive ophitic to sub-ophitic dolerite has been encountered in drill holes MC 14 and Mac 33 (Figs. 3.1-3.5). K-Ar age determinations from pyroxenes in the dolerite Age provide an age of  $396 \pm 10$  ma, which is interpreted as a minimum age reset by the Devonian Tabberabberan Orogeny (Corbett and Komysan, 1989). The dolerite has a similar rock geochemistry to the Hellyer basalt and may be the last of that Cambrian magmatic event. The dolerite is closely associated spatially with the Que River Shale, which supports a correlation with the Hellyer basalt. Komysan (1986) mapped a dolerite unit to the north of Mt Charter and examinations indicate that it is the same as that in Mac 33 and MC 14. The dolerite has chilled margins in sharp contact with the Que River Shale, indicating that the shale was partially or totally lithified when the dolerite intruded.

**Plate 9:** A/ (Top). Massive, black Que River Shale, cut by pyrite-silica veins and silica-carbonate veins (Mac 27, 644.9). B/ (Bottom). Finely laminated volcanoclastic horizon interbedded with the Que River Shale. The white layer is composed of broken quartz and feldspar phenocrysts, small pyritic clasts are also visible. (MC 13, 260.1 m)

**Plate 10:** Thin section of the massive shale unit. Broken quartz phenocrysts (white) are set within a fine-grained sediment matrix. Cross cutting the section is a quartz-carbonate vein.

**Plate 11:** A/ (Top). Laminated volcanoclastic andesite ash layer with visible broken feldspar phenocrysts and pyrite clasts with a thin layer of Que River Shale (MC 13, 252.7 m; Left is down hole). B/ (Bottom) Massive to laminated siltstone with minor pyrite clasts and quartz-carbonate veins (MC 13, 255.4 m)

**Plate 12:** Thin section of laminated siltstone. Minor laminations can be partly seen to overlap a chloritically altered clast (mag 25x)

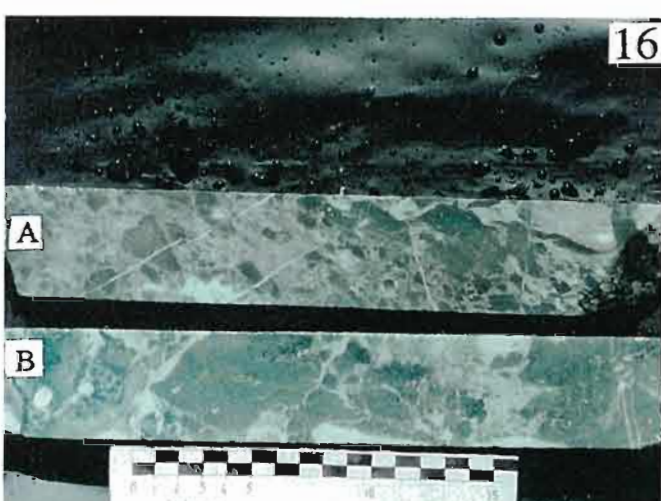
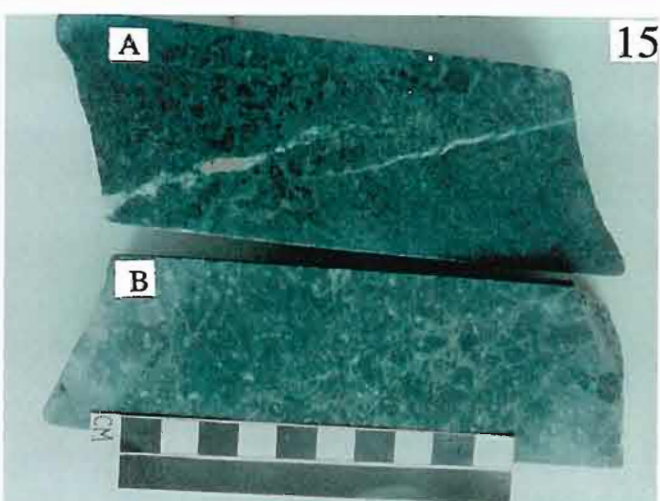
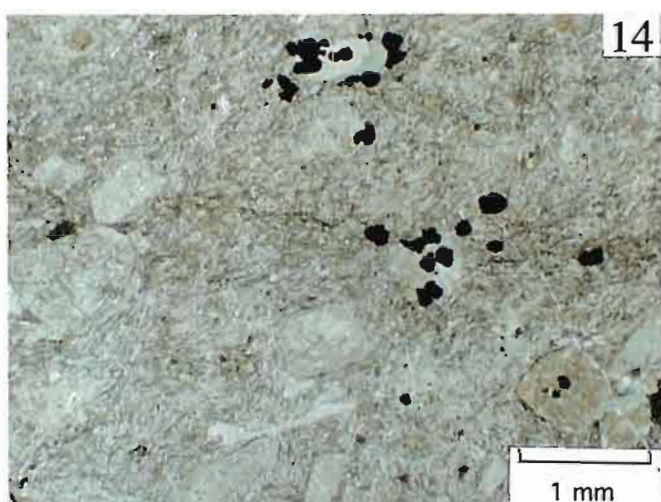
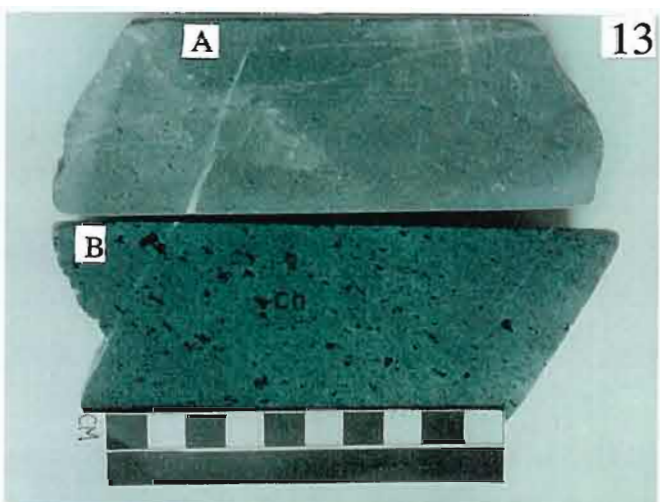
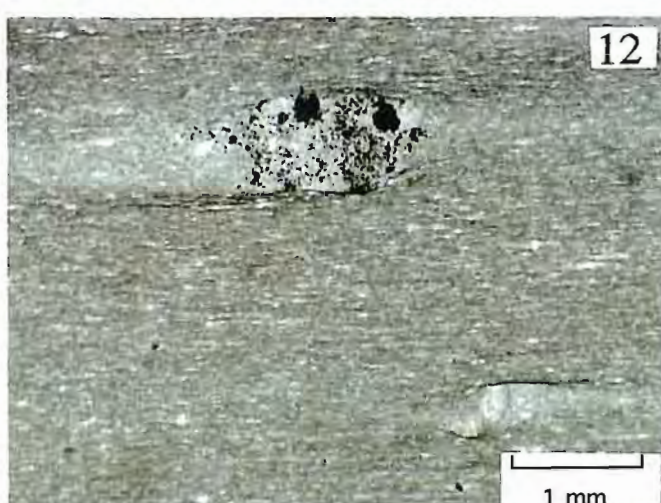
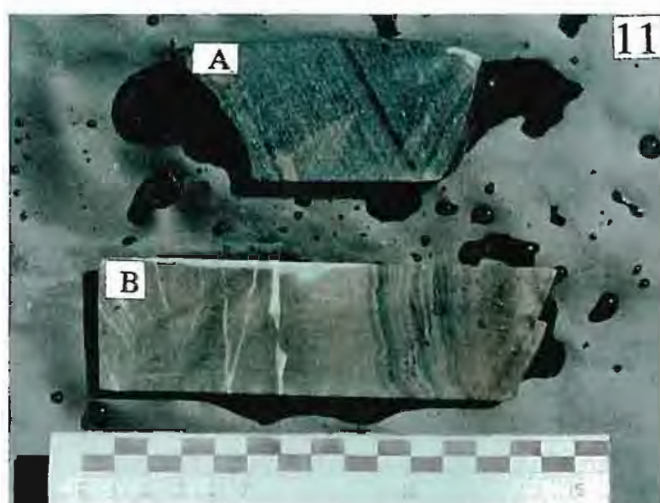
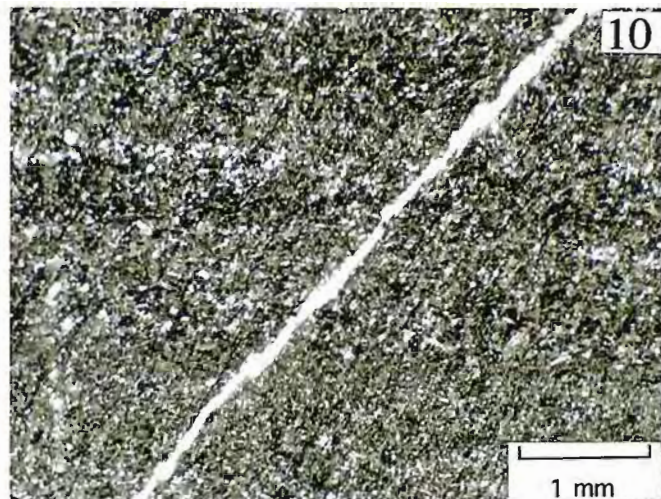
**Plate 13** A/ (Top) Chloritically altered weakly feldspar-phyric andesite lava. Original mafic minerals have been replaced by a later stage chlorite alteration (Mac 33, 676m). B) (Bottom) Massive to weakly feldspar-phyric andesite lava with regional prehnite-pumpellyite overprint.

**Plate 14:** Thin section of chloritically altered andesite lava. The chlorite is visible as olive green patches on the original mafic phenocrysts. Other minerals include chromites (opaque) and plagioclase (brownish; mag 25 x).

**Plate 15:** A/ (Top). An aphyric andesite lava that appears to have some hydrofracturing cutting the lithology (Mac 35, 780m). B/ (Bottom). Perlitically (?) cracked dacite to andesite lava (Mac 33, 524m).

**Plate 16:** A/ (Top). Matrix supported monomict andesite breccia. The matrix to the andesite clasts has been overprinted by silica-sericite alteration (MC 14, 345 m). B/ Clast supported hydrofractured andesite breccia with infilling carbonate matrix. Andesite clasts are predominantly weakly feldspar-phyric. (Mac 35, 234.3m).







### 3.9 LOCAL STRUCTURE

The structure of the area is dominated by two N.N.W.-N.W. trending faults (Fig. 3.7). The Mt Charter Fault forms the southern boundary of the Que-Hellyer Volcanics (Corbett and Komyshan, 1989) (Fig. 3.7). This fault is exposed at the surface on the Murchison Highway as an intensely cleaved zone within shales and greywackes and has been identified in DDH HP 1 indicating that it has a dip greater than 80° (Barwick, 1991) (Fig. 1.3). The second major fault in the area has been mapped by Aberfoyle geologists and Komyshan (1986) (Fig. 3.7) as marking the contact between the Que River Shale and andesite lavas (A. McNeill pers comm, 1995). Within the stratigraphy are an interpreted series of smaller scale sub-parallel faults to the major structures. These faults are important to mineral exploration as they may have been conduits for mineralising solutions. The study area has also been subjected to folding, producing a series of symmetrical synclinal and anticlinal structures that trend N.E and are shallowly plunging to the N.E. These faults can be linked with the Tabberabberan Orogeny that occurred during the Devonian (Corbett and Komyshan, 1989).

### 3.10 STRATIGRAPHIC CROSS SECTIONS

Two cross sections have been constructed across the area (Fig. 3.7) to assist in interpreting the facies relationships and to consider any lithological controls on the mineralisation. The major section is a S.W.-N.E (Fig. 3.8) that incorporates drill holes Mac 27, Mac 35, MC 12, MC 13 and MC 14 (Fig. 3.8). Due to faulting and the variable nature of the Que-Hellyer Volcanics, Mac 33 has been excluded from this section as it is considered to be too far off-section. The second section is a W.N.W-E.S.E. (Fig. 3.9) section that incorporates the stratigraphy from DDH's Mac 27, Mac 33 and MC 14 (Fig. 3.9). These cross sections highlight the interfingering relationships of the basalts and the andesites with the dacites and the Que River Shale. Comparing Figure 3.8 and Figure 3.9 the stratigraphy of the W.N.W-E.S.E section, appears to be more complex than the S.W.-N.E. section and highlights the diverse nature of the Que-Hellyer Volcanics stratigraphy (Note: Coherent units and brecciated units

have been classified as one lithological unit to simplify the sections, eg. coherent basalts and brecciated basalts are grouped together to form the main basalt horizon).

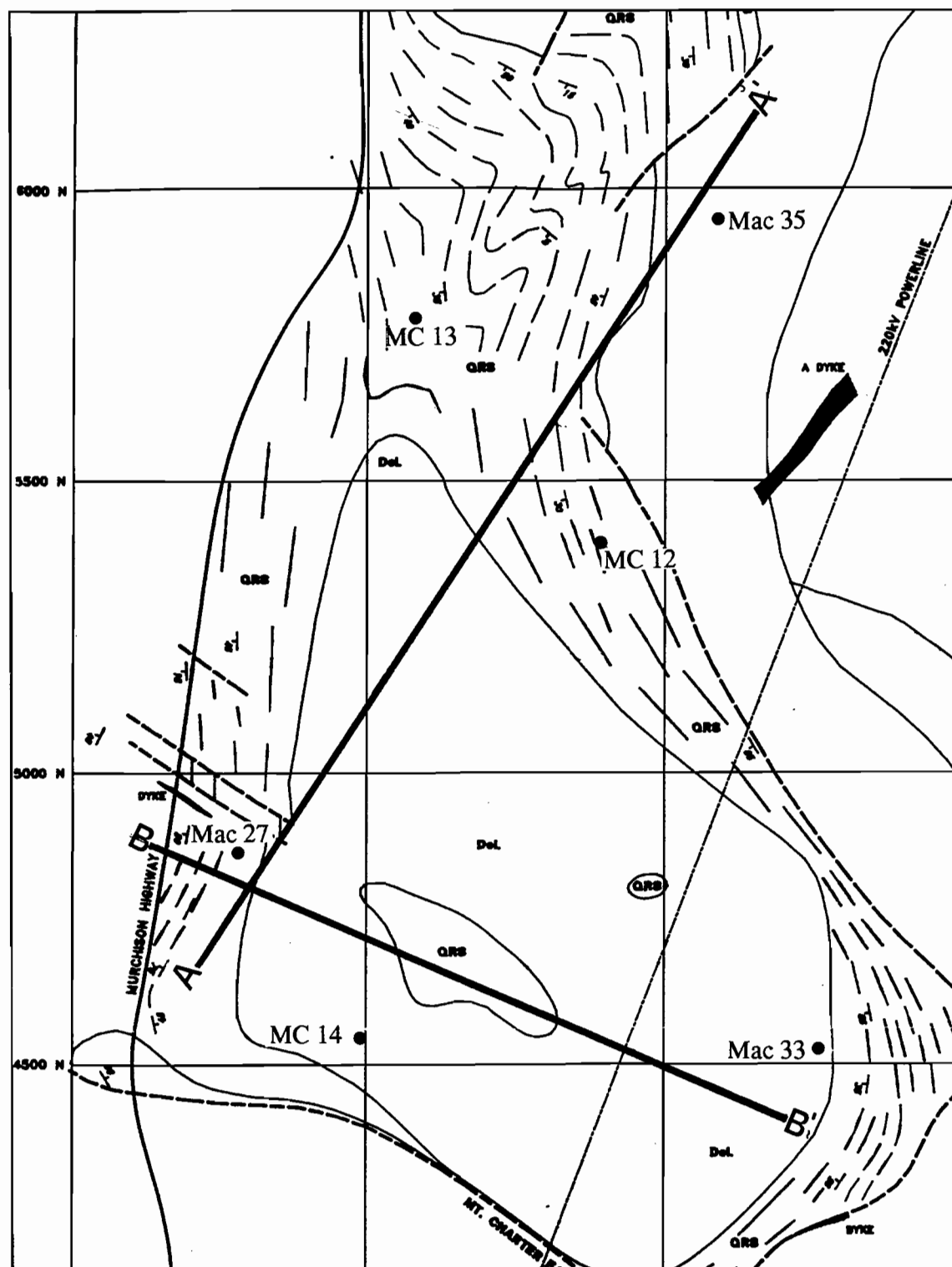
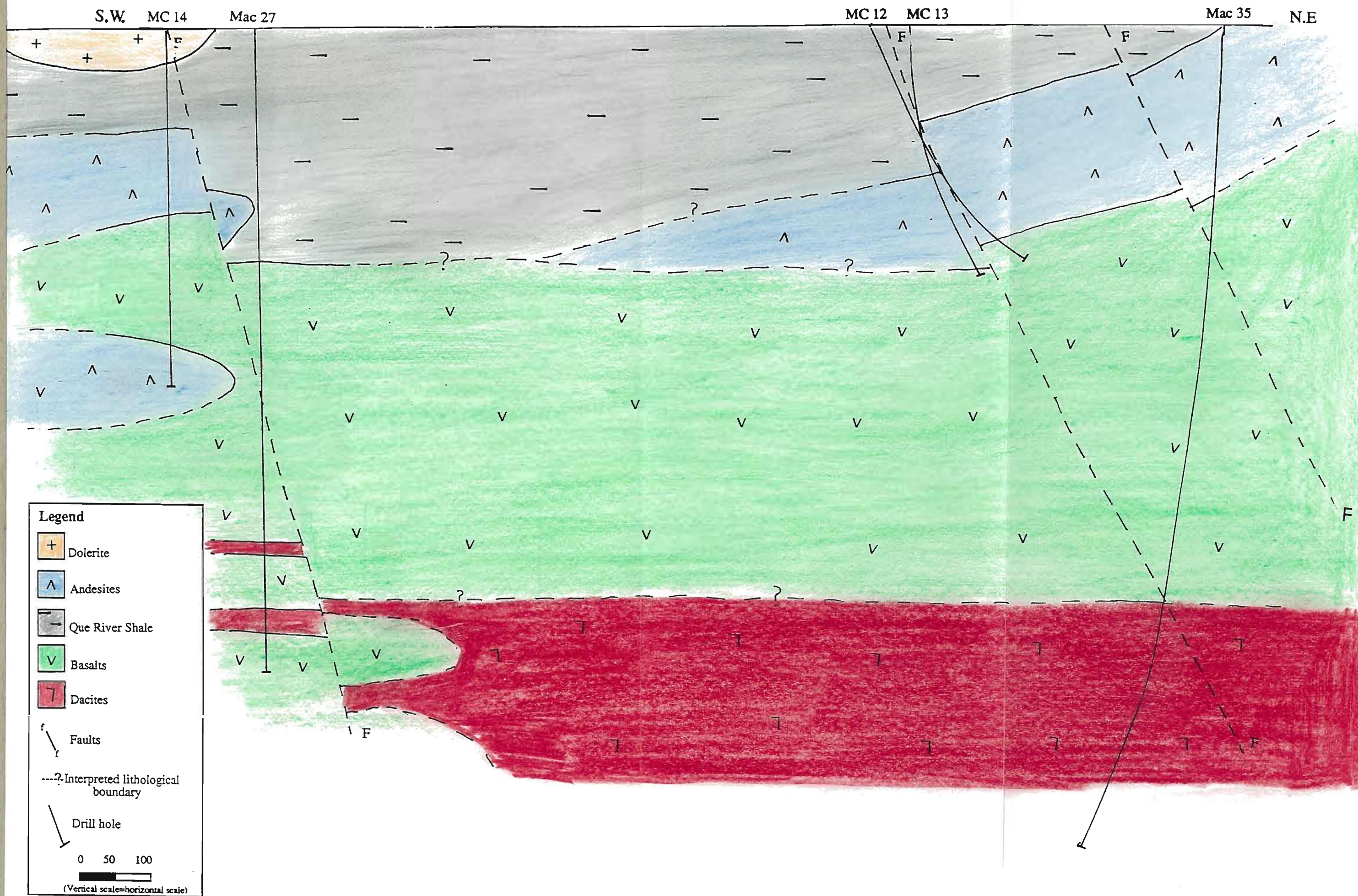


Figure 3.7: Lines of cross section for stratigraphic interpretations.



Figure 3.8: Schematic Cross Section For A-A'



Legend

- + Dolerite
- ^ Andesites
- Que River Shale
- v Basalts
- 7 Dacites

Faults

Interpreted lithological boundary

Drill hole

0 50 100

(Vertical scale=horizontal scale)



Figure 3.9: Schematic Cross Section For B-B'

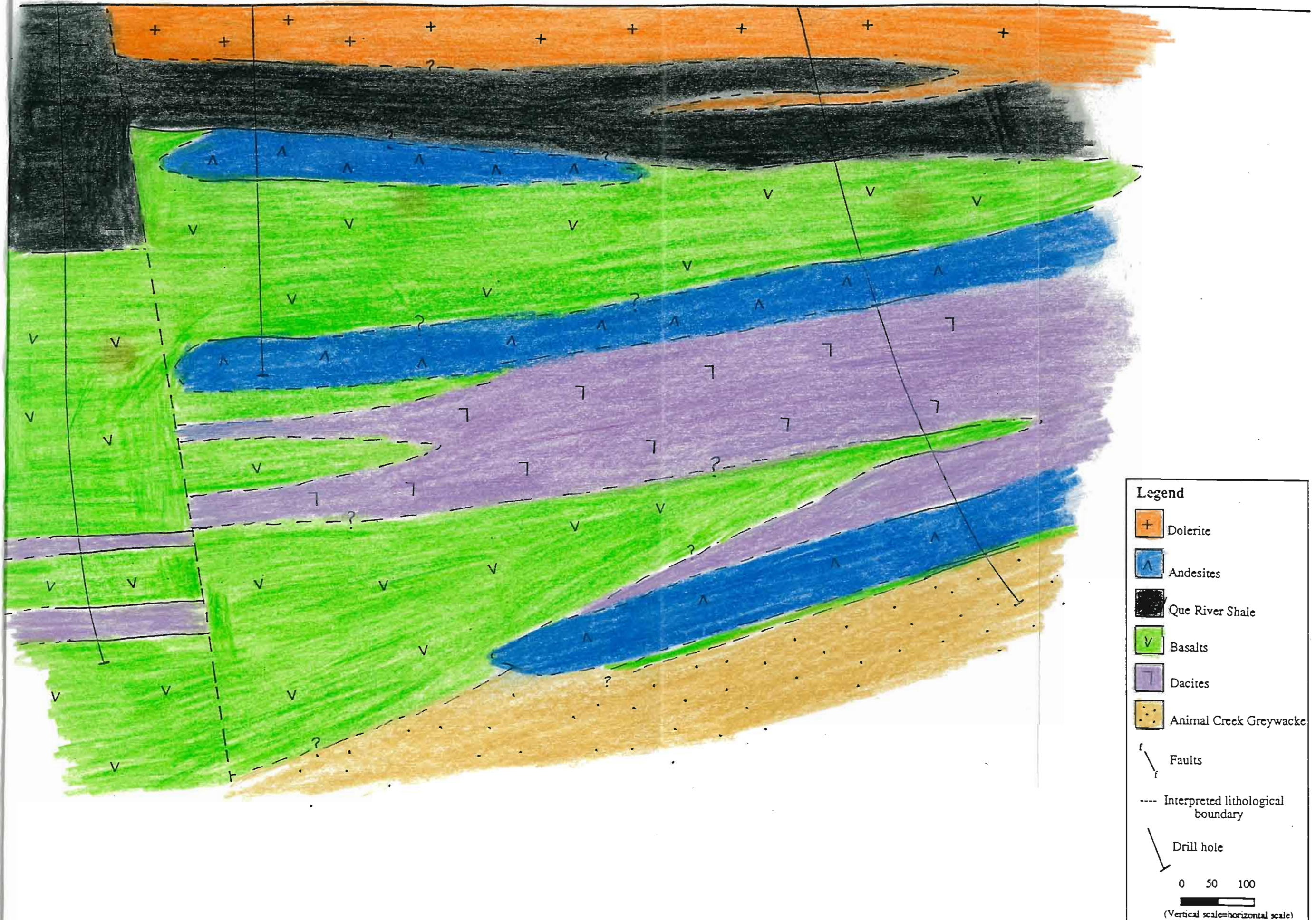
W.S.W.

Mac 27

MC 14

Mac 33

E.S.E.



**Legend**

- Dolerite
- Andesites
- Que River Shale
- Basalts
- Dacites
- Animal Creek Greywacke
- Faults
- Interpreted lithological boundary
- Drill hole

0 50 100  
 (Vertical scale=horizontal scale)



### 3.11 SUMMARY

The stratigraphy at High Point is dominated by the Que-Hellyer Volcanics, which are represented by a thick package of mixed sequence lithologies and the upper basalts and andesites. The Que-Hellyer Volcanics are overlain by a relatively thick sequence of Que River Shale. The Animal Creek Greywacke is the basal unit encountered in drill core occurring as cross bedded siltstones and sandstones. Disconformably overlying the Animal Creek Greywacke is a package of dacites and volcanoclastic units that form the mixed sequence, or mine sequence, of Corbett (1992) and Wallace and Waters (1992). The package has a maximum thickness of up to 100 m which is similar to that for other localities.

The dacites are conformably overlain and interfinger with a sequence of coherent basaltic horizons and breccias. The basalts are augite  $\pm$  olivine-phyric units that appear to be the equivalent of the upper basalts of the Que-Hellyer Volcanics. They attain a maximum of 600 m in thickness (Mac 35) (Fig. 3.8). The presence of the peperitic margins suggests that the basalts were emplaced when the Que River Shale was still wet and unconsolidated. Deeper in the stratigraphy, the basalts are considered to be intrusive, based upon their interpreted contacts with the dacites.

The Que River Shale conformably overlies the volcanic packages in the High Point area. This unit consists of massive, black, fine-grained shale that has been derived from a distal felsic volcanic source (Corbett, 1992). The shale marks the end of major proximal volcanism in the area, and the beginning of a period of relatively quiet sedimentation. Thickness of the shale reaches 250 m, with minor thin interbedded volcanoclastic layers that are up to 4 m thick.

A coherent package of andesite horizons and related breccias interfinger and overlie the basalts at High Point. The andesites are interpreted to be both intrusive dykes and sills based on the contacts with the shale (peperitic andesites), basalts (fingers of both andesites and basalts) and dacites (possible chilled margins). The combined total thickness for the mixed sequence and the upper basalts and andesites is up to a maximum of 1 km, as observed in Mac 35. This

is equivalent to the total thickness previously recorded for the whole sequence and is due to a combination of structural thickening by Devonian folding and a sub-basin within the main Que-Hellyer basin.

A series of sub-ophitic dolerite dykes with prominent chilled margins have intruded the shale. These dykes are interpreted to be the last stage of basaltic volcanism associated with the Que-Hellyer Volcanics.

---

## Chapter 4

### Alteration

---

#### 4.1 INTRODUCTION

The High Point area has been subjected to several generations of alteration. The various types of alteration provide vectors to possible mineralisation. Alteration was logged in this study in an attempt to quantify the alteration intensity and possible alteration zonation. Petrographic studies have been employed to confirm field observations.

There are three aims for the alteration study:

- 1/ To characterise the main styles of alteration and to construct an alteration paragenesis;
- 2/ To define any alteration zonation corresponding to the stratigraphy, and/ or mineralisation; and
- 3/ To compare the alteration at High Point with that documented from the Hellyer and Que River deposits.

#### 4.2 ALTERATION PETROGRAPHY

##### 4.2.1 Silica alteration

Two forms of silicification have been recognised in the High Point lithologies. The most common is strong silicification and baking of the sediment matrix in the basalt-shale and the andesite-shale peperites (Plate 17A). The matrix is comprised of blue grey silica and contains minor pyrite, sphalerite and chalcopyrite. Genesis of the blue chert alteration appears

to have occurred syn to early post peperite genesis. This form of silica or chert is similar to the interpillow chert of the upper basalts and andesites at Hellyer.

The second, less abundant form of silica alteration is restricted to vein style quartz alteration (Plate 18A). These veins (less than 1 cm wide) consist of light grey quartz with minor amounts of carbonate that cross cut the earlier blue chert and occur at varying angles to the drill core. The intensity of this style of alteration ranges from weak to moderate and occurs right throughout the stratigraphy.

#### 4.2.2 Silica-sericite

Silica-sericite alteration of the High Point lithologies is typically light grey to white and ranges in intensity from weak to strong. The silica-sericite alteration is observed as two forms: pervasive texturally preserving silica-sericite (Plate 17A); or localised texturally destructive silica-sericite (Plates 19A-19B). The pervasive style occurs as millimetre wide rims around andesite clasts in the andesite-mudstone peperites (Plate 17A), and is almost exclusively restricted to clasts that are greater than 2.5 cm in diameter. The intense silica-sericite alteration appears to be highlighting original glassy quenched margins (Fig. 4.1) and the clasts display original textures such as feldspar phenocrysts. In most cases clasts smaller than 2.5 cm in diameter are completely overprinted by the silica-sericite, however, original feldspar crystal shapes are still visible within the clasts.

The localised, texturally destructive silica-sericite alteration gives the rock a pseudo-fragmental appearance similar to that described by Allen (1992) and McPhie *et al.* (1993). The pseudo-fragmental texture is created by the concentration or localisation of hydrothermal fluids along a microfault, and is the result of the concentration of the fluids that created the silica-sericite alteration rims around the andesite clasts in the andesite-mudstone peperites. This texture is characterised by strong intensities and has destroyed most of the original textural features of the host lithologies. Minor disseminated pyrite, sphalerite, galena, and chalcopyrite, is observed with the pseudo-fragmental alteration texture, indicating that the mineralisation is either directly associated with the silica-sericite alteration, or is post silica-sericite alteration.



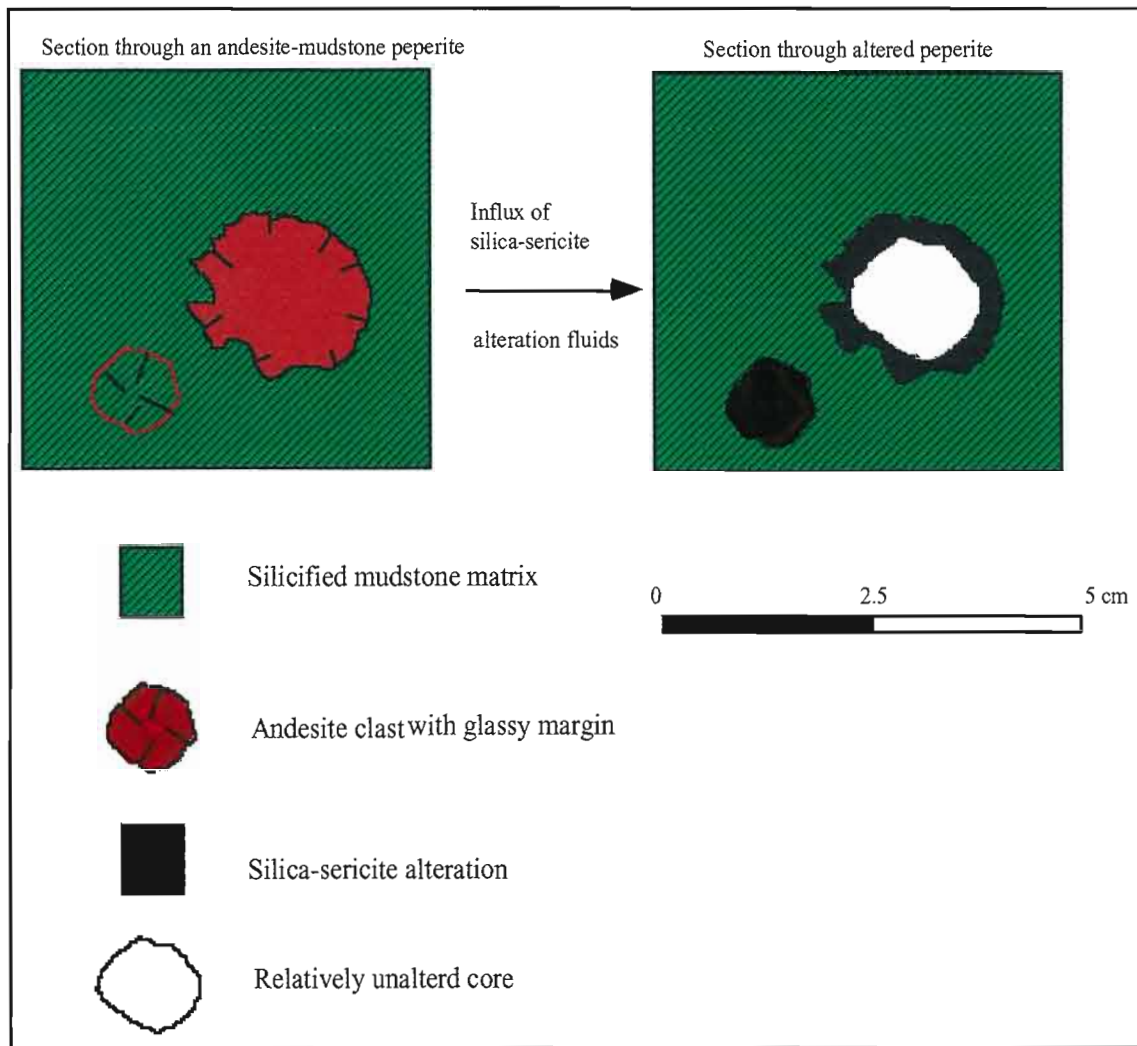


Figure 4.1: Genesis of silica-sericite alteration rims around andesite clasts within andesite-mudstone peperites.

#### 4.2.3 Chlorite alteration

Pervasive chlorite alteration is restricted to the basaltic and andesitic units. The intensity of chlorite alteration varies depending on lithology. In coherent volcanic units it ranges from weak to moderate (Plate 13B), whereas the volcanic breccias have undergone strong to intense chlorite alteration (Plates 20A, 24A), presumably due to the higher primary porosity. Original textures in the chlorite altered clasts of the lava breccias have been almost completely detextured. Petrographic examinations of the breccias reveals the plagioclase phenocrysts are partially preserved, whereas augite and olivine have been completely replaced by chlorite. In contrast, olivine and augite in the coherent volcanics are mostly pristine, with only minor replacement by chlorite.

Chlorite alteration produced alteration rims around clasts in the andesite-mudstone and basalt-mudstone peperites. This texture is interpreted to have formed when fluids have preferentially altered the originally glassy margins of the clasts within the peperites in a similar process to the silica-sericite rims. The chlorite alteration rims are up to 2 cm in width and the colour grades from black (outer rim) into a light olive green (inner margins).

The chlorite alteration assemblage can be further subdivided into a silica chlorite zone and a chlorite zone. A lithological control upon the two chlorite sub-zones is undetermined, however it is suggested that possibly the breccia units within the basalt units are influencing the two separate chlorite assemblages.

#### **4.2.4 Fuchsite alteration**

At High Point basaltic units have undergone fuchsite (chrome mica) alteration. The fuchsite occurs as either intense, texturally destructive, massive replacements (Plate 21A) or as small millimetre-sized disseminated, texturally preserving spots (Plate 20 B). The massive fuchsite ranges from apple green to a very light green in colour and reaches a maximum intensity of 5. The disseminated fuchsite spots are closely associated with lemon-coloured sericite.

#### **4.2.5 Silica-albite alteration**

Silica-albite alteration is localised to the upper of sections of drill holes Mac 35, MC 12, and MC 13 (Fig. 4.4). It is almost exclusively restricted to the andesite sills intersected by these holes. This style of alteration occur in a similar fashion to the silica-sericite assemblage, as a weak to moderate pervasive texturally preserving overprint and as texturally destructive pseudo-fragmental alteration texture (Plate 22). Minor hematite dusting has given the rock a light pink to orange colour similar to classic "potassic" alteration from porphyry Cu deposits (eg. Lowell and Guilbert, 1970).

**Plate 17:** A/ (Top) Silicified and sericitised andesite-mudstone peperite. The matrix of the peperite has been silicified. Clasts within the peperite have either silica-sericite rims or are totally altered by silica-sericite. B/ (Bottom).Silica-sericite and chlorite alteration of a basaltic peperite.

**Plate 18:** A/ (Top). Light grey-white silica vein cross cutting an andesite lava with smaller earlier stages of veins.

**Plate 19:** A/ (Top). Pseudo-fragmental appearance of silica-sericite alteration with an andesite lava. Minor chalcopyrite is visible within the alteration. B/ Pervasive silica-sericite-pyrite alteration texture

**Plate 20:** A/ (Top). Chlorite alteration of clasts within what was originally a peperite. The chlorite can be seen to change in colour from a dark green to a light green. The matrix of the peperite has been altered by an early stage of silica alteration. B/ (Bottom). Light green disseminated fuchsite spots are within a lemon coloured sericite, which has been cross cut by a carbonate-silica vein.

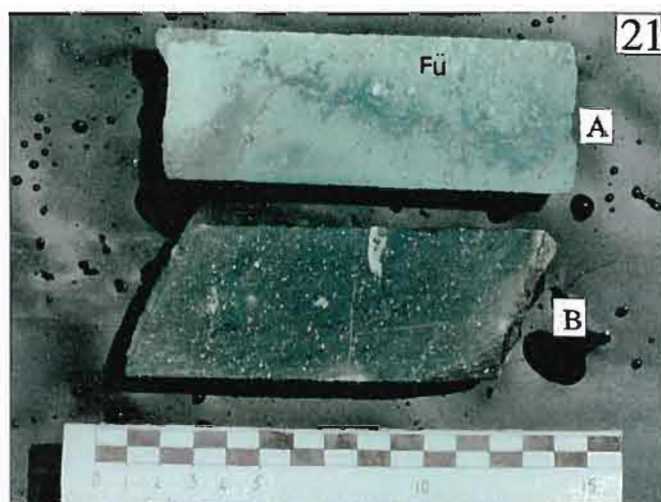
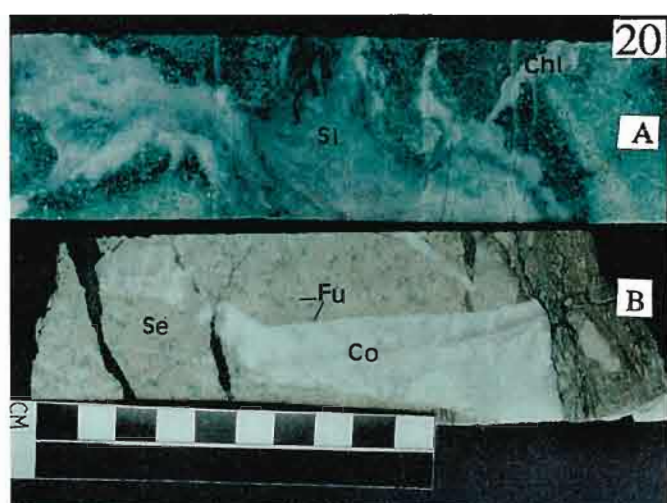
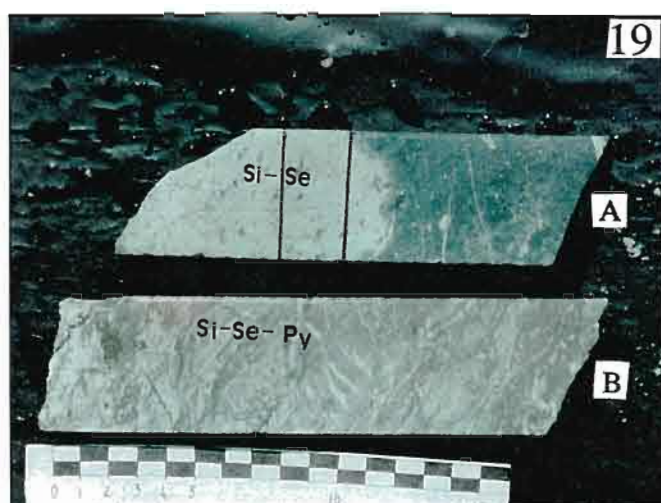
**Plate 21:** A/ (Top). Texturally massive fuchsite alteration of basaltic lava with minor fine grained galena. B/ (Bottom) A relatively unaltered basalt lava.

**Plate 22:** Silica-albite alteration with hematite dusting that is overprinting an earlier chlorite alteration (Mac 33, 364m-366m).

**Plate 23:** A/ (Top) Potassic alteration of amygdales in an amygdaloidal basalt (Mac 35, 288.4m). B/ (Bottom). Carbonate hydrofracturing of andesite (Mac 35, 207).

**Plate 24:** A/ (Top). Complex alteration pattern of a basaltic peperite. The main features are the late stage cross-cutting epidote vein, the different colours of chlorite and the K-feldspar alteration of the amygdales (Mac 35, 295.5 m). B/ (Bottom) Potassic alteration in the base of MC 13 (310m).





#### 4.2.6 Potassic alteration

Rare, weak to moderate, bright pink potassic alteration occurs in the deeper sections of DDH MC 13 within basaltic host rocks. Potassic alteration is associated with small (0.5 cm) wide amygdales that are infilled by K-feldspar and quartz (Plates 23A, 24A, 24 B). Pink to orange K-feldspar massive to bladed euhedral crystals up to 3 mm long and 1mm wide occur as a selvage around the later amygdales. This selvage is overgrown by white to clear quartz with granular chlorite infilling the centre of the amygdales.

#### 4.2.7 Epidote alteration

Epidote alteration occurs as pervasive, texturally preserving, small patchy aggregates (Fig. 4.2). In general the pervasive epidote alteration found in association with either silica-albite or chlorite alteration or with regional metamorphic minerals (prehnite and pumpellyite). Epidote also occurs in association with pale green chlorite in thin veins (possibly tension gashes) and rare amygdales and as rare, 1cm wide veins, that are perpendicular to the core axis. Vein epidote occurs as small (less than 1mm) acicular crystals in association with poorly crystalline quartz and appears to be the last alteration/ mineralisation event of the High Point area (Plate 24A).

### 4.3 PARAGENESIS

The paragenesis of alteration assemblages at High Point is complex (Fig. 4.3). The earliest event is interpreted to be the silicification of the mudstone matrix in the andesite-mudstone and basalt-mudstone peperites. Initial silicification was followed by silica-sericite alteration which cross cuts the mudstone matrix (Fig. 4.2 and Plate 17A). Chlorite alteration cross cuts and partially overprints both the silicified mudstone matrix and the silica-sericite alteration assemblages (Fig. 4.2). The timing of the silica-albite and sericite-fuchsite assemblages is unconstrained but both are thought to precede the potassic and epidote alteration assemblages. Potassic alteration is a later stage event similar to that reported by McGoldrick *et al.* (1990) and McGoldrick and Large (1992). Epidote alteration is the final event, as it cross



cuts all other phases of alteration. It is attributed to the Devonian metamorphic overprint associated with the Tabberabberan Orogeny.

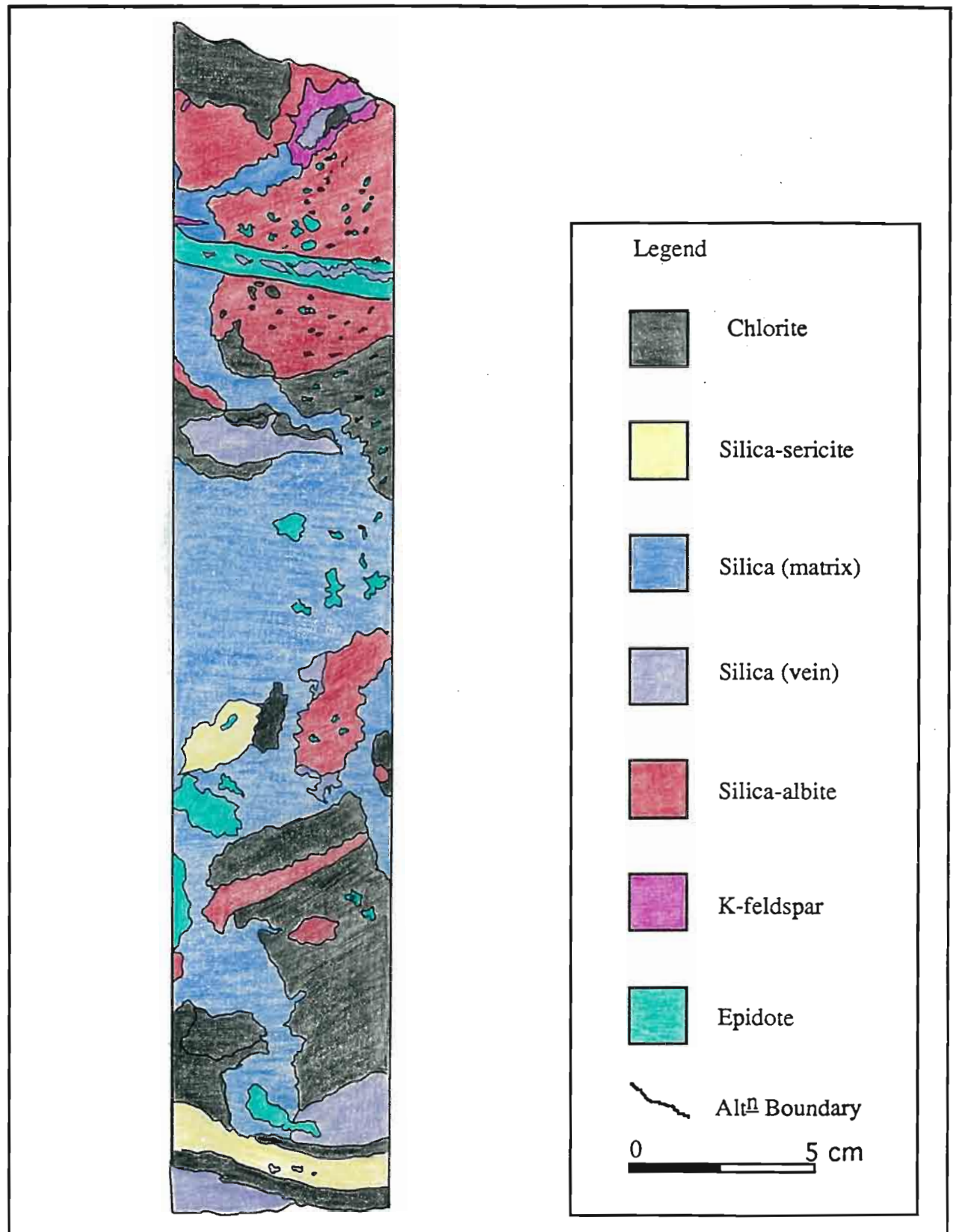


Figure 4.2: Overprinting relationships of alteration at High Point. (Core from Mac 35, 293 m).

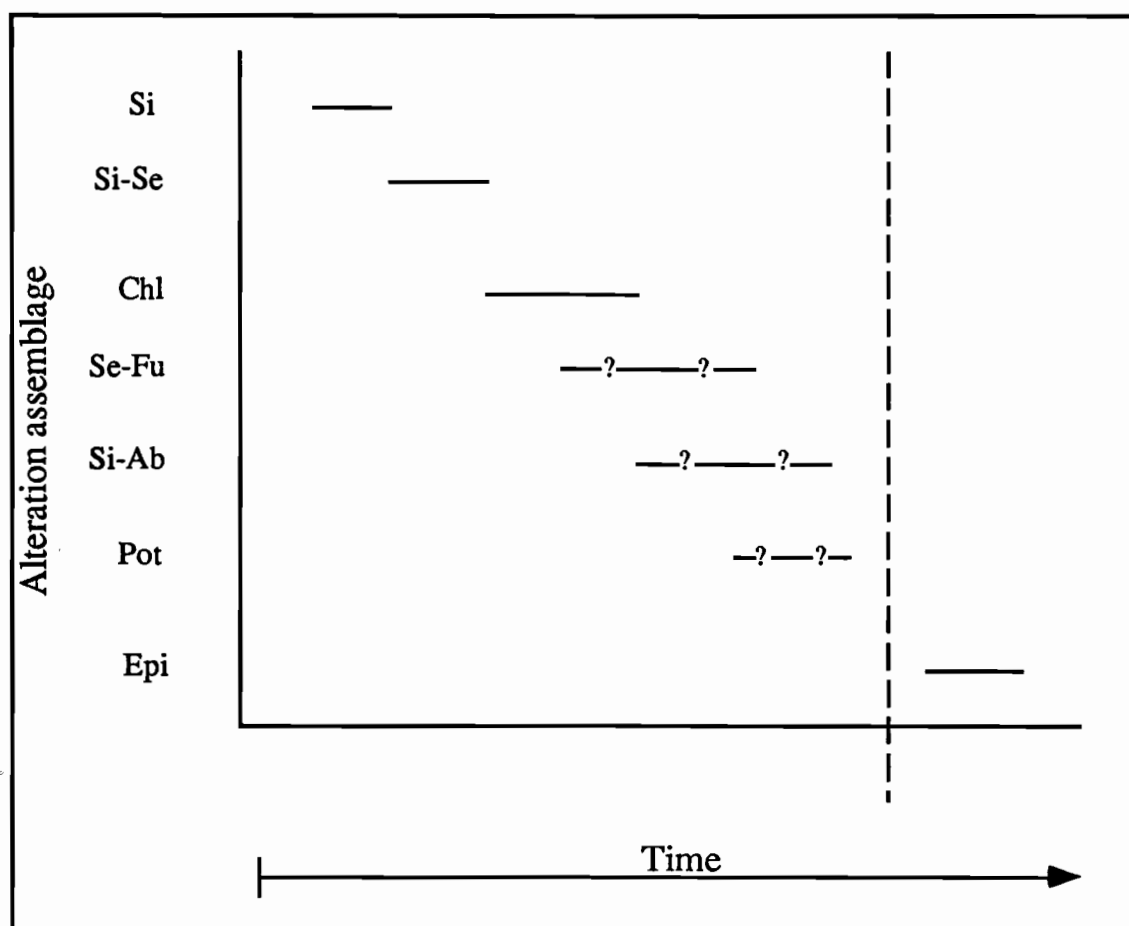
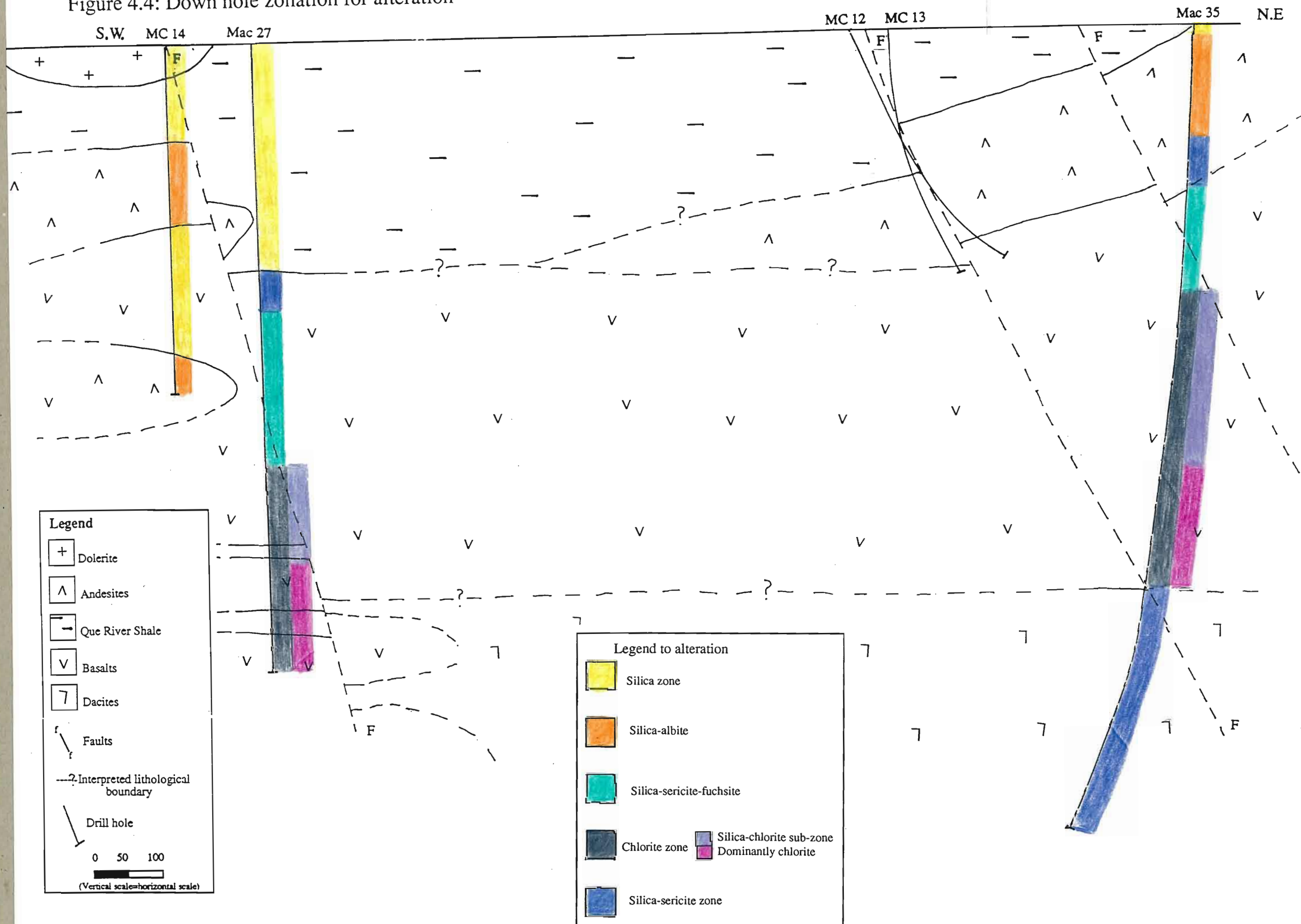


Figure 4.3 Paragenetic sequence of alteration assemblages. (Si= Silica, Se= Sericite, Chl= Chlorite, Fu= Fuchsite, Pot= Potassic and Epi= Epidote).

#### 4.4 ZONATION

The broad spatial distribution of various alteration assemblages recognised at High Point are illustrated in Figure 4.4. The alteration assemblages define a vertical zonation pattern, suggesting that the alteration assemblages were lithology dependent. Silica-albite alteration is restricted to the upper andesite sill in DDH Mac 35, MC 12 and MC 13. Sericite-fuchsite alteration only occurs in the upper to middle sections of the basalts (Fig. 4.4). The chlorite assemblage is also restricted to the basaltic and lies directly below the sericite-fuchsite alteration zone. This zone can be further subdivided into a silica chlorite zone and a chlorite zone. The Silica-sericite alteration occurs in all three volcanic packages, but is best developed in the dacites intersected deep in drill hole Mac 35.

Figure 4.4: Down hole zonation for alteration





## 4.5 DISCUSSION

### 4.5.1 VHMS related alteration

The alteration recorded at High Point is similar to that recorded at the VHMS deposits hosted by the Que-Hellyer Volcanics, and from other regions of the world including mainland Australia, Canada and the Kuroko district. Although the alteration assemblages immediately surrounding VHMS deposits are highly variable, distinct patterns are evident (Large, 1992). Footwall alteration associated with VHMS deposits occur as two main styles: footwall alteration pipes below the massive sulphide; and semi-conformable alteration zones that are regionally extensive (Morton and Franklin, 1987). Strong silica metasomatism is characteristic of the upper part of the alteration pipes, particularly in the Kuroko deposits of Japan (Shirozo, 1974; Urabe *et al.*, 1983) and the VHMS deposits of Cyprus (Lydon, 1984). Four distinct alteration zones have been identified in footwall alteration pipes. They are: (1) an inner zone of intense silica-pyrite  $\pm$  chlorite with abundant stringer sulphides, (2) a chlorite-pyrite  $\pm$  carbonate surrounding the siliceous core, (3) a sericite-chlorite-pyrite shell, and (4) a sericite-quartz-pyrite outer-most zone (Large, 1992).

At the Millenbach (Riverin and Hodgson, 1980; Knuckey *et al.*, 1982) and Corbet (Knuckey and Watkins, 1982) deposits of the Noranda area in Canada the footwall alteration pipes consist of inner chloritised cores surrounded by a sericite alteration zone. The major chloritic core is characterised by major additions of iron and magnesium along with depletions of calcium, sodium and silicon. This reflects the destruction of the feldspar component of the original felsic or mafic volcanic rock during the process of chloritisation (Roberts and Sheahan, 1988). The Hellyer deposit also displays classic zonation of footwall alteration, from the inner siliceous core through a zone of chlorite altered units to a zone of sericite and to the peripheries of the zone which are a sericite-quartz assemblage (Gemmell and Large, 1992) (Fig. 4.2).

Hangingwall alteration of VHMS deposits is typically either absent or when present poorly developed, however alteration assemblages are still recognisable. Deposits such as

Mount Chalmers (Queensland) have a weakly developed sericite-chlorite alteration assemblage in the hangingwall rhyolite volcanoclastics (Large and Both, 1980). In contrast, the hangingwall assemblages at Woodlawn (Peterson and Lambert, 1979) and Scuddles (Ashley *et al.*, 1988) have intense chlorite-quartz  $\pm$  carbonate alteration in the volcanics that overlie the massive sulphide bodies. Hangingwall alteration at Hellyer is characterised by the presence of fuchsite, and a broad zone of pervasive calcite and veining (Drown, 1990). This style of hangingwall alteration is also present at Que River (Wallace, 1989). McArthur (1989) reported silica-albite and silica-albite-chlorite assemblages within the pillow lava sequence overlying the orebody.

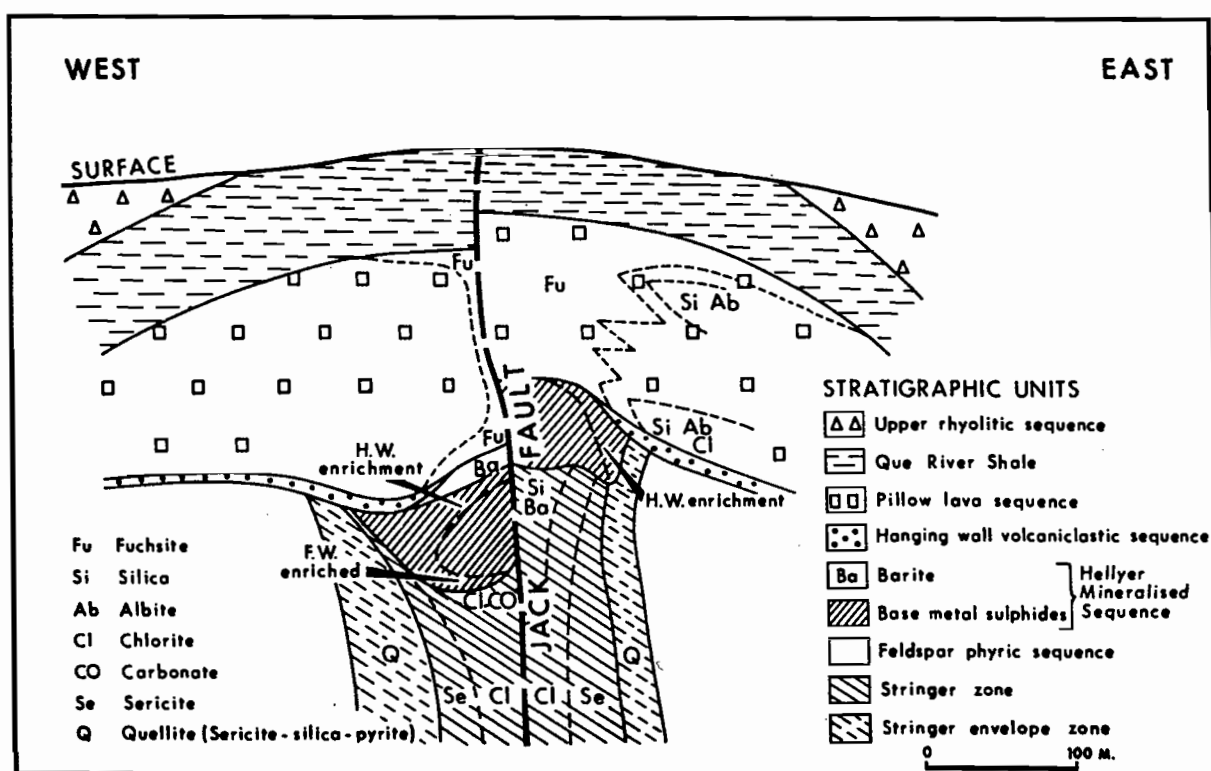


Figure 4.5: Zonation of major alteration at Hellyer (After McArthur, 1989).

Obvious comparisons can be drawn between the alteration at High Point and the Hellyer and Que River deposits. The silica-sericite assemblage at High Point appears to be the equivalent of the sericite zone described at Hellyer by Gemmell and Large (1992), and the chlorite alteration assemblage at High Point is equivalent to the chlorite zone at Hellyer. The presence of silica-sericite and chlorite alteration assemblages at High Point suggest that the dacites and lower basalts are part of a footwall alteration zone to possible economic base metal mineralisation in the area. By analogy with Que River and Hellyer, the fuchsite and silica albite alteration may represent weak hangingwall alteration at High Point. The origin of the fuchsite alteration at Hellyer is ascribed to the breakdown of primary chromium-rich pyroxenes in the basalts (Jack, 1989). This is also the most likely scenario for the formation of fuchsite at High Point.

#### 4.5.2 K-Feldspar alteration

K-Feldspar alteration in the Mount Read volcanics has been discussed by Polya *et al.* (1986) and Eastoe *et al.* (1987), who noted. K-feldspar occurs either as primary phenocrysts or as a secondary alteration product related to Cambrian Granites. Common occurrences of K-feldspar are in pre-ore volcanics in areas such as Red Hills (Fig. 2.2), Mount Farrell (Fig. 2.2), Jukes (Doyle, 1990) and Mount Darwin (Jones, 1993) and is an overprint of a quartz-calcite-sericite assemblage in the Rosebery-Hercules area.

K-Feldspar alteration is also present at Que River (McGoldrick *et al.*, 1990; McGoldrick and Large, 1992; Offler and Whitford, 1992). The most common occurrence at Que River is at the peripheries of the main PQ lens, where it is interpreted to be a primary alteration assemblage that is associated with the initial Cambrian alteration event (Offler and Whitford, 1992).

The K-feldspar alteration at High Point is of uncertain origin. The K-feldspar may be a VHMS-related alteration product, or it may be related to a sub-surface Cambrian granite similar to the Darwin Granite and the Murchison Granite (Jones, 1993; Large *et al.*, submitted). Due to the limited distribution of this alteration style, it is not possible to conclude a definite origin for the K-feldspar assemblage.

### 4.5.3 Epidote

Epidote can occur in variety of environments including high temperature assemblages (Battey, 1981; Duda and Rejl, 1986), deep semi-conformable alteration zones beneath Canadian Archaean VHMS deposits (Galley, 1993; Galley *et al.*, 1993; Skirrow and Franklin, 1994), and within metamorphic terrains (Deer *et al.*, 1992). Epidote occurs in a wide range of metamorphic conditions from greenschist and amphibolite facies rocks to lower grade rocks with temperatures and pressures as weak as 320 °C and 130 atm. respectively (Deer *et al.*, 1992). Offler and Whitford (1992) reported epidote from the Que River deposit and attributed it to a Devonian Orogenic event. A low grade metamorphic origin is most likely for the pervasive epidote alteration at High Point due to its association with albite, prehnite-pumpellyite and calcite.

## 4.6 SUMMARY

Several alteration have occurred at High Point. Silicification of the peperite matrix was followed by the pervasive and pseudo-fragmental white silica-sericite alteration. This in turn was followed by pervasive black chlorite, pervasive and pseudo-fragmental silica-albite alteration and apple green fuchsite alteration assemblages. Late stage cooling of fluids is interpreted to represent K-feldspar infilling amygdales. These assemblages are all interpreted to represent Cambrian hydrothermal activity and are partly similar to the alteration at Hellyer and Que River. The last stage of alteration within the area is represented by cross cutting veins and small disseminated aggregates of epidote that is attributed to a Devonian metamorphic overprint. during the Devonian Tabberrabberan Orogeny. The various Cambrian alteration assemblages are vertically zoned and lithologically controlled. The vertical zonation consists of silica-albite (andesite-related) overlying sericite-fuchsite alteration (basalt-related) which in turns overlies a chlorite zone (basalt-related). The lower-most alteration assemblage is silica-sericite alteration and is primarily related to the dacitic units.

---

## Chapter 5

### Geochemistry

---

#### 5.1 INTRODUCTION

A geochemical study of the High Point lithologies was undertaken to address four main aims.

These aims are:

- 1/ To classify the lithologies using geochemical data;
- 2/ To compare the geochemical data from High Point with other geochemical data from the Que-Hellyer Volcanics (ie. Corbett and Komyshan (1989) and Crawford *et al.*, (1992); and
- 3/ To geochemically characterise the Mount Charter dolerite and compare it with the upper basalts to test a possible correlation between the two lithologies.

The major source for geochemical data was from core fillet grind assays collected during routine sampling by Aberfoyle geologists as part of their exploration program. This data does not contain analyses for Nb, Y, Sr and Rb. In addition, twenty selected relatively unaltered samples were analysed for the major, minor and trace elements that included Nb, Y, Sr and Rb. The results from this sampling and the core fillet grinds are included in Appendix 2.

### 5.2.1 Analytical methods

The analyses of the core fillet grinds and the selected samples was conducted by Analabs (Burnie) and paid for wholly by Aberfoyle. Elemental analysis (including major, minor and trace) were determined using X-ray fluorescence techniques and acid digestions (See Appendix 2 for full techniques). Care was taken during the preparation not to contaminate the samples with Cr, hence a tungsten carbide disc mill was used during milling of the crushed samples. Major and minor elements were analysed using the methods of Norrish and Hutton (1969), and the trace elements were analysed using pressed boric acid-backed powder pills, of approximately 6g in weight. Whole rock analyses have been recalculated to 100 % volatile free.

## 5.2 RESULTS

### 5.2.1 Introduction

The results from the geochemical analysis for Mac 33, Mac 35 and the selected samples are included in Appendix 2. Representative results from Mac 33, Mac 35 and the selected samples of these holes are included in Table 5.1, 5.2 and, 5.3 receptively. Data from Corbett and Komyshan (1989) and Crawford *et al.* (1992) used for comparison with the Que Hellyer Volcanics, are included in Tables 5.4 and 5.5 respectively.

#### 5.2.1.1 High Point results

Data from High Point are initially categorised using hand sample and thin section descriptions (Chapter 3.2) that place the rocks into either the mixed sequence dacites, or the upper basalts and andesites (Table 5.1-5.3). These units are further classified according to immobile element abundances.

Rock type	Dacite	Dacite	Dacite	Andesite	Andesite	Andesite	Basalt	Basalt	Basalt
Sample No	622362	622370	622371	622368	622369	622405	622356	622357	622358
Distance (M)	308.8-320.2	379-389	389-392	360-372.5	372.5-379	751-755.8	234.4-239	239-254.4	254.4-266.4
Hole No	Mac 33	Mac 33	Mac 33	Mac 33	Mac 33	Mac 33	Mac 33	Mac 33	Mac 33
SiO <sub>2</sub>	61.91	64.50	63.77	61.28	58.88	59.49	62.10	59.94	60.72
Al <sub>2</sub> O <sub>3</sub>	16.81	17.19	16.96	15.48	15.82	17.48	16.05	15.99	16.24
MnO	0.85	0.58	0.60	0.74	0.73	0.52	0.88	0.82	0.78
Fe <sub>2</sub> O <sub>3</sub>	9.20	7.99	7.61	9.94	10.45	11.59	10.24	9.89	8.87
MnO	0.41	0.25	0.30	0.27	0.38	1.02	0.44	0.47	0.49
K <sub>2</sub> O	1.60	0.25	2.39	1.95	1.62	1.37	1.38	1.73	1.80
MgO	3.74	2.80	2.38	6.54	7.06	8.66	5.48	5.08	4.31
CaO	4.87	2.59	4.30	7.84	9.55	4.38	4.61	7.50	7.77
P <sub>2</sub> O <sub>5</sub>	1.58	0.57	1.07	1.60	2.10	0.72	1.29	2.15	2.04
Na <sub>2</sub> O	3.97	6.40	3.80	2.25	2.27	3.94	3.96	3.30	3.01
Total %	100.00	100.00	100.00	100.00	100.00	100.00	100.00	100.00	100.00
Cu	58	130	145	83	140	245	84	71	74
Pb	68	25	1030	83	52	<5	1130	1050	155
Zn	1815	188	1723	706	216	253	2178	1086	312
Ag	<2	<2	<2	<2	<2	<2	<2	<2	<2
Au	<0.008	<0.008	<0.008	<0.008	<0.008	<0.008	<0.008	<0.008	<0.008
Ba	2537	1158	140	1113	1449	335	1770	1382	1469
As	10	9	46	18	7	3	5	13	20
Cr	41	164	21	927	45	25	13	10	19
Zr	182	173	178	163	166	197	190	193	182
Ti	4690	3920	3210	4040	4040	2550	4670	4790	4500
Ti/Zr	25.77	22.66	18.03	24.79	24.34	28.98	24.58	24.82	24.73

Table 5.1: Selected geochemical data from Mac 33.(Note: Major elements are expressed in weight (%), all others are in ppm)

Rock type	Dacite	Dacite	Dacite	Andesite	Andesite	Andesite	Basalt	Basalt	Basalt
Sample No	622561	622562	622565	622489	622490	622491	622514	622515	622516
Distance(m)	798-807	807-818	842-856	40-50	50-60	60-70	288-300	300-312	312-322
Hole No.	Mac 35	Mac 35	Mac 35	Mac 35	Mac 35	Mac 35	Mac 35	Mac 35	Mac 35
SiO <sub>2</sub>	66.75	65.33	67.98	61.64	61.60	60.82	48.05	49.30	51.34
Al <sub>2</sub> O <sub>3</sub>	15.36	15.93	15.54	17.77	16.89	17.19	12.32	12.19	12.03
SiO <sub>2</sub>	66.75	65.33	67.98	61.64	61.60	60.82	48.05	49.30	51.34
TiO <sub>2</sub>	0.46	0.49	0.43	0.55	0.58	0.56	0.58	0.59	0.55
Fe <sub>2</sub> O <sub>3</sub>	6.82	6.97	5.30	7.38	7.91	7.79	9.10	8.34	8.26
MnO	0.18	0.18	0.19	0.15	0.15	0.16	0.42	0.33	0.30
K <sub>2</sub> O	2.36	2.21	2.99	1.98	1.60	1.19	1.41	1.01	1.00
MgO	1.95	2.01	1.29	2.83	4.13	4.29	6.86	6.29	6.98
CaO	3.33	3.55	3.64	3.35	2.95	3.17	18.27	18.74	17.10
P <sub>2</sub> O <sub>5</sub>	0.15	0.14	0.10	0.31	0.30	0.30	0.61	0.59	0.55
Na <sub>2</sub> O	2.62	3.19	2.55	4.05	3.90	4.52	2.38	2.61	1.89
Total %	100	100	100	100	100	100	100	100	100
Cu	26	23	100	102	106	82	186	199	166
Pb	16	38	29	65	63	37	108	187	85
Zn	80	98	58	217	204	221	240	548	256
Ag	<2	<2	<2	<2	<2	<2	<2	<2	<2
Au	<0.008	<0.008	<0.008	<0.008	<0.008	<0.008	<0.008	<0.008	<0.008
Ba	541	769	751	1247	867	423	2167	1036	798
As	2	4	2	7	4	6	15	13	6
Cr	8	17	9	17	17	15	634	619	591
Zr	248	285	230	175	180	171	142	142	139
Ti	2631	2732	2446	3177	3305	3200	3110	3188	3005
Ti/Zr	10.61	9.59	10.63	18.15	18.36	18.71	21.90	22.45	21.62

Table 5.2: Selected geochemical data from Mac35. (Note: Majors are expressed in weight %, all others in ppm)



Rock type	dacite	dacite	dacite	andesite	andesite	andesite	basalt	basalt	basalt
Sample No	1001	1002	1013	1007	1008	1010	1009	1011	1014
Hole (Depth)	12 (173.5)	33 (531.5)	27 (750.1)	14 (521.7)	14 (171.8)	12 (184.2)	35 (303)	35 (276.4)	13 (321.9)
SiO <sub>2</sub>	71.73	65.27	63.15	63.15	59.35	58.24	47.33	46.84	50.93
Al <sub>2</sub> O <sub>3</sub>	12.52	13.09	14.21	15.15	15.62	18.34	12.84	13.54	16.31
TiO <sub>2</sub>	0.41	0.31	0.46	0.46	0.71	0.56	0.57	0.58	0.65
Fe <sub>2</sub> O <sub>3</sub>	4.42	4.46	5.72	4.35	7.86	10.00	8.65	8.95	10.61
MnO	0.16	0.09	0.32	0.19	0.44	0.28	0.30	0.53	0.32
CaO	3.41	9.77	4.28	6.49	4.75	2.27	18.75	16.74	8.22
K <sub>2</sub> O	2.35	2.15	5.02	3.11	2.94	1.90	1.27	1.34	1.99
MgO	1.37	0.71	4.03	2.40	4.03	3.19	7.28	7.61	7.86
P <sub>2</sub> O <sub>5</sub>	0.29	0.08	0.30	0.31	0.86	0.31	0.60	0.60	0.58
Na <sub>2</sub> O	3.36	4.07	2.51	4.39	3.45	4.91	2.41	3.27	2.54
S	0.75	0.51	0.49	0.73	0.37	0.46	0.57	0.60	0.02
Total (%)	100.00	100.00	100.00	100.00	100.00	100.00	100.00	100.00	100.00
Cu	48	46	81	79	34	49	179	111	137
Pb	1083	108	296	661	94	311	83	5	26
Zn	937	60	234	1026	12200	1001	139	180	100
Ni	5	8	37	30	38	7	130	132	100
Ba	1300	1483	3894	1960	2934	1406	744	1763	1732
Zr	123	214	147	141	199	176	143	147	153
Cr	6	6	112	67	81	10	486	483	364
Ti	2367	2001	2661	2556	3944	3387	3050	3146	3675
Ti/Zr	19.24	9.35	18.10	18.13	19.82	19.24	21.33	21.40	24.02
Rb	64	64	137	79	55	68	31	31	51
Sr	382	375	502	394	461	619	471	393	787
Y	18	38	22	22	36	29	23	21	26
Zr	123	214	147	141	199	176	143	147	153
Nb	5	13	8	7	10	9	8	10	10
Zr	123	214	147	141	199	176	143	147	153
Y	18	38	22	22	36	29	23	21	26

Table 5.3: Selected Geochemical data. (Note: Majors are expressed in weight %, all others are in ppm)

### 5.2.1.2 Results from Que-Hellyer Volcanics

Two groups of data are included from the Que-Hellyer Volcanics for comparison with geochemical data from High Point. Locations of the samples taken after Corbett and Komysan (1989) are included in Appendix 2. Sample locations for the data obtained by Crawford *et al.*, (1992) (Tables, 5.4-5.5) are also included with those of Corbett and Komysan (1989) (Appendix 2).

Rock type Sample No	Basalt 334161	Basalt Z7251	Andesite 334162	Andesite MR437
Hole (Depth)	HL6 (200.1m)	HP2 392m	HL 6 208.5m	913959
SiO <sub>2</sub>	49.9	52.9	55.6	56.2
TiO <sub>2</sub>	0.85	0.52	0.77	0.6
Al <sub>2</sub> O <sub>3</sub>	14.1	13.6	18.6	13.1
FeO	9.77	8.51	10.5	9.02
MnO	0.16	0.14	0.23	0.18
MgO	11.6	15.2	4.6	8.2
CaO	8.83	6.5	3.08	7.96
Na <sub>2</sub> O	1.22	1.53	4.12	3.06
K <sub>2</sub> O	3.07	0.99	1.93	1.31
P <sub>2</sub> O <sub>5</sub>	0.43	0.12	0.57	0.41
Total	100	100	100	100
Ba	BDL	13337	3407	1114
Rb	50	27	46	24
Sr	404	183	595	612
Y	32	16	32	21
Nb	13	5	11	8
Zr	195	75	187	131
Ni	n.a.	380	17	87
Cr	n.a.	1133	5	370
V	n.a.	223	302	282
Sc	n.a.	28	31	32
Ti/Zr	25.2	41.6	24.7	27.5

Table 5.4: Geochemical data from the Que-Hellyer Volcanics (After Crawford *et al.*, 1992).

Rock type	Dacites		Upper andesites and basalts				Dolerites		
Sample No	P200	P191	P192	P218	P177	P097	P021	P011	P216
SiO <sub>2</sub>	70.9	73.43	73.76	60.84	58.55	61.87	52.83	52.92	53.35
TiO <sub>2</sub>	0.32	0.28	0.26	0.36	0.5	0.63	0.36	0.62	0.5
Al <sub>2</sub> O <sub>3</sub>	16.17	14.8	14.45	19.07	14.46	16.71	16.15	14.69	13.96
Fe <sub>2</sub> O <sub>3</sub>	0.98	2.1	2.01	1.44	1.08	10.99	1.17	1.03	0.76
FeO	2.45	0.79	1.86	7.07	5.35	3.43	6.49	7.46	7.29
MnO	0.11	0.04	0.05	0.22	0.76	0.04	0.15	0.16	0.16
MgO	1.24	0.05	0.31	3.64	6.07	3.02	8.06	10.48	10.99
CaO	2.99	0.35	0.24	0.56	6.63	0.15	12.44	8.23	10.48
Na <sub>2</sub> O	1.18	5.35	2.57	5.24	4.12	0.49	1.72	2.65	1.35
K <sub>2</sub> O	3.57	2.74	4.45	1.45	2.35	2.49	0.52	1.62	0.98
P <sub>2</sub> O <sub>5</sub>	0.09	0.07	0.04	0.11	0.13	0.18	0.11	0.14	0.18
Total	100	100	100	100	100	100	100	100	100
Ba	730	1800	2300	1050	1550	6900	165	800	390
Rb	150	81	135	73	85	93	48	61	59
Sr	26	260	210	240	280	34	125	370	270
Y	19	28	26	16	54	31	10	16	12
Nb	8	7	6	7	5	9	BDL	8	4
Zr	140	165	175	200	95	170	58	94	82
Co	5	8	7	9	23	33	42	37	36
Ni	5	4	BDL	24	55	150	105	165	140
Cr	125	82	47	31	410	770	155	790	820
V	260	31	28	91	230	280	280	250	230
Sc	35	15	14	15	33	40	40	34	30
Cu	12	9	20	8	8	99	47	57	21
Pb	26	8	9	BDL	8	11	4	6	10
Zn	11	37	150	74	760	140	62	77	75
Ti/Zr	14	9	9	11	32	22	37	40	37

Table 5.5: Geochemical data from the Que-Hellyer Volcanics (After Corbett and Komysan, 1989). (Note majors are expressed in weight (%), all others are in ppm)

### 5.3 GEOCHEMICAL CLASSIFICATION OF VOLCANICS

The data obtained from geochemical sampling allows characterisation of each of the three main volcanic units. The basaltic sequences are characterised by having high Ti/Zr values that rarely extend below 20, or above 55; they are further characterised by having Cr values less than 50 ppm, to values in excess of 1000 ppm, for analysed samples (Fig. 5.1). P<sub>2</sub>O<sub>5</sub> values for the basalts display a wide spread (0.1-0.7 %) (Fig. 5.3) in comparison to the andesites that plot within a tight group from approximately 0.25 ppm to 0.35 ppm. Andesites also display a small variance in terms of Ti/Zr values (0.16 to 0.20) (Figs. 5.1-5.3) with the exception of one data point that plots at a value of 0.33. Characteristic of the dacites are low to very low P<sub>2</sub>O<sub>5</sub> values (less than 0.15), typically lower than the andesites. However, Ti/Zr are slightly more variable than for the andesites. The spurious data points for both the andesites and dacites (marked on Figs. 5.1-5.3) may indicate possible mobilisation of P<sub>2</sub>O<sub>5</sub> during alteration. Chromium analysis for the dacites indicates that Cr-rich fluids have passed through the units. This is consistent with field observations, where minor fuchsite was recorded within the dacites as well as the basalts and andesites.

### 5.4 IMMOBILE ELEMENT GEOCHEMISTRY

Element mobility describes the chemical changes that take place within a rock after formation-generally during interaction with fluids (Rollinson, 1993). Element mobility occurs during either weathering, diagenesis, metamorphism or hydrothermal alteration (Rollinson, 1993). Immobile elements are those elements that retain their original abundances during fluid interaction. Elements considered to be immobile under all but the most intense fluid interaction include Ti, Al, Nb, Y, Zr and P (Finlow-Bates and Stumpfl, 1981; Rollinson, 1993). Mobile elements under a variety of fluid interaction conditions include Si, Fe, Mn, Mg, Ca or Na (Table 5.6). Workers such as Pearce and Cann (1971, 1973) and Winchester and Floyd (1979)

Figure 5.1: Cr versus Ti/Zr

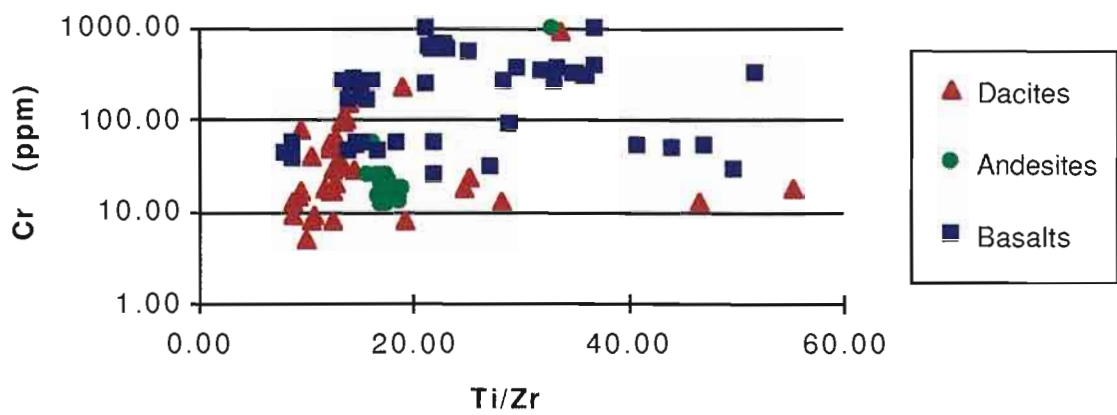


Figure 5.2: Cr\*P2O5 versus Ti/Zr

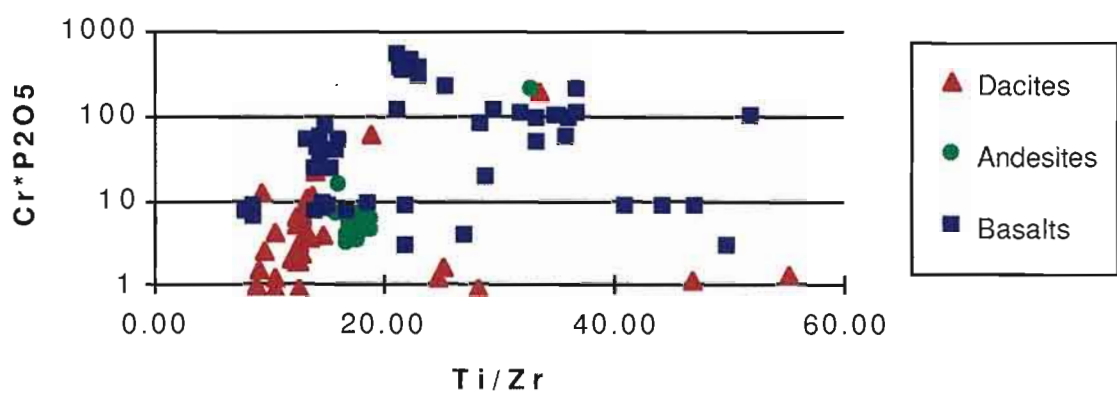
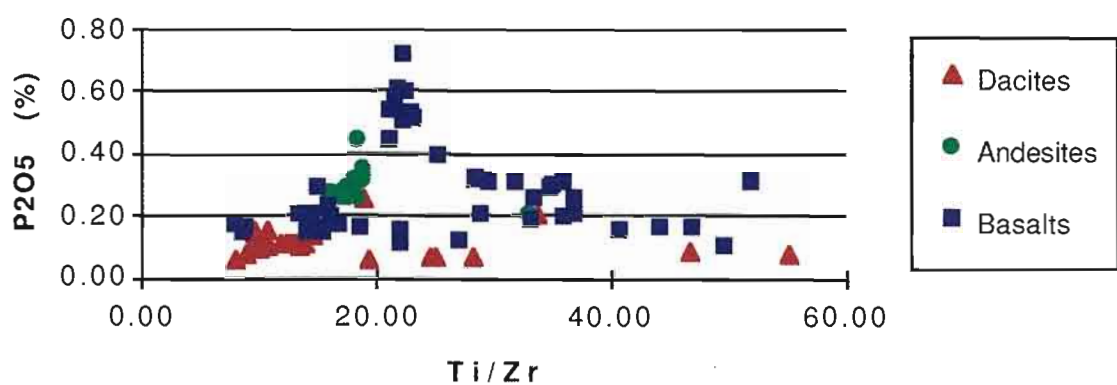


Figure 5.3: P2O5 versus Ti/Zr



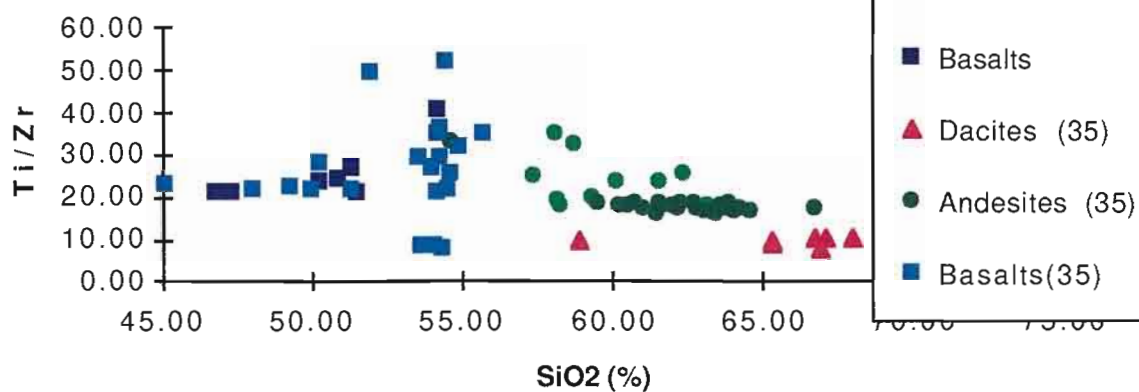
have used immobile elements to subdivide basaltic rocks according to their tectonic setting on the basis of their trace element characteristics.

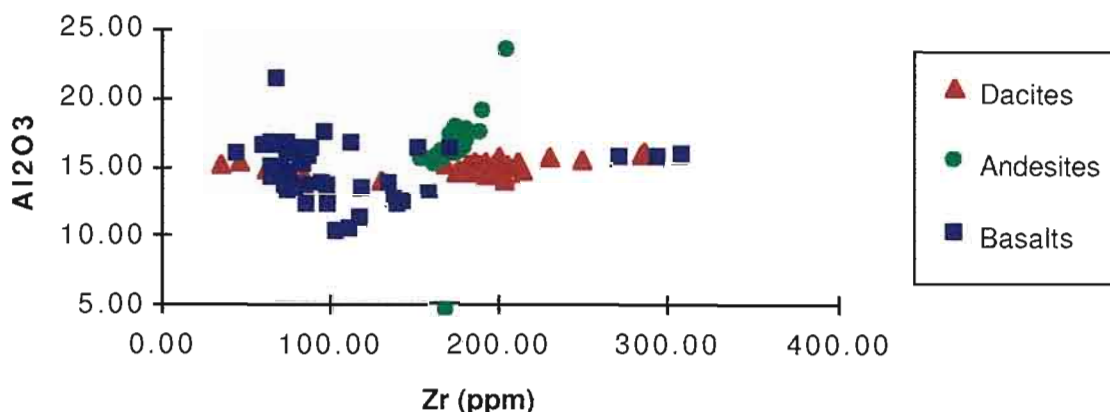
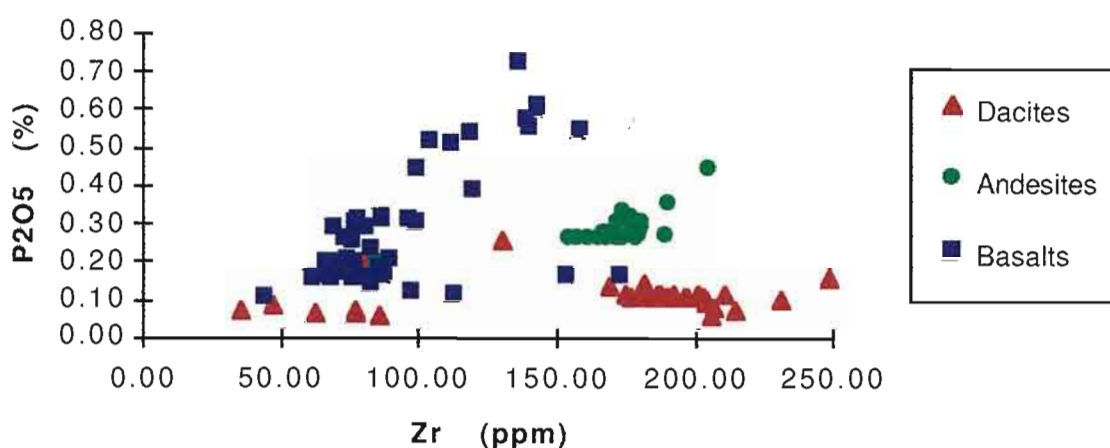
Rock type		Si	Ti	Al	Fe	Mn	Mg	Ca	Na	K	P	Reference
Komatiite		×						×	×	×		Arndt (1983)
Basalt	Hydrothermal alteration	-			-	-	+	-	-	-		Mottl (1983)
Basalt	Hydrothermal alteration	+	-		-	-	-	-	+			MacGeehan and MacLean (1980)
Basalt	Submarine weathering	-			+		-	-	-	+		Pearce (1976)
Basalt	Weathering	-					-	-	-	-		Pearce (1976)
Basalt	Greenschist facies metamorphism				×		×		×	×		Pearce (1976), Gelinis <i>et al.</i> (1982)
Basalt	Amphibolite facies metamorphism	×						×	×			Rollinson (1983)
Granite	Weathering				×		×	×	-	×		Nesbitt and Young (1989)
Granite	Contact metamorphism			+	-		-	-	-	+		Vernon <i>et al.</i> (1987)
'Granite'	Granulite facies metamorphism						-			×		Allen <i>et al.</i> (1985)
Calcareous sediments	Medium grade metamorphism								-	-		Ferry (1983)
Calcareous sediments	Contact metamorphism	×			×		×					Burcher-Nurminen (1981)
Sandstone-clay	Diagenesis	×			×		×	×		×		Boles and Franks (1979)

Key: ×, element mobile; -, element depleted; +, element enriched.

Table 5.6 Major element mobility in common rock types under a variety of hydrothermal conditions. (After Rollinson, 1993).

Finlow-Bates and Stumpfl (1981) noted that the immobile elements can sometimes be mobilised together by the same fluid interaction event (eg. hydrothermal alteration). To confidently use immobile elements for comparisons of tectonic settings, the mobility of the so-called immobile elements must be checked. A scatter plot of the immobile elements plotted against one another would indicate that the elements are, in fact mobile, however a linear trend may indicate that all the immobile elements have been mobilised together (McGeehan and McLean, 1980). Discrimination of immobile elements and mobile elements can be resolved by plotting different pairs, where a large number of elements plotting in a linear array is more likely to indicate that they are all immobile rather than mobilised together (Whitford *et al.*, 1989). Plots of the High Point data suggest that elements such as Ti, Zr, Nb, Y and Al are immobile elements for the analysed samples (Figs. 5.4-5.8).

Figure 5.4: Ti/Zr versus SiO<sub>2</sub>

**Figure 5.7: Al<sub>2</sub>O<sub>3</sub> versus Zr****Figure 5.8: P<sub>2</sub>O<sub>5</sub> versus Zr**

## 5.5 COMPARISON WITH QUE-HELLYER VOLCANICS

Geochemical data from this study have been compared to other data from volcanic units within the Mount Read belt. From the High Point data it is possible to distinguish three distinct geochemical suites that correspond to three of the suites described by Crawford *et al.*, (1992). The authors describe five separate suites for the Mount Read belt however, only three are of relevance and are described below. Suite I rocks are voluminous and includes the Eastern sequence, Central Volcanic Complex, Tyndall Group and the andesitic lavas of the Que-Hellyer footwall sequence. Geochemically this suite of rocks are transitional, medium to high-K calc-alkaline and are the least light REE-enriched of the calc-alkaline lavas of the Mount Read Volcanics. In comparison with suite I rocks, suite II lithologies are more



enriched in  $P_2O_5$ , and light REE and have high-K calc-alkaline affinities; they include units such as the hornblende-porphyrritic andesites and dacites mainly from the upper part of the southern Central Volcanic Complex. The final suite used for comparison with the High Point lithologies is suite III, which comprises the upper basalts and andesites from the Que-Hellyer hangingwall sequence, the Lynch Creek basalts and the intrusive basalts in the Howard Plain area. The suite III rocks are typically low  $TiO_2$  (0.4-.5%), low  $P_2O_5$  (<0.1%) basalts, to low  $TiO_2$  (0.4-0.8%) but strongly  $P_2O_5$ -enriched basalts.

The High Point dacites are characterised by low  $P_2O_5/TiO_2$ , low to medium  $Ti/Zr$  ratios and low  $TiO_2$  contents (Figs. 5.9-5.11). Plotted on these figures are the fields that Crawford *et al.* (1992) defined for each of the five geochemical suites in the Mount Read Volcanics. From figures 5.9-5.11 the dacites are best correlated with suite I and from figures 5.9-5.11 the data for the andesites at High Point plot mainly within the boundaries of suite II. These andesites typically contain low to medium  $TiO_2$  and Cr and are relatively enriched in  $P_2O_5$ , here they are considered to be temporal equivalents of suite II. The basalts at High Point (as described in Section 3.4 and 5.3) are the equivalent of the suite III units of Crawford *et al.* (1992). The field that defines the suite III lithologies does not completely enclose all the High Point basalt data, mainly due to the alteration events that have affected Cr.

## 5.6 GEOCHEMICAL COMPARISON OF DOLERITES

A geochemical study was undertaken of the Mount Charter dolerites to evaluate the possibility that it is a Cambrian unit related to the upper basalts of the Que-Hellyer Volcanics rather than a Devonian unit as mapped by Komyshan (1986). To establish the likelihood of the body being co-magmatic with the upper basalts, the geochemical features of the dolerites were plotted for Cr,  $P_2O_5$  and  $Cr \cdot P_2O_5$  against  $Ti/Zr$  (Figs. 5.12-5.14) both from this study and from Corbett and Komyshan (1989) and Crawford *et al.* (1992). The dolerite is characterised by medium to high Cr values,  $Ti/Zr$  values between 35 and 40, and  $P_2O_5$  levels between 0.1 and 0.2 weight %. Therefore, these values for the dolerite are within the fields for the upper basalts, implying that they are broadly co-magmatic. The geological relationships (Section

and the geochemical signature indicate that the dolerites are in fact, a Cambrian intrusive rather than a Devonian intrusive as previously described by Corbett and Komyshan (1989).

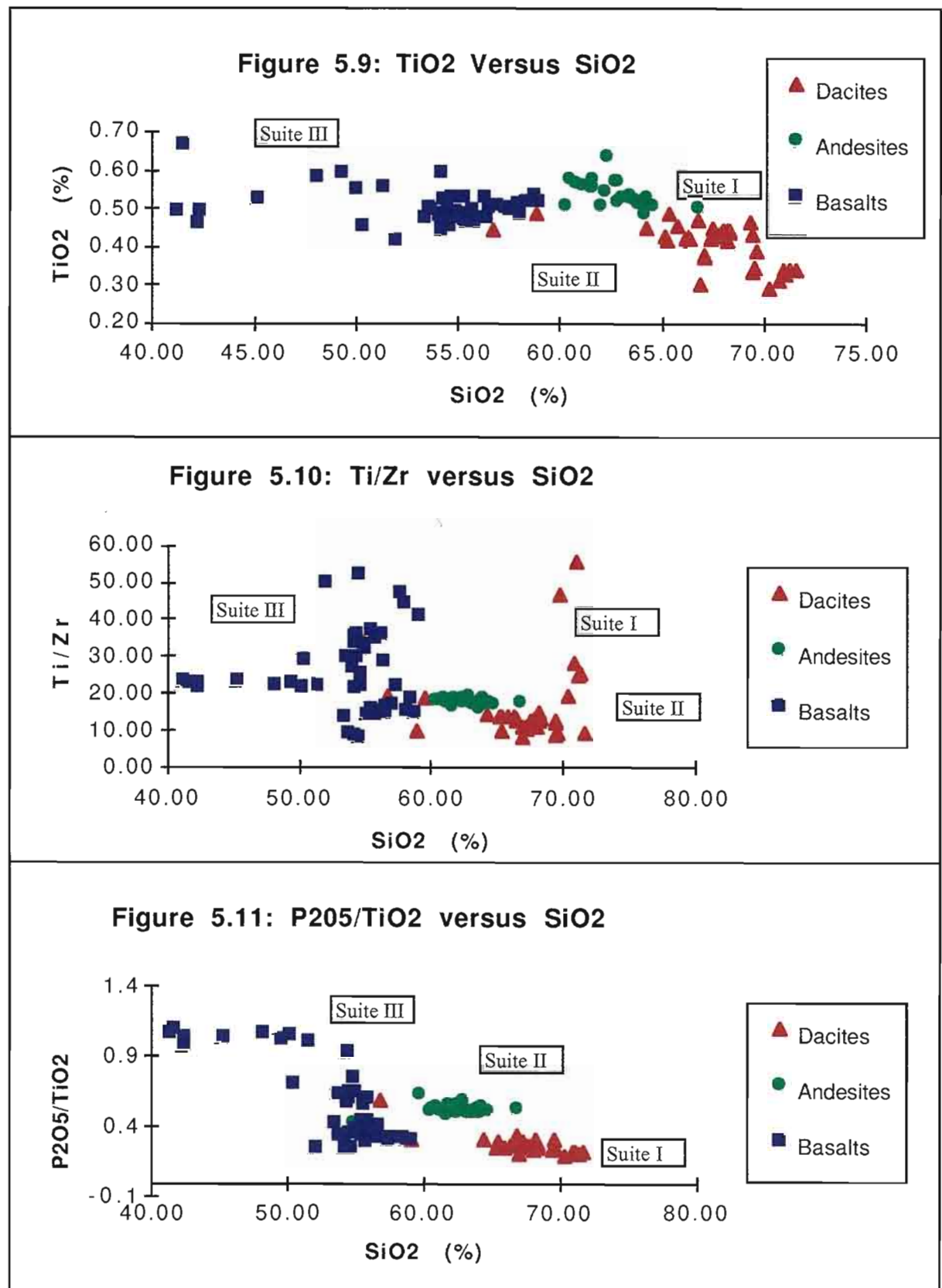


Figure 5.12: Cr\*P2O5 versus Ti/Zr

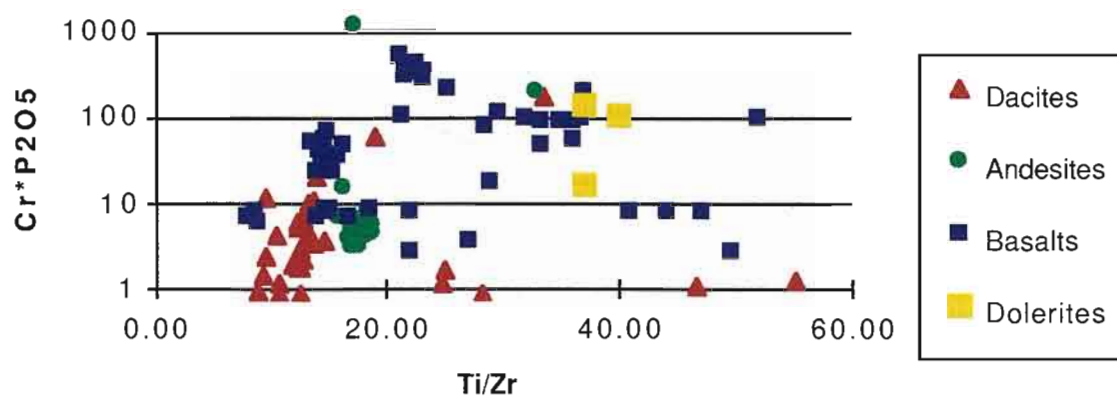


Figure 5.13: Cr versus Ti/Zr

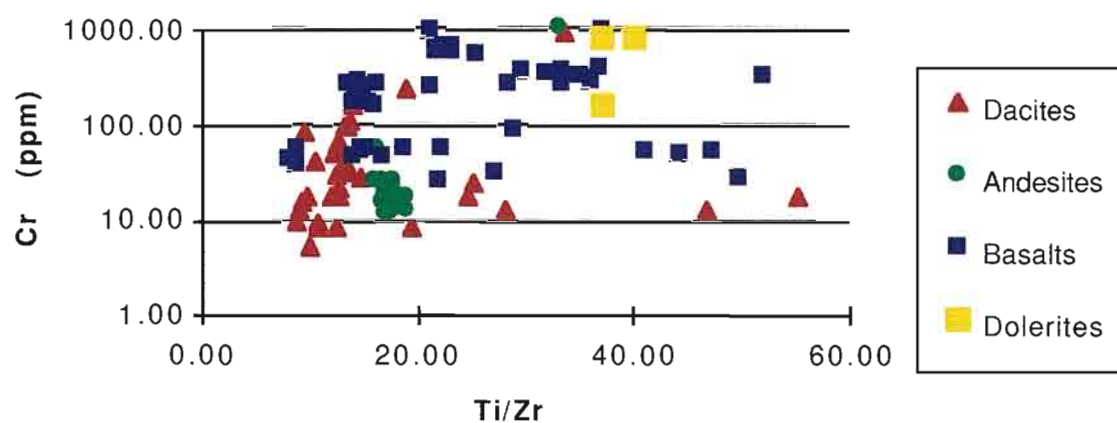
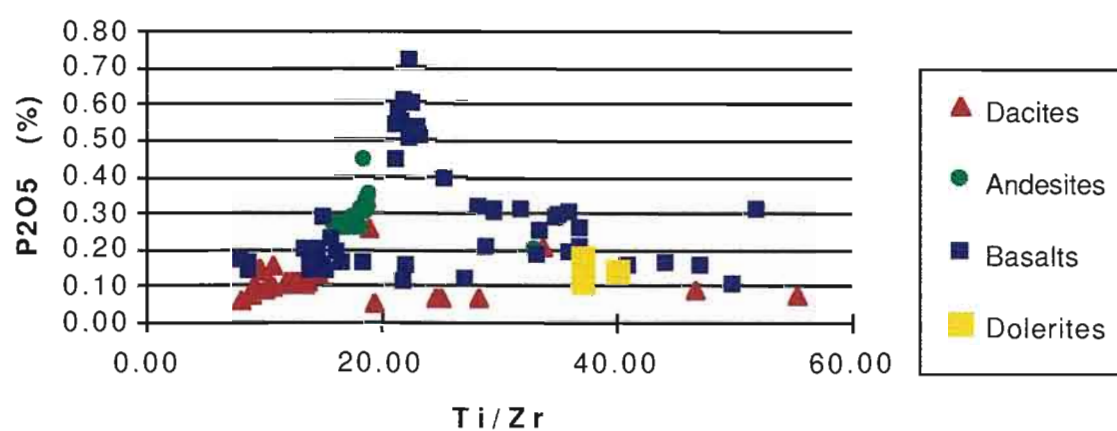


Figure 5.14: P2O5 versus Ti/Zr



## 5.7 ALTERATION INDICES

The alteration index is defined as the  $(K_2O + MgO)/(K_2O + MgO + CaO + Na_2O)$  (Ishikawa *et al.*, 1976) and measures relative enrichment and depletions of oxides during alteration. At Hellyer, Gemmell and Large (1992) observed that the alteration index increased toward the centre of the footwall alteration system. The zonation is a maximum of 91 in the siliceous core, decreasing to 36 in the unaltered andesites. At High Point, the alteration indices (Tables 5.1-5.3) are much more varied and range from 96 down to 17 indicating that there is a larger degree of variability in the alteration index at High Point compared to Hellyer. Typical alteration indices (ie. between 20 and 40) indicate that the rocks are relatively unaltered where the majority of values are below 45. These values indicate that the alteration in High Point area is equivalent to the unaltered andesites and the stringer envelope zone of the footwall alteration at Hellyer (Fig 5.15). As discussed previously (Chapter 4), the alteration at High Point is comparable to that at Hellyer, however the alteration index suggests that the High Point lithologies are relatively unaltered. It is further suggested that the fluids that formed the High Point alteration assemblages were not as focussed, intense or at as high temperature as those that formed the stringer zone (Se, Chl, Si ; AI.80) at Hellyer.

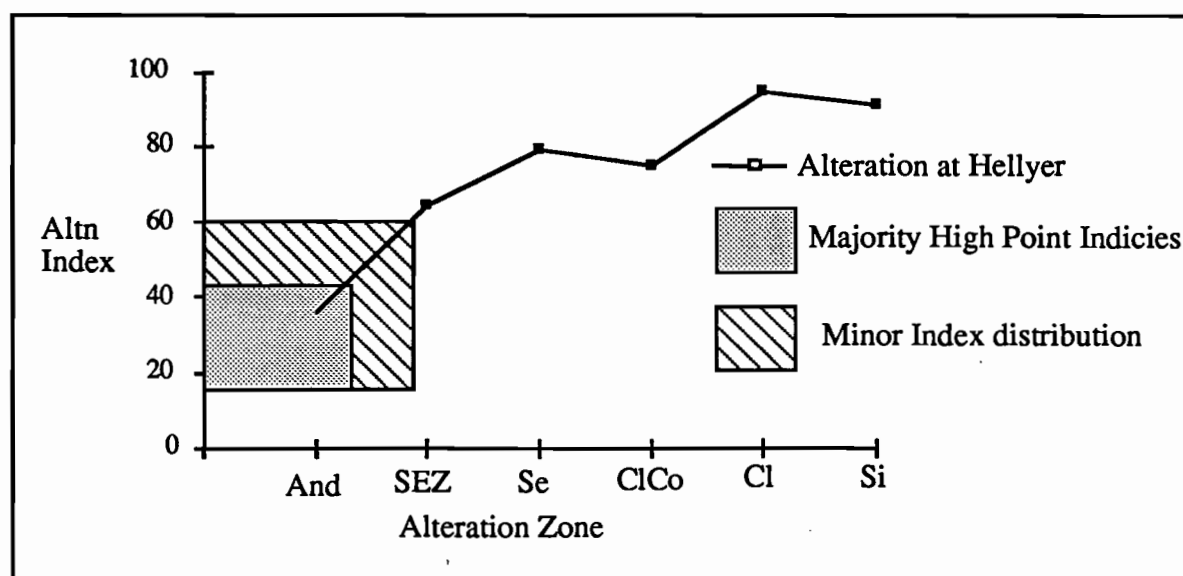


Figure 5.15: Comparison of alteration index for the High Point area with the alteration index for the alteration zones in the stringer system at Hellyer. And= unaltered andesite, SEZ= stringer envelope zone, Se= sericite, Cl= chlorite, Co= carbonate (primarily calcite), Si= siliceous core (After Gemmell and Large, 1992).

The alteration index was also used in this study to determine if any association occurs with alteration and mineralisation. There appears to be no distinct correlation with the mineralisation and alteration index from the plots of down hole depth versus zinc and alteration index for Mac 33, Mac 35 and the combination of data.

## 5.7 SUMMARY

In summary, the High Point volcanics can be classified according to hand sample and thin section descriptions and by geochemical signatures. The dacites are characterised by low  $P_2O_5$ , low Ti/Zr ratios and low  $P_2O_5/TiO_2$  ratios and correlate with suite I volcanics of Crawford *et al.* (1992). The andesite units are the temporal equivalents of suite II lithologies owing to the similar enrichments of  $P_2O_5$ , similar  $P_2O_5/TiO_2$  and Ti/Zr values. The upper basalts of the Que-Hellyer Volcanics that have been classified as suite III lithologies are represented in the High Point area by the basalt lavas and lava breccias (Chapter 3.4). This correlation has been drawn by the similarities with the  $P_2O_5/TiO_2$ , Ti/Zr, the  $Cr^*P_2O_5$  versus Ti/Zr plot and the  $P_2O_5$  versus Ti/Zr plots. From these plots it is also possible to re-interpret the Mount Charter dolerites as a Cambrian intrusive that is co-magmatic with the upper basalts of the Que-Hellyer Volcanics.

The study of alteration index  $(K_2O + MgO)/(K_2O + MgO + CaO + Na_2O)$  demonstrates that the High Point lithologies are relatively unaltered in comparison with the stringer system underlying Hellyer. The values for the alteration index at High Point indicates that the area is similar to the unaltered andesites and the stringer envelope zone as indicated by similar alteration assemblages. The equivalent alteration at High Point compared with Hellyer is less intense and less focussed, and possibly formed at lower temperatures. Plots for alteration indices and mineralisation indicate there is no distinct correlation between mineralisation and the alteration index at High Point.